

Gö-VIP-15: Dr. Malte Tiburcy/Prof. Dr. Wolfram-Hubertus Zimmermann

Institut für Pharmakologie und Toxikologie

Originalpublikation: *Defined Engineered Human Myocardium with Advanced Maturation for Applications in Heart Failure Modelling and Repair. In: Circulation, Mai 2017; 135 (19): 1832-1847 Epub 6.2.2017 (DOI:10.1161/CIRCULATIONAHA.116.024145)*

Autoren: Malte Tiburcy^{1,2}; James E. Hudson^{1,2}; Paul Balfanz^{1,2}; Susanne Schlick^{1,2}; Tim Meyer^{1,2}; Mei-Ling Chang Liao^{1,2}; Elif Levent^{1,2}; Farah Raad^{1,2}; Sebastian Zeidler^{1,2,3}; Edgar Wingender^{2,3}; Johannes Riegler⁴; Mouer Wang⁴; Joseph D. Gold^{4,5}; Izhak Kehat⁶; Erich Wettwer^{1,7}; Ursula Ravens⁷; Pieterjan Dierickx⁸; Linda W. van Laake⁸; Marie Jose Goumans⁹; Sara Khadjeh¹⁰; Karl Toischer¹⁰; Gerd Hasenfuss¹⁰; Larry A. Couture¹¹; Andreas Unger¹²; Wolfgang A. Linke^{2,10,12}; Toshiyuki Araki¹³; Benjamin Neel¹³; Gordon Keller¹⁴; Lior Gepstein⁶; Joseph C. Wu^{4,5}; Wolfram-Hubertus Zimmermann^{1,2}

- (1) Institute of Pharmacology and Toxicology, University Medical Center Göttingen, Germany.
- (2) German Center for Cardiovascular Research (DZHK), partner site Göttingen
- (3) Institute of Bioinformatics, University Medical Center Göttingen, Germany
- (4) Stanford Cardiovascular Institute and
- (5) Department of Radiology, Molecular Imaging Program, Stanford University School of Medicine, Stanford, USA
- (6) The Sohnis Laboratory for Cardiac Electrophysiology and Regenerative Medicine, Technion-Israel Institute of Technology, Haifa, Israel.
- (7) Institute of Pharmacology and Toxicology, Technical University Dresden, Germany
- (8) University Medical Center Utrecht and Hubrecht Institute, Utrecht, The Netherlands
- (9) Leiden University Medical Center, Leiden, The Netherlands
- (10) Clinic for Cardiology and Pneumology, University Medical Center Göttingen, Germany.
- (11) Center for Applied Technology, Beckman Research Institute, City of Hope, Duarte, USA.
- (12) Department of Cardiovascular Physiology, Institute of Physiology, Ruhr University Bochum, Germany.
- (13) New Laura and Isaac Perlmutter Cancer Center at New York University Langone, New York, USA
- (14) McEwen Centre for Regenerative Medicine, Toronto, Canada.



Dr. med. Malte Tiburcy



Prof. Dr. Wolfram-Hubertus Zimmermann

Zusammenfassung des wissenschaftlichen Inhalts

Humane Herzmuskelzellen (Kardiomyozyten) aus pluripotenten Stammzellen haben sich zu einem wichtigen Modellsystem der kardiovaskulären Grundlagenforschung entwickelt. Darüber hinaus ist auch eine klinische Anwendung für die Zell-basierte Herzreparatur z.B. als „Herzpfaster“ denkbar. Eine zentrale Limitation von aus embryonalen oder induzierten pluripotenten Stammzellen abgeleiteten Herzmuskelzellen ist deren phänotypische Unreife. Aufgrund des offensichtlichen „Entwicklungsblocks“ in klassischen Zellkulturformaten wird die Eignung von Herzmuskelzellen aus embryonalen oder induzierten pluripotenten

Stammzellen infrage gestellt. Im Rahmen einer aktuellen Arbeit haben wir die Hypothese überprüft, dass aus pluripotenten Stammzellen abgeleitete Herzmuskelzellen in einem definierten 3D-Kulturformat in der Lage sind, bereits in der Kulturschale einen postnatalen Phänotyp zu erreichen. Über das sogenannte „Tissue Engineering“ ist es uns erstmalig gelungen, aus definierten Zelltypen (Herzmuskelzellen und Fibroblasten) unter definierten Kulturbedingungen und ohne Verwendung tierischer Seren humane Herzmuskelgewebe (sogenannte Engineered Heart Muscle - EHM) zu erzeugen. Ein bisher in alternativen Kulturformaten nicht erreichter Reifegrad wurde sowohl morphologisch (Sarkomerbildung mit M-Banden), funktionell (Nachweis einer klassischen Kraft-Frequenz-Beziehung), molekular (RNAseq Profile im direkten Vergleich mit embryonalem, fetalen und adulten Herzgewebe) sowie pharmakologisch (Ansprechen auf Katecholaminstimulation) nachgewiesen. Reifung ist eine wichtige Voraussetzung für die Anwendung von EHM in der Überprüfung der Arzneimittelsicherheit ebenso wie in der Etablierung von Krankheitsmodellen für die Entwicklung individualisierter Therapieansätze („Präzisionsmedizin“). Beispielhaft konnten wir zeigen, dass durch chronische Katecholamin-Applikation ein charakteristischer Herzinsuffizienz-Phänotyp hervorgerufen und durch parallele Anwendung spezifischer Katecholamin-Rezeptorblocker inhibiert werden kann. Darüber hinaus konnte die Skalierbarkeit des EHM-Ansatzes für therapeutische Anwendung, d.h. die Remuskularisierung des insuffizienten Herzens, demonstriert werden.

WEITERE INFORMATIONEN:

Dr. med. Malte Tiburcy: m.tiburcy@med.uni-goettingen.de

Prof. Dr. Wolfram-Hubertus Zimmermann: w.zimmermann@med.uni-goettingen.de

Institut für Pharmakologie und Toxikologie

Robert-Koch-Str. 40, 37075 Göttingen

Telefon: 0551/39-5781

Defined Engineered Human Myocardium With Advanced Maturation for Applications in Heart Failure Modeling and Repair

Editorial, see p 1848

BACKGROUND: Advancing structural and functional maturation of stem cell–derived cardiomyocytes remains a key challenge for applications in disease modeling, drug screening, and heart repair. Here, we sought to advance cardiomyocyte maturation in engineered human myocardium (EHM) toward an adult phenotype under defined conditions.

METHODS: We systematically investigated cell composition, matrix, and media conditions to generate EHM from embryonic and induced pluripotent stem cell–derived cardiomyocytes and fibroblasts with organotypic functionality under serum-free conditions. We used morphological, functional, and transcriptome analyses to benchmark maturation of EHM.

RESULTS: EHM demonstrated important structural and functional properties of postnatal myocardium, including: (1) rod-shaped cardiomyocytes with M bands assembled as a functional syncytium; (2) systolic twitch forces at a similar level as observed in bona fide postnatal myocardium; (3) a positive force-frequency response; (4) inotropic responses to β -adrenergic stimulation mediated via canonical β_1 - and β_2 -adrenoceptor signaling pathways; and (5) evidence for advanced molecular maturation by transcriptome profiling. EHM responded to chronic catecholamine toxicity with contractile dysfunction, cardiomyocyte hypertrophy, cardiomyocyte death, and N-terminal pro B-type natriuretic peptide release; all are classical hallmarks of heart failure. In addition, we demonstrate the scalability of EHM according to anticipated clinical demands for cardiac repair.

CONCLUSIONS: We provide proof-of-concept for a universally applicable technology for the engineering of macroscale human myocardium for disease modeling and heart repair from embryonic and induced pluripotent stem cell–derived cardiomyocytes under defined, serum-free conditions.

Malte Tiburcy, MD
James E. Hudson, PhD
Paul Balfanz
Susanne Schlick, MS
Tim Meyer, PhD
Mei-Ling Chang Liao, PhD
Elif Levent, PhD
Farah Raad, PhD
Sebastian Zeidler, PhD
Edgar Wingender, PhD
Johannes Riegler, PhD
Mouer Wang, MD
Joseph D. Gold, PhD
Izhak Kehat, MD, PhD
Erich Wettwer, PhD
Ursula Ravens, MD, PhD
Pieterjan Dierickx, PhD
Linda W. van Laake, MD, PhD
Marie Jose Goumans, PhD
Sara Khadjeh, PhD
Karl Toischer, MD
Gerd Hasenfuss, MD
Larry A. Couture, PhD
Andreas Unger, PhD
Wolfgang A. Linke, PhD
Toshiyuki Araki, PhD
Benjamin Neel, MD, PhD
Gordon Keller, PhD
Lior Gepstein, MD, PhD
Joseph C. Wu, MD, PhD
Wolfram-Hubertus
Zimmermann, MD

Correspondence to: Wolfram-Hubertus Zimmermann, MD, Institute of Pharmacology and Toxicology, University Medical Center Göttingen, Georg-August-University, Robert-Koch-Str 40, 37075 Göttingen, Germany. E-mail w.zimmermann@med.uni-goettingen.de

Sources of Funding, see page 1844

Key Words: heart failure
■ models, cardiovascular
■ regeneration ■ stem cells
■ tissue engineering

© 2017 American Heart Association, Inc.

Clinical Perspective

What Is New?

- Proof-of-concept for the engineering of scalable force-generating human myocardium from a variety of human pluripotent stem cells and biopsy-derived fibroblasts under defined, serum-free conditions.
- Evidence for morphological, molecular, and functional maturation beyond the present state-of-the-art is demonstrated (eg, positive force-frequency response, sarcomere assembly with robust M-band formation).
- Simulation of a human heart failure phenotype in the dish with (1) contractile dysfunction, (2) loss of a positive force-frequency response, (3) adrenergic signal desensitization, (4) cardiomyocyte hypertrophy, and (5) biomarker release (N-terminal pro B-type natriuretic peptide) by chronic catecholamine stimulation.
- Implantability of scalable engineered human myocardium patches is demonstrated.

What Are the Clinical Implications?

- Robustness and readiness of defined, serum-free engineered human myocardium for applications in translational studies is demonstrated.
- Advanced morphological, molecular, and functional maturation, and organotypic responses to physiological (positive force-frequency response) and pathological (norepinephrine-induced heart failure) stimuli, as well, are key for the utility of engineered human myocardium in heart failure modeling.
- Simulated heart failure in engineered human myocardium may be exploited for the development of novel heart failure therapeutics.
- The reported defined, serum-free protocol will facilitate the engineering of human myocardium according to current good manufacturing practice for applications in tissue-engineered heart repair.

The availability of human embryonic stem cells (ESCs)¹ and human-induced pluripotent stem cells (iPSCs)² and the scalability of their directed differentiation into bona fide cardiomyocytes, as well,³⁻⁷ have facilitated the rapid evolution of myocardial tissue engineering. Early tissue-engineering studies in chick embryo and rodent models have established electromechanical stimulation as an important engineering paradigm,⁸⁻¹⁰ which has now been translated to human models.¹¹⁻¹⁶ The accumulating evidence for advanced maturation in 3-dimensional versus monolayer cultures provides a solid rationale for applications in phenotypic screens¹¹ and heart repair.^{17,18} As the use of myocardial tissue engineering increases in academia and industry, it is essential to establish conditions readily adaptable to current good manufacturing practice. To

achieve this goal, it is imperative to define the essential elements required for the structural and functional maturation of tissue-engineered myocardium under defined, serum-free conditions. Last, robust and reproducible utility in ESC- and iPSC-based models is of pivotal importance.

In this study, we report a systematic approach for the design of engineered human myocardium (EHM) with structural and functional properties observed in the postnatal heart. Unbiased transcriptome profiling provided evidence for advanced maturation in EHM in comparison with parallel monolayer cultures. To demonstrate the applicability of EHM for the modeling of "human heart failure in the dish," we introduce a catecholamine overstimulation protocol with outcomes similar to what is typically observed in clinical heart failure. Last, we provide proof-of-concept for the scalability and in vivo applicability of defined EHM as an important step toward clinical translation of tissue-engineered heart repair.

METHODS

Human Pluripotent Stem Cell Lines

We utilized: H9.2¹⁹; HES3 (Embryonic Stem Cell International) including the transgenic derivative HES3-ENVY²⁰; HES2 (Embryonic Stem Cell International) including the transgenic derivative HES2-RFP²¹; H7¹ (WiCell); hiPS-G1 (generated in-house using Sendai Virus reprogramming, Cytotune Kit, Thermo Fisher); hiPS-BJ (Dr Toshiyuki Araki, New York), approved according to the German Stem Cell Act by the Robert-Koch-Institute to W.-H.Z.: permit #12; reference number: 1710-79-1-4-16.

Cardiomyocyte Differentiation and Purification

Differentiated embryoid bodies (H9.2, HES3, HES3-ENVY, HES2, hiPS-BJ) were shipped to Göttingen at room temperature and arrived within 72 to 96 hours. Cardiomyocytes from H7 (L. A. Couture, City of Hope) were shipped at -80°C . Frozen human cardiomyocytes were stored at -152°C . Most experiments were performed with HES2-RFP and hiPS-G1 lines differentiated in monolayers according to Hudson et al²² with modifications. In brief, pluripotent stem cells (PSCs) were plated at 5×10^4 to 1×10^5 cells/cm² on 1:30 Matrigel in phosphate-buffered saline (PBS)-coated plates and cultured in Knockout DMEM, 20% Knock-out Serum Replacement, 2 mmol/L glutamine, 1% nonessential amino acids, 100 U/mL penicillin, and 100 $\mu\text{g}/\text{mL}$ streptomycin (all Life Technologies) mixed 1:1 with irradiated human foreskin fibroblast (HFF)-conditioned medium with 10 ng/mL fibroblast growth factor-2 (FGF2) or TeSR-E8 (STEMCELL Technologies). After 1 day the cells were rinsed with Roswell Park Memorial Institute (RPMI) medium and then treated with RPMI, 2% B27, 200 $\mu\text{mol}/\text{L}$ L-ascorbic acid-2-phosphate sesquimagnesium salt hydrate (Sigma-Aldrich), 9 ng/mL Activin A (R&D Systems), 5 ng/mL BMP4 (R&D Systems), 1 $\mu\text{mol}/\text{L}$ CHIR99021 (Stemgent), and 5 ng/mL FGF-2 (Miltenyi Biotec) for 3 days. Following another wash with RPMI medium, cells were cultured from day 4 to 13

with 5 $\mu\text{mol/L}$ IWP4 (Stemgent) followed by RPMI, 2% B27, 200 $\mu\text{mol/L}$ L-ascorbic acid-2-phosphate sesquimagnesium salt hydrate. Where indicated, cardiomyocytes were metabolically purified by glucose deprivation²³ from day 13 to 17 in RPMI without glucose and glutamine (Biological Industries), 2.2 mmol/L sodium lactate (Sigma-Aldrich), 100 $\mu\text{mol/L}$ β -mercaptoethanol (Sigma-Aldrich), 100 U/mL penicillin, and 100 $\mu\text{g/mL}$ streptomycin. Please refer to [online-only Data Supplement Table 1](#) for an overview of the different cardiac differentiation protocols^{3,17,19,22,24} used in this study.

EHM Generation

An overview of the protocols to generate human EHM is displayed in Table. Details can be found in the [online-only Data Supplement Material](#).

Table. Overview of EHM Protocols

Component	Starting Protocol	Matrix Protocol	Serum-Free Protocol
EHM reconstitution mixture			
Collagen rat (research grade), mg /EHM	0.4		
Collagen bovine (medical grade), mg /EHM		0.4	0.4
Matrigel, %, v/v	10		
Base medium	DMEM	DMEM	RPMI
Horse serum, %	10		
Chick embryo extract, %	2		
Fetal bovine serum, %		20	
B27 (without insulin), %			4
EHM culture medium			
Base medium	Iscove	Iscove	Iscove*
Fetal bovine serum, %	20	20	
B27 (without insulin), %			4
IGF-1, ng/mL			100
FGF-2, ng/mL			10
VEGF ₁₆₅ , ng/mL			5
TGF- β 1, ng/mL			5
Nonessential amino acids, %	1%	1%	1%
Glutamine, mmol/L	2	2	2
Penicillin, U/mL	100	100	100
Streptomycin, $\mu\text{g/mL}$	100	100	100
β -Mercaptoethanol, $\mu\text{mol/L}$	100	100	

DMEM indicates Dulbecco modified Eagle medium; EHM, engineered human myocardium; FGF-2, fibroblast growth factor-2; IGF-1, insulin-like growth factor 1; RPMI, Roswell Park Memorial Institute medium; TGF- β 1, transforming growth factor- β 1; and VEGF₁₆₅, vascular endothelial growth factor 165.

*Alternatively other basal medium with ≥ 1.2 mmol/L calcium.

Analyses of Contractile Function

Contraction experiments were performed under isometric conditions in organ baths at 37°C in gassed (5% CO₂/95% O₂) Tyrode solution (containing: 120 NaCl, 1 MgCl₂, 0.2 CaCl₂, 5.4 KCl, 22.6 NaHCO₃, 4.2 NaH₂PO₄, 5.6 glucose, and 0.56 ascorbate; all in mmol/L). Spontaneous beating frequency was determined at 2 mmol/L calcium after 10 minutes of equilibration of EHMs. EHMs were electrically stimulated at 1.5 to 2 Hz with 5 ms square pulses of 200 mA. EHMs were mechanically stretched at intervals of 125 μm until the maximum systolic force amplitude (force of contraction [FOC]) was observed according to the Frank-Starling law. Responses to increasing extracellular calcium (0.2–4 mmol/L), increasing stimulation frequencies (1, 2, 3 Hz), and adrenergic stimulation with isoprenaline (1 $\mu\text{mol/L}$) followed by functional antagonism by the muscarinic agonist carbachol (10 $\mu\text{mol/L}$) at $\approx\text{EC}_{50}$ calcium of individual EHMs were investigated. Where indicated, an isoprenaline concentration response curve was performed in the presence or absence of specific β_1 -adrenoceptor antagonist CGP-20712A (300 nmol/L, Sigma-Aldrich) or specific β_2 -adrenoceptor antagonist ICI-118551 (50 nmol/L, Sigma-Aldrich). Postrest potentiation was assessed after 2 minutes of stimulation at 1.5 to 2 Hz and pauses of 10 s. The last stimulated beat amplitude was compared with the first stimulated beat amplitude after the pause. Only EHMs without spontaneous contractions during the stimulation pause were included in the analysis.

EHM Heart Failure Model

L-Norepinephrine hydrochloride (NE) and endothelin-1 were prepared in distilled water containing 200 $\mu\text{mol/L}$ L-ascorbic acid-2-phosphate sesquimagnesium salt hydrate (all from Sigma-Aldrich). EHMs were treated with indicated concentrations for 7 days. N-Terminal pro B-type natriuretic peptide was measured by using the Elecsys kit (Roche Diagnostics).

EHM Dissociation

To isolate single cells, EHMs were incubated in collagenase 1 solution (2 mg/mL in calcium-containing PBS in the presence of 20% fetal bovine serum) at 37°C for 60 to 90 minutes. EHM were washed with PBS (without calcium) and further incubated in Accutase (Millipore), 0.0125% Trypsin (Life Technologies), 20 $\mu\text{g/mL}$ DNase (Calbiochem) for 30 minutes at room temperature. Cells were then mechanically separated and transferred into PBS with 5% fetal bovine serum for live cell flow cytometry. To preserve rod-shaped morphology of EHM-derived cardiomyocytes, 30 mmol/L 2,3-butanedione monoxime was added to the collagenase solution, and the final cell suspension was quickly transferred to 4% formaldehyde (Histofix, Roth). EHM-derived cells were spread out on glass slides (Superfrost plus, Menzel-Gläser) in distilled water and air dried.

Human Samples

Human fetal heart tissue (3 biopsies from a single donation) was obtained after elective abortion material (vacuum aspiration) without medical indication following informed consent. The collection of fetal material was approved by the Ethical Committee of the Leiden University Medical Center (MEC-P08.087).

Human heart samples were collected from the left ventricles of nonfailing donor hearts (n=4 donor hearts) not suitable for transplantation as approved by the Ethical Committee of the University Medical Center Göttingen (31/9/00). Gingiva samples were obtained from otherwise healthy donors during elective periodontal surgical treatment as approved by the Ethical Committee of the University Medical Center Göttingen (16/6/09). Cardiac fibroblasts were purchased from Lonza. The study was conducted in accordance with the Declaration of Helsinki by the World Medical Association.

RNA Sequencing

RNA was prepared using Trizol (Life Technologies) following the manufacturer's instruction. RNA integrity was assessed with the Agilent Bioanalyzer 2100. Total RNA was subjected to library preparation (TruSeq Stranded Total RNA Sample Prep Kit from Illumina) and RNA-sequencing on an Illumina HighSeq-2000 platform (SR 50 bp; >25 Mio reads/sample). Sequence images were transformed with the Illumina software BaseCaller to bcl files, which were demultiplexed to fastq files with CASAVA (v1.8.2). Fastq files were mapped to GRCh38/hg38 using STAR 2.4 or TopHat2²⁵ and reads per kilobase of transcript per million (RPKM) were calculated based on the Ensembl transcript length as extracted by biomaRt (v2.24). We only considered protein_coding transcripts for further analysis. Gene ontology analysis was performed through DAVID.²⁶ To determine cardiomyocyte and fibroblast transcriptomes the following algorithm was applied: (1) counts (>10) of purified PSC-derived cardiomyocytes (HES2, iCELL, hiPS-G1; n=3 from each line) and fibroblasts from 3 different sources (heart, skin, gingiva; n=3 from each source) were pooled and the differentially expressed genes ($P < 0.05$, corrected by Benjamini-Hochberg method for multiple testing²⁷) between cardiomyocyte and fibroblast pools determined using edgeR²⁸; (2) log₂ changes of differentially expressed genes were calculated and genes omitted with a log₂ difference lower than mean log₂ of all cardiomyocyte genes; (3) resulting cardiomyocyte- and fibroblast-enriched genes were screened for RPKM values in adult healthy heart and all genes with RPKM <1 in adult heart were omitted.

3D Printing of Flexible Holders for EHM Patches

Flexible holders for the EHM patch construction were printed on a Connex350 (Stratasys) 3D printer using the biocompatible MED610 polymer as stiff base and TangoBlack polymer for the flexible poles. Support material was sprayed off using a Balco Powerblast waterjet. Holders were incubated for 15 minutes in isopropanol to dissolve traces of support material, sprayed again, rinsed, and soaked in water for at least 5 days to bleed out leftovers from the polymerization process. Holders were then sterilized by plasma cleaning for 30 s (Harrick Plasma).

Imaging of EHM Patch Function

For each measurement, plates were recorded inside a 37°C climate chamber for at least 2 minutes at 50 frames per second resolution using a Basler acA2000 8 bit monochrome camera with a Kowa 35-mm lens from ≈45-cm distance. Back light was set to bleach background pixels and facilitate video analysis

by a custom-made Matlab code. The region of interest was manually adjusted to patch size, nonbackground pixels were selected by an intensity cutoff, and the Matlab `imdilate` and `imfill` commands were used to close gaps and fill holes in the tissue leaving pixels belonging to patch and poles white (1) and everything else black (0). The number of white pixels represents the surface area s_a at time t and was converted to fractional area change (FAC) by division through the maximum s_a of a contraction cycle. Contraction peaks, ie, the time points of maximal FAC, were identified automatically; FAC and beating frequency, determined from peak-to-peak intervals, were averaged over 2 minutes.

Implantation of Human Patches

EHM patches were epicardially implanted into immunosuppressed athymic (nude) rats (Charles River) as described previously.¹⁷

Flow Cytometry and Immunofluorescence Staining

Quantitative and qualitative analyses were performed after antibody labeling ([online-only Data Supplement Table II](#)) as described previously.²⁹

Statistical Analyses

Data are presented as mean±standard error of the mean. Statistical differences between 2 groups were tested by 2-sided unpaired or paired Student *t* tests. In case of ≥3 groups, 1-way or 2-way unpaired or repeated-measures ANOVA with appropriate post hoc testing was performed. The performed tests are specified in the respective figure legends. Statistical testing was performed with GraphPad Prism 6.

Additional methods are described in the [online-only Data Supplement Material](#).

RESULTS

Definition of Cell Composition in EHM

EHM formation comprises 2 macroscopically distinguishable phases (Figure 1A): (1) EHM consolidation in casting molds with an onset of spontaneous beating in variably sized areas within 24 hours, and (2) EHM maturation with coordinated and rhythmic contractions of the whole tissue after 3 days and onward ([online-only Data Supplement Movie I](#)). In pilot experiments, we defined 1.5×10^6 ESC (H9.2 and HES3)-derived cardiomyocytes suspended in 500-μL collagen type I/Matrigel hydrogels as the optimal condition for the construction of force-generating EHM ([online-only Data Supplement Table I](#)).

Using HES2 and hiPSC-BJ cardiac differentiation cultures with different cardiomyocyte content, we found that EHM containing a cardiomyocyte:nonmyocyte composition of 1:1 at the time of force assessment developed maximal contractile forces (Figure 1B). This was in agreement with recent reports¹⁵ and our own experience in rodent models³¹ on the critical role of

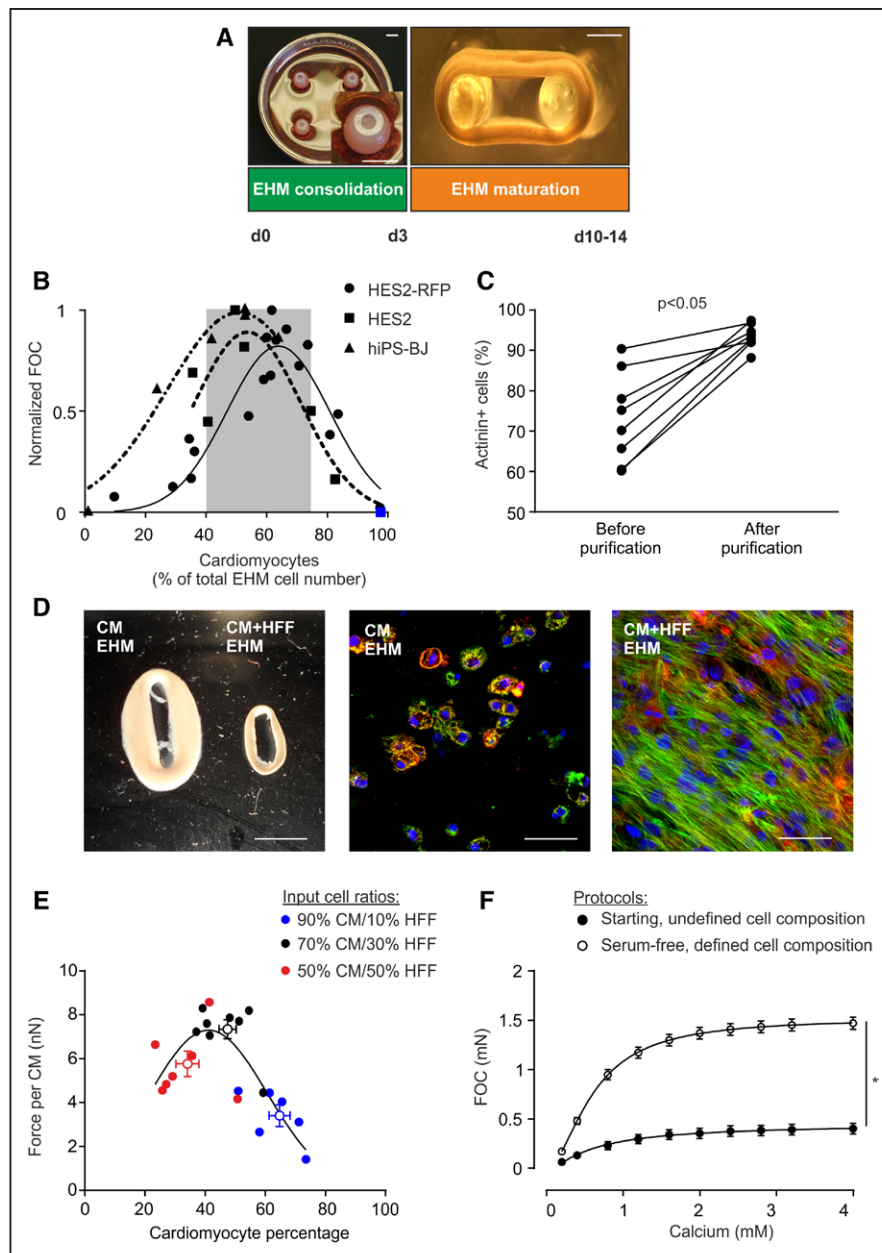


Figure 1. Defining human EHM.

A, EHM generation is characterized by 2 phases: EHM consolidation for 3 days (**Left**, casting mold with 4 EHMs; **Inset**, magnification of EHM in mold) and EHM maturation for at least 7 days under mechanical load (**Right**, EHM on flexible PDMS holders). Bars: 5 mm (**Left**), 1 mm (**Right**). **B**, Force of contraction (FOC; normalized to maximal FOC) in relation to output cardiomyocyte percentage (actinin⁺ cells) of EHM made from HES2-RFP, HES2, and hiPS-BJ lines. Blue square indicates an EHM sample constructed from SIRPA2A-selected³⁰ cardiomyocytes. Gray area indicates optimal cardiomyocyte percentage across indicated lines (mean±SD). **C**, Purification of cardiomyocytes for defined EHM generation. Quantification of cardiomyocyte purity (actinin⁺ cells) before and after enrichment by metabolic selection; n=8, $P<0.05$ by 2-tailed, paired Student *t* test. **D**, Macroscopic appearance of EHM with >92% CM (CM EHM) and EHM with >92% CM supplemented with HFF (70:30% CM+HFF EHM). Immunostaining for actinin (green), f-actin (red), and nuclei (blue) in CM EHM (**Middle**) and CM+HFF EHM (**Right**). Bars: 5 mm (**Left**), 50 μm (**Middle** and **Right**). **E**, Titration of the optimal CM:HFF ratio. Output CM percentage and force per CM in 2-week-old EHM made with indicated input cell ratios of purified CMs and HFFs. Colors indicate the input CM:HFF ratio of respective EHMs (each circle represents one individual EHM with an additional empty circle indicating the mean±SEM of the respective groups). **F**, Force of contraction (FOC) recorded under increasing calcium concentrations and electric stimulation at 1.5 Hz in 4-week EHMs constructed according to the undefined Starting Protocol (n=19; Table) and defined, Serum-free Protocol (n=59; Table); pooled data from EHM generated from different ESC and iPSC lines (please refer also to [online-only Data Supplement Figure IV](#) for detailed information); * $P<0.05$ by 2-way ANOVA with the Tukey multiple comparisons post hoc test. ANOVA indicates analysis of variance; CM, cardiomyocyte; EHM, engineered human myocardium; ESC, embryonic stem cell; HFF, human foreskin fibroblast; iPSC, induced pluripotent stem cell; and SEM, standard error of the mean.

nonmyocytes for the engineering of force-generating myocardium. We next formally tested the effect of the cardiomyocyte:nonmyocyte ratio by using metabolic selection²³ for cardiomyocyte purification (Figure 1C) and HFFs; EHM constructed directly from enriched cardiomyocyte populations did not condense and contained mostly rounded cardiomyocytes (Figure 1D; [online-only Data Supplement Movie II](#)). The addition of HFFs at a 70%/30% cardiomyocyte/fibroblast input ratio was optimal for the construction of force-generating EHM loops with a cardiomyocyte:fibroblast output ratio of $\approx 1:1$ (Figure 1E), confirming our initial findings (Figure 1B).

By defining the nonmyocyte input, we observed advanced cardiomyocyte maturation with reduced variability in the functional maturation of EHM ([online-only Data Supplement Figure IA](#)) and a higher mean actinin fluorescence intensity per cell, indicating higher sarcomeric protein content per individual cardiomyocyte ([online-only Data Supplement Figure IB](#)). Furthermore, the classical inotropic and lusitropic (relaxation) responses to isoprenaline were enhanced in defined EHM ([online-only Data Supplement Figure IC](#)). The number of immature ventricular cardiomyocytes (defined by simultaneous expression of MLC2A and MLC2V) was greatly reduced by EHM culture with more pronounced ventricular maturation in defined EHM ([online-only Data Supplement Figure ID and IE](#)). Defining the nonmyocyte population in EHM not only reduced intraline ([online-only Data Supplement Figure IA](#)), but also interline variability ([online-only Data Supplement Figure IF](#)). Moreover, expression of pluripotency-associated genes and cell cycle activity in cardiomyocytes and nonmyocytes were markedly reduced in defined EHM ([online-only Data Supplement Figure II](#)). Taken together, we conclude that defining the nonmyocyte cell fraction increases the robustness of the EHM protocol also with respect to its organotypic contractile function and ventricular fate.

Development of a Defined, Serum-Free EHM Construction Protocol Toward Current Good Manufacturing Practice

The EHM Starting Protocol, which was devised from our original rodent tissue engineering protocol,²⁹ included a variety of undefined matrix (Matrigel) and serum (horse serum, fetal calf serum, chick embryo extract) components (Table). We first defined the matrix components and observed that EHM could be constructed from medical-grade bovine collagen without Matrigel (Matrix Protocol), without any reduction in functionality ([online-only Data Supplement Figure IIIA and IIIB](#)). The addition of laminin (5 $\mu\text{g}/\text{EHM}$) or fibronectin (5 $\mu\text{g}/\text{EHM}$) to the Matrix Protocol did not further improve EHM function ([online-only Data Supplement Figure IIIC](#)). Factorial screens, including the assessment of the B27 supplement, were performed next with the aim to replace all animal culture

medium components. To expedite the initial screens, we used simple HES2-cardiomyocyte aggregate cultures ([online-only Data Supplement Figure IIID](#)) and subsequently tested putative cardio-instructive factors in EHM. We first selected a particular B27 medium supplementation (4% with insulin) based on cell viability. We subsequently selected growth factors (FGF-2, insulin-like growth factor 1 [IGF-1], transforming growth factor- $\beta 1$ [TGF- $\beta 1$], vascular endothelial growth factor 165 [VEGF₁₆₅]) for EHM testing according to the following criteria: (1) neutral or enhanced cell viability, and (2) enhanced cardiomyocyte actinin content or cardiomyocyte size. Last, we confirmed that the combination of FGF-2, IGF-1, TGF- $\beta 1$, and VEGF₁₆₅ was maximally effective in supporting the formation of force-generating EHMs ([online-only Data Supplement Figure IIIE](#)). In agreement with the important role of extracellular matrix remodeling in early EHM cultures,²⁹ we found that TGF- $\beta 1$ treatment in the consolidation phase (day 0–3) was necessary for enhanced EHM function ([online-only Data Supplement Figure IIIE](#)). It is interesting to note that we observed that antioxidants were not critical for EHM function and that omitting insulin (B27 minus insulin) enhanced EHM function in comparison with insulin-containing B27 ([online-only Data Supplement Figure IIIF](#)). This led to the definition of a minimal Serum-free Protocol containing 4% B27 without insulin plus TGF- $\beta 1$, IGF-1, FGF-2, VEGF₁₆₅ (Table). Last, testing of the basal media identified calcium supplementation to physiological concentrations (1.2 mmol/L) as a critical parameter for optimal outcome ([online-only Data Supplement Figure IIIG](#)). Collectively, these experiments established a defined, Serum-free Protocol with markedly enhanced contractile performance in comparison with the undefined Starting Protocol (Figure 1F; [online-only Data Supplement Movie III](#)) and applicability to various ESC- and iPSC-EHM models ([online-only Data Supplement Figure IV](#)).

Evidence for Structural and Functional Maturation of EHMs

We next investigated whether the defined, Serum-free Protocol supports EHM maturation. Enzymatic dispersion of EHMs revealed cardiomyocytes with an elongated phenotype with sarcomeres in registry (Figure 2A, [online-only Data Supplement Figure VA](#)). In comparison with serum-containing EHM cultures and in line with the functional outcome (Figure 1F), intact rod-shaped cardiomyocytes from EHMs constructed according to the Serum-free Protocol presented with a larger volume ($12\,101 \pm 1\,240$ versus $5\,649 \pm 1\,410 \mu\text{m}^3$), but similar aspect ratio (7.6 ± 0.4 versus 6.7 ± 0.9 ; $n=28/10$). In comparison with 2D monolayer cardiomyocyte cultures and EHM constructed according to the Starting Protocol, sarcomere size was larger in EHM constructed according to the defined, Serum-free Protocol (1.93 ± 0.01 versus 1.81 ± 0.01 ver-

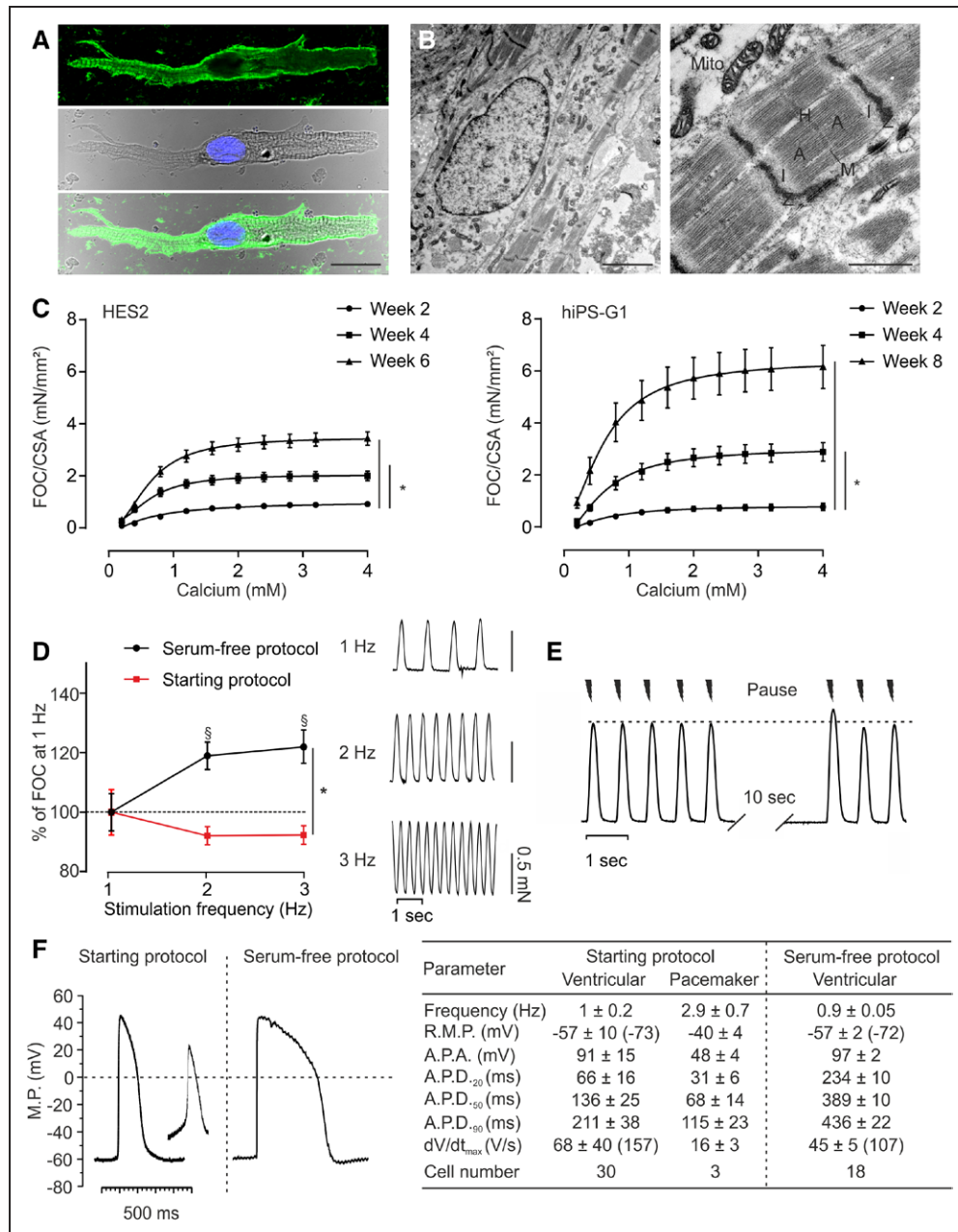


Figure 2. Morphological and functional maturation of EHM.

A, Immunostaining of isolated cardiomyocyte from 4-week EHM (hiPS-G1). **Top**, myosin heavy chain (green); **Middle**, brightfield image with nucleus labeled with Hoechst (blue); **Bottom**, overlay; bar: 20 μ m). **B**, Electron micrographs of 4-week EHMs (hiPS-G1), low-power (**Left**, bar: 2.5 μ m) and high-power magnification (**Right**, characteristic sarcomere structures are labeled; Mito, mitochondria; bar: 1 μ m). **C**, FOC per cross-sectional area (CSA) of serum-free EHM from HES2 and hiPS-G1 at the indicated time points in culture; n=12/14/8 for weeks 2/4/6 in HES2 EHM and n=7/10/8 for weeks 2/4/8 in hiPS-G1 EHM **P*<0.05 by 2-way ANOVA with the Tukey multiple comparison post hoc test. **D**, Force-frequency response of hiPS-G1-EHM (at 4 weeks in culture) generated according to the Starting Protocol (red; n=8) and defined, Serum-free Protocol (black; n=21). [§]*P*<0.05 versus 1 Hz of the respective group by 2-way ANOVA with the Tukey multiple comparison post hoc test; **P*<0.05 by 2-way repeated measures ANOVA followed by the Sidak multiple comparison test. **E**, Representative force traces recorded from hiPS-G1-EHM (at 4 weeks in culture) at 1.5-Hz stimulation with an intermittent stimulation pause (10 s); enhanced FOC at the reintroduction of electric stimulation, ie, postrest potentiation, is characteristic for cardiomyocytes with mature intracellular calcium storage and release (the dotted line marks prepause baseline maximal FOC). **F**, Representative action potentials recorded by impaling electrode measurements in EHM developed under the Starting Protocol (HES3) and the Serum-free Protocol (HES2); the table summarizes data recorded from together 51 independent action potential recordings; values in parentheses indicate maximally negative RMP and fastest dV/dt_{max} recorded in the respective groups. ANOVA indicates analysis of variance; APA, action potential amplitude; APD, action potential duration; EHM, engineered human myocardium; MP, membrane potential; and RMP, resting membrane potential.

mus $1.84 \pm 0.01 \mu\text{m}$; >120 sarcomeres were analysed in 12/8/10 cardiomyocytes in the respective groups. The low cardiomyocyte volume ($20\,000\text{--}35\,000 \mu\text{m}^3$ reported in adult human cardiomyocytes³²) was mainly attributable to a smaller cell width in EHM (width: 13 ± 0.5 versus $20\text{--}35 \mu\text{m}$; length: 92 ± 4 versus $60\text{--}150 \mu\text{m}$ in adult human cardiomyocytes^{32,33}). Note that cardiomyocytes in EHM exhibited a similar width as observed in 6-week-old infant heart ($4\text{--}12 \mu\text{m}$ ³³). Ultrastructural analyses revealed that cardiomyocytes in EHM displayed a remarkable degree of sarcomere organization with clearly distinguishable Z, I, A, H, and M bands (Figure 2B, [online-only Data Supplement Figure IVB](#)). Consistent with earlier reports on largely absent M bands, even in extended stem cell-derived cardiomyocyte monolayer cultures³⁴ and tissue-engineered models,^{11–13,15} we found little organization of M bands in monolayer cardiomyocytes, but a high degree of organization in EHM-derived cardiomyocytes ([online-only Data Supplement Figure IVC](#)). Also, enhanced MLC2V organization and presence of n-cadherin⁺ intercalated disk-like structures were observed in EHM cardiomyocytes ([online-only Data Supplement Figure IVB and IVC](#)).

Functional maturation was a continuous process with enhanced inotropic responses to calcium in older EHM (Figure 2C); this was despite similar cardiomyocyte content ([online-only Data Supplement Figure VIA](#)). Because EHM cross-sectional area decreased over time in culture ([online-only Data Supplement Figure VIB](#)), we opted to correct FOC by cross-sectional area to allow a direct comparison of the different models (HES and iPSC) and their developmental stages (Figure 2C); uncorrected FOC is displayed in [online-only Data Supplement Figure VIC](#)). The average maximal FOC developed by EHM after 8 weeks in culture ($6.2 \pm 0.8 \text{ mN/mm}^2$ at 1.5 Hz; $n=8$) exceeded the reported FOC ($\approx 1 \text{ mN/mm}^2$ at 1 Hz) in papillary muscle from human infants (3–14 months after birth)³⁵ markedly, but remained lower than the FOC recorded in adult non-failing myocardium ($\approx 25 \text{ mN/mm}^2$ at ≈ 1.5 Hz).³⁶ It is interesting to note that a positive force-frequency behavior (Bowditch phenomenon), which is absent in newborns and present in infants,³⁵ was clearly developed in defined, serum-free EHM ($+19 \pm 5\%$ at 2 Hz, $+22 \pm 6\%$ at 3 Hz versus 1 Hz, studied at 4 weeks) in contrast to EHM constructed according to the undefined Starting Protocol (Figure 2D). In agreement with this finding, postrest potentiation (enhanced FOC by $+9 \pm 1\%$ [$n=7$] in the first electrically stimulated beat after a stimulation pause) was observed, providing evidence for intracellular calcium storage and release by the sarcoplasmic reticulum (Figure 2E).

Electrophysiological studies revealed that EHMs comprised mainly working myocardium-like cells without pronounced spontaneous phase 4 depolarization (Figure 2F). This suggests that the spontaneous contractions of EHM are under the control of a small portion of pacemaker cells in EHM ($<10\%$ of all cells analyzed).

Molecular Maturation of EHM

We next sought to use an unbiased approach to determine whether signs of molecular maturation could be identified inline with the observed structural and functional maturation of EHM. Hence, we first determined the differential transcriptome in high purity ($94 \pm 2\%$ ACTN2⁺ by flow cytometry, $n=9$) PSC-derived cardiomyocytes ($n=777$ transcripts; HES2, hiPS-G1, hiPS-CDI; each $n=3$) and fibroblasts ($n=200$ transcripts; skin-, gingiva-, heart-derived fibroblasts; each $n=3$) by RNA sequencing (Figure 3A). As anticipated cardiomyocyte, the cardiomyocyte (CM) transcriptome was highly enriched for sarcomeric transcripts, and the fibroblast transcriptome was enriched for transcripts encoding for extracellular matrix-associated proteins and proteins mediating cell-cell or cell-matrix interactions (Figure 3B, refer to [online-only Data Supplement Tables III and IV](#) for a full list of the identified CM and fibroblast transcriptomes including a comparison with fetal and adult heart expression levels).

We next used the CM transcriptome to establish a temporal gene expression profile from embryonic to adult heart, taking embryonic CMs (22-day-old monolayer HES2 CM, $n=3$), fetal heart ($n=3$), and adult heart ($n=4$) as reference time points. We classified 3 gene clusters: (1) genes with continuous increase (adult CM genes; $n=218$; Figure 3C, upper box), (2) genes with continuous decrease (embryonic CM genes; $n=128$; Figure 3C, lower box), and (3) genes without clear trajectory ($n=431$) in expression (refer to [online-only Data Supplement Table V](#) for a full list of genes in each of the 3 clusters). Transcriptional profiling revealed that transcription of 174 and 110 of the adult CM genes was enhanced and transcription of 94 and 72 of the embryonic CM genes was reduced in parallel EHM (6 weeks) and 2D (60 days) cultures, respectively. Direct comparison of the CM maturation gene transcripts (embryonic plus adult CM genes; $n=346$) showed higher frequencies of fetal-adult gene expression levels in EHM, indicating enhanced molecular maturation in EHM versus 2D (Figure 3D). In comparison with 2D cultures, but also with undefined EHM cultures, a significant upregulation of pivotal CM genes involved in “ventricular cardiac muscle tissue morphogenesis” (gene ontology:0055010) further confirmed the cardiotypic development and a high degree of maturation in EHM constructed according to the defined, Serum-free Protocol (Figure 3E, [online-only Data Supplement Figure VII](#)).

Simulation of Heart Failure in EHM by Neurohumoral Overstimulation

The sympathetic nerve system controls heart function via the release of catecholamines and subsequent adrenoceptor activation. Experimentally, acute addition of isoprenaline (β_1 - and β_2 -adrenoceptor agonist) is used

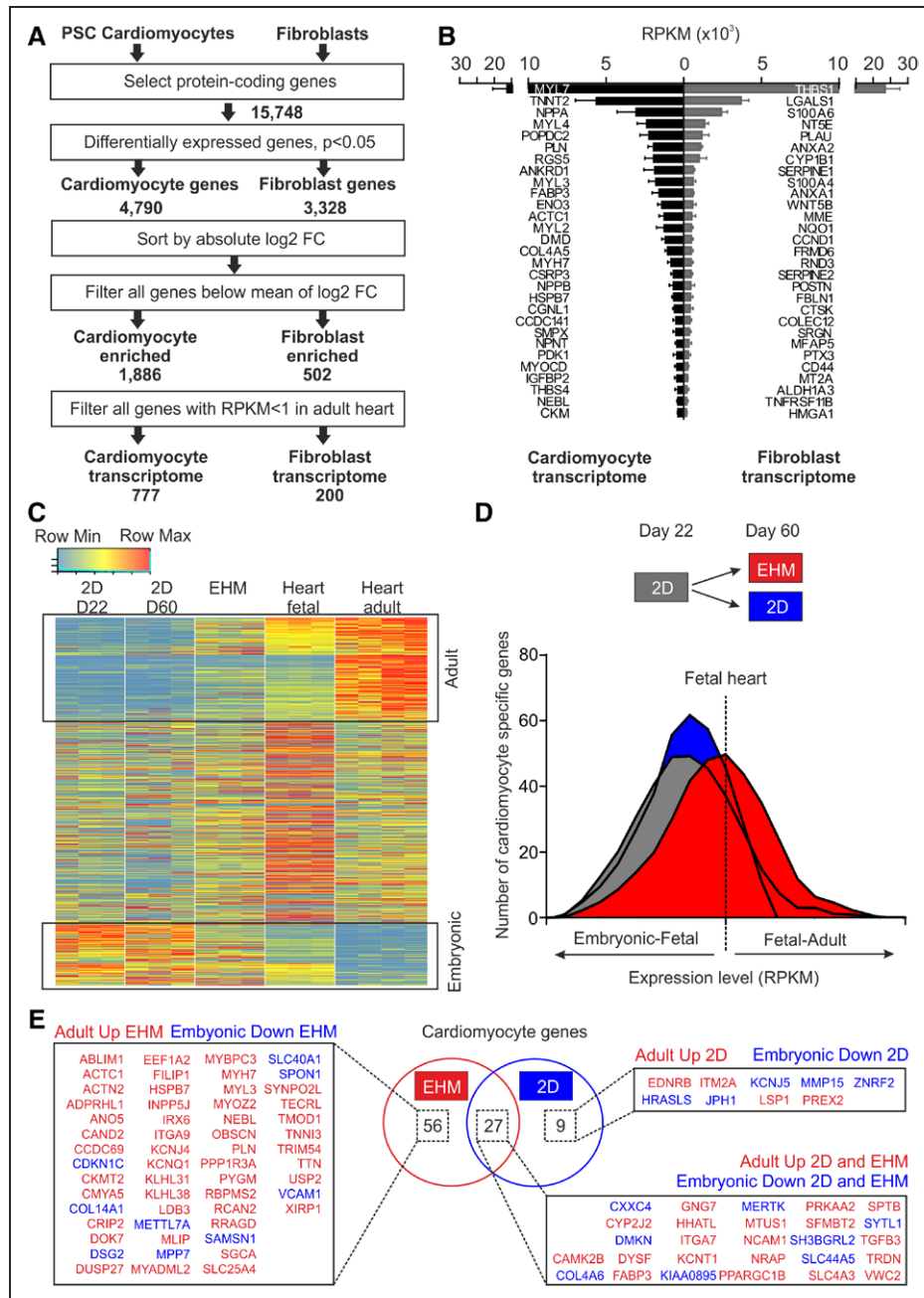


Figure 3. Molecular maturation of serum-free EHM.

A, Strategy to determine cardiomyocyte and fibroblast transcriptomes from RNAseq data obtained from purified pluripotent stem cell-derived (PSC) cardiomyocytes ($n=3$ hES2 RFP, $n=3$ iCell CM, $n=3$ hiPS-G1) and primary fibroblasts ($n=3$ HFF, $n=3$ human cardiac fibroblasts, $n=3$ human gingiva fibroblasts). **B**, RPKM values of the 29 most abundantly expressed transcripts in PSC-derived cardiomyocytes and primary fibroblasts. **C**, Heatmap of cardiomyocyte transcripts in 22-day-old cardiomyocyte monolayer cultures (2D D22), 60-day-old cardiomyocyte monolayer cultures (2D D60), 6-week-old EHMs (note that cardiomyocyte age in these EHMs was similar to 2D D60 cultures), fetal heart, and adult heart. Boxed areas indicate cardiomyocyte maturation genes; adult, increasing expression with development (upper box), and embryonic, decreasing expression with development (lower box). **D**, Histogram of cardiomyocyte gene expression level (RPKM) in comparison with fetal heart as reference. Comparison of 22-day-old cardiomyocyte monolayer cultures (2D, gray box) as starting point, 60-day-old cardiomyocyte monolayer cultures (2D, blue box), and 6-week EHM cultures (red box). **E**, Venn diagram and corresponding list of differentially expressed cardiomyocyte maturation genes with specific regulation in EHM, 60-day-old cardiomyocyte monolayer cultures (2D), or both (overlap in Venn diagram; $P < 0.05$ corrected for multiple testing by Benjamini-Hochberg method). CM indicates cardiomyocyte; EHM, engineered human myocardium; FC, fold change; HFF, human foreskin fibroblast; and RPKM, reads per kilobase of transcript per million.

to simulate organotypic responses to catecholamine stimulation, including enhanced force development (inotropy), beating frequency (chronotropy), and relaxation (lusitropy); chronic application of norepinephrin (NE; α_1 -, α_2 -, β_1 - > β_2 -adrenoceptor agonist) is classically used to induce pathological CM hypertrophy.

Although effects on chronotropy have been well established in human PSC-derived CMs, so far, there is little evidence for regular inotropic responses,^{11,13,15} suggesting functional immaturity of the β -adrenergic signaling cascade. Transcriptome analyses revealed lower transcript abundance for most adrenergic receptors, including, in particular, the β_1 (*ADRB1*)- and β_2 (*ADRB2*)-adrenoceptors, in EHM versus adult myocardium (online-only Data Supplement Figure VIII A). Irrespective of the transcript levels, we observed a robust inotropic response of EHM to isoprenaline, which was significantly enhanced in serum-free versus serum-containing cultures (online-only Data Supplement Figure VIII B and VIII C). It is interesting to note that EHM displayed a similar sensitivity (EC_{50} : 10 ± 1 nmol/L; online-only Data Supplement Figure VIII D) to isoprenaline as that reported for nonfailing myocardium.³⁷ Classical pharmacological β_1 - and β_2 -adrenoceptor blocking experiments with CGP-20712A and ICI-118551, respectively, revealed that $32 \pm 6\%$ of the acute inotropic effect in EHM were mediated via *ADRB1* (online-only Data Supplement Figure VIII E).

Chronic catecholamine overstimulation (serum levels in patients with heart failure: 1–10 nmol/L NE) contributes to heart failure development and progression.³⁸ In iPSC models, results have been variable with recent reports demonstrating the need for defined media to elicit CM hypertrophy.³⁹ We asked whether EHMs would exhibit the clinically observed heart failure phenotype, including β -adrenergic desensitization, CM hypertrophy, and the release of biomarkers (such as brain natriuretic peptide⁴⁰). To recapitulate sympathetic overstimulation, we exposed EHM to NE at clinically relevant concentrations (0.001–1 μ mol/L) for 7 days. We also included a group of EHMs exposed to endothelin-1 (0.01 μ mol/L), a well-established inducer of CM hypertrophy via the alternative Gq-protein transduction pathway.⁴¹ Similarly as observed in patients, chronic NE stimulation induced contractile dysfunction in a concentration-dependent manner (Figure 4A) with desensitization to acute β -adrenergic stimulation (Figure 4B), which, according to its underlying mechanism, only occurred under NE and not endothelin-1. To enable a cell type-specific analysis of cell size and cell composition, we developed a color-coded EHM model comprising RFP⁺-CMs and GFP⁺-fibroblasts amenable to flow cytometry analyses (Figure 4C, online-only Data Supplement Movie IV). This allowed us to confirm enhanced CM hypertrophy (Figure 4D, online-only Data Supplement Figure IX) and death (Figure 4E) in response to increasing NE concentrations. We also

found the clinically relevant biomarker N-terminal pro B-type natriuretic peptide released in a concentration-dependent manner (Figure 4F) and a blunted force-frequency response in serum-free, but not serum-containing EHM (online-only Data Supplement Figure XA). A consistent observation was that the pathological phenotype was, in general, more pronounced in serum-free EHM (summarized in online-only Data Supplement Figure XB) with a significantly reduced hypertrophic response in serum-containing EHM. This finding is consistent with earlier data on the hypertrophy-masking effects of serum in human PSC-derived CMs.³⁹ It is notable that the pathological phenotype could be partially or fully prevented by β_1 -adrenoceptor and α_1 -adrenoceptor blockade with metoprolol and phenoxybenzamine, respectively, demonstrating the applicability of EHM in the in vitro simulation of heart failure and its prevention by pharmacological means (Figure 4G).

Scaling of EHM for Heart Repair

Remuscularization of myocardial scar tissue in the failing heart will require sizable muscle surrogates. Accordingly, we tested whether large EHM can be engineered under the defined, Serum-free EHM Protocol. We also reasoned that casting patches rather than loops would facilitate scaling toward clinical needs. Accordingly, we developed stamps with flexible tips by 3D printing for the penetration of EHM mixtures cast into a size-adapted mold (Figure 5A). This allowed us to scale EHM patches variably, reaching sizes for clinical translation (15×17 mm and 35×34 mm containing 10×10^6 and 40×10^6 CMs respectively; thickness: 0.5 ± 0.1 mm, $n=5$; Figure 5B and 5C). Cells in EHM patches were homogeneously distributed and structurally organized along traction force lines (Figure 5C). It is important to note that EHM patches and loops contracted similarly (online-only Data Supplement Movie V). Because nondisruptive measurements will finally be essential to document EHM patch quality, we developed an optical force assessment strategy by correlating FOC recorded in individual EHM loops with FAC in EHM patches from the same production runs. This analysis revealed a correlation of FOC and FAC recorded in EHM loops and patches, respectively (online-only Data Supplement Figure XI); further refinement of this measure will be required to account for homogeneity, shape, and force distribution of the different culture formats.

In continuation of a recently completed experimental series for the assessment of feasibility and safety of EHM grafting,¹⁷ we now tested whether EHM patches would be retained after engraftment. In line with our recent study with EHM loops, we could demonstrate that EHM patches formed sizable and structurally highly developed grafts in RNU rats (Figure 5D through 5F), which were progressively vascularized (Figure 5G).

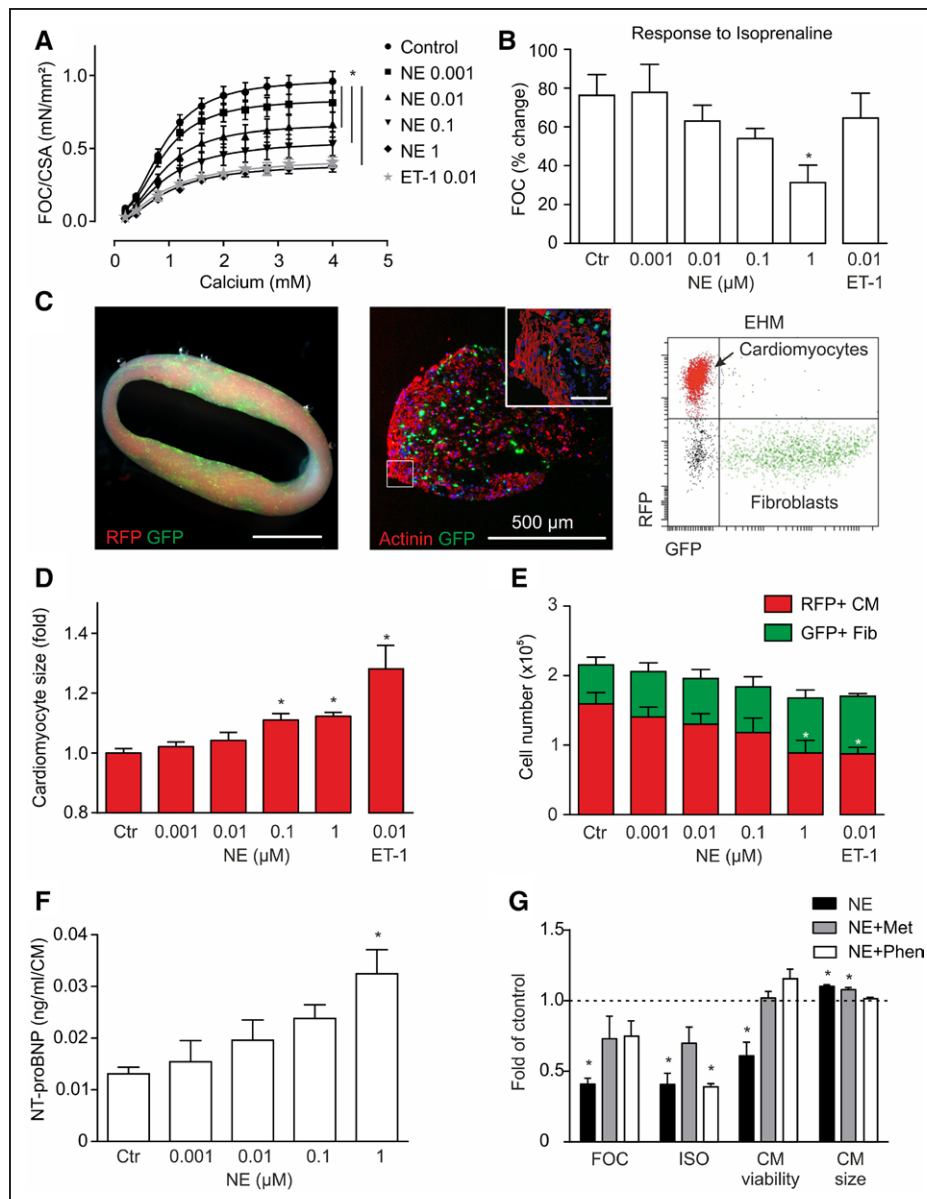


Figure 4. Modeling heart failure in color-coded EHM.

A, Effect of 7-day treatment with indicated concentrations (in $\mu\text{mol/L}$) of norepinephrine (NE) or endothelin-1 (ET-1) on FOC of EHM; $*P < 0.05$ versus Control by 2-way ANOVA with the Tukey multiple comparison post hoc test, $n = 8$ to 10 per Control and NE groups, $n = 4$ for ET-1 group. **B**, Inotropic response to acute isoprenaline (ISO) stimulation in EHM previously exposed to 7-day NE or ET-1 at the indicated concentrations (same EHM as in **A**); $*P < 0.05$ versus Control (Ctr) by 1-way ANOVA with the Tukey multiple comparison post hoc test. **C, Left**, Macroscopic view of color-coded EHM (RFP+CM: red, GFP+Fib: green); scale bar: 1 cm. **Middle**, Cross section of color-coded EHM (red: actinin+CM, green: GFP+Fib); scale bar: 500 μm ; **Inset**, magnification, scale bar: 50 μm . **Right**, Flow cytometry of RFP+CM and GFP+Fib after enzymatic dispersion of color-coded EHM. **D**, CM size measured by determination of RFP median fluorescence intensity (MFI, please refer to [online-only Supplement Figure IX](#) for experimental details); $*P < 0.05$ versus Ctr by 1-way ANOVA with the Tukey multiple comparison post hoc test. **E**, Cell type distribution in color-coded EHM assessed by total cell quantification after enzymatic dispersion and subsequent flow cytometry for the separation of RFP+CM and GFP+Fib (from same EHM as in **A**); $*P < 0.05$ for cardiomyocyte number versus Ctr by 1-way ANOVA with the Tukey multiple comparison post hoc test. **F**, NT-proBNP secretion per CM into the culture medium ($n = 3/\text{group}$). **G**, Maximal FOC, response to ISO, CM viability, and CM size in comparison with control (dashed line) in EHM treated with 1 $\mu\text{mol/L}$ NE with and without preincubation with 5 $\mu\text{mol/L}$ metoprolol (Met) or 5 $\mu\text{mol/L}$ phenoxybenzamine (Phen); $*P < 0.05$ versus Ctr by 1-way ANOVA with the Tukey multiple comparison post hoc test ($n = 4$ –10/group). ANOVA indicates analysis of variance; CM, cardiomyocyte; EHM, engineered human myocardium; Fib, fibroblast; FOC, force of contraction; and NT-proBNP, N-terminal pro B-type natriuretic peptide.

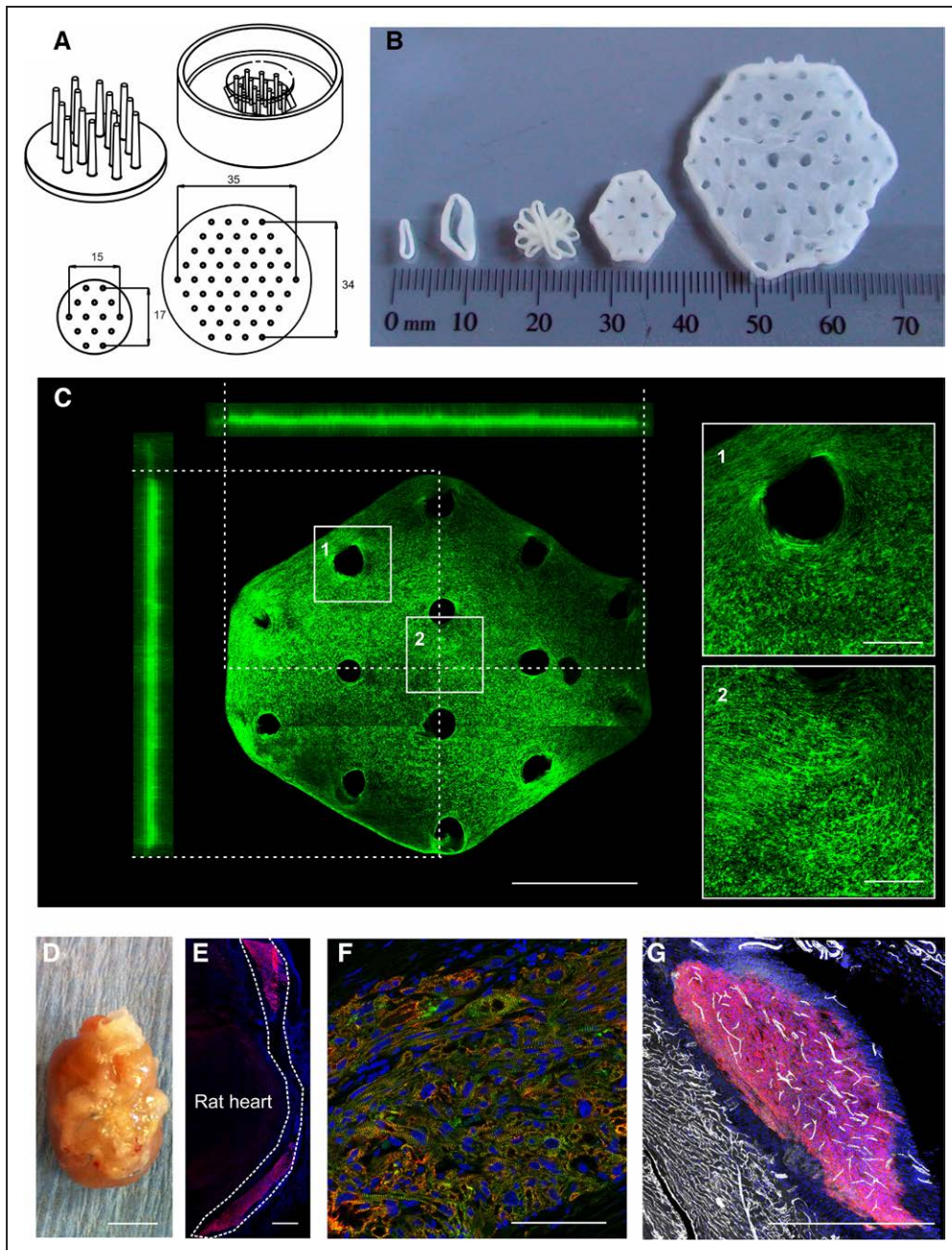


Figure 5. Scaling of EHM for heart repair.

A, Technical drawings of the EHM patch manufacturing devices: **Top left**, 3D-printed patch holder with flexible poles; **Top right**, inverted patch holder positioned in hexagonal casting mold; **Bottom**, top view on patch holder for small and large EHM patch with dimensions in millimeters. **B**, Display of different EHM designs (from left to right): small (1.5×10^6 cells/500 μ L) and big (2.5×10^6 cells/900 μ L) loops, fusion of 5 big loops according to technology reported earlier for rat,⁴² small (10×10^6 cells/2 mL) and clinical-sized large (40×10^6 cells/8 mL) patch. **C**, Overview and 90° projections of an immunostained (f-actin in green) small EHM patch (image stitched together from $24 \times 850 \times 850$ μ m tiles); boxed areas magnified on right for a demonstration of cell orientation. Bars: 5 mm (overview) and 1 mm (magnifications). **D**, Explanted rat heart 4 weeks after epicardial implantation of an EHM patch in a RNU rat; bar: 1 cm. **E**, Overview of human EHM on rat heart, immunostaining of human MYH7 (red), dashed line outlines the human EHM; bar: 500 μ m. **F**, Immunostaining of human EHM 107 days after implantation, cardiac troponin T (red), sarcomeric actinin (green), nuclei (blue); bar: 100 μ m. **G**, Immunostaining of CD31 (white) and human specific β 1-integrin (red); bar: 500 μ m. EHM indicates engineered human myocardium.

DISCUSSION

Our study demonstrates that differentiated, force-generating human heart muscle can be generated *in vitro* under defined, serum-free conditions for applications in heart failure modeling and tissue-engineered heart repair. While the definition of cell composition and culture conditions reduced variability and procedural complexity, it also supported CM structural and functional maturation beyond the current state-of-the-art. The reported protocol is adaptable to current good manufacturing practice and thus serves as the basis for highly standardized *in vitro* assay development and clinical translation of tissue-engineered heart repair.

A number of factors have been previously identified to support maturation of human CMs in tissue-engineered heart muscle, such as mechanical stimulation¹³ and electric stimulation,¹² and the coculture of CMs and fibroblasts, as well.¹⁵ In this study, we systematically screened culture conditions and identified the minimal requirements for EHM formations under highly defined conditions (Table: Serum-free Protocol). So far unrecognized were the need for an adaptation of extracellular calcium to physiological levels (1.2 mmol/L) and supplementation of TGF β -1 during EHM consolidation. The requirement for calcium adaptations was identified serendipitously while testing different basal media with normal and reduced (RPMI 0.42 mmol/L) calcium. This observation is in agreement with the previously reported essential role of calcium for myofibrillogenesis in the mouse.⁴³ The mode of action of TGF β -1 during EHM consolidation appears to be enhanced fibroblast-mediated extracellular matrix remodeling, which was found earlier to be crucial in rodent EHM models.²⁹ Last, addition of IGF-1, FGF-2, VEGF,¹⁶⁵ and B27 without insulin were sufficient to replace all serum supplements. The use of clinical grade bovine collagen instead of the widely used Matrigel supplemented hydrogels⁴⁴ further assisted in defining culture conditions.

Using our highly defined EHM protocol, we observed advanced structural, functional, and molecular maturation of CMs. In fact, to our knowledge, the following maturation characteristics have not been reported so far: (1) structural maturation with a rod-shaped CM morphology and sarcomers with distinguishable M bands; both parameters are rarely observed even in extended (1-year) monolayer cultures⁴⁵; (2) dominant ventricular structural and functional maturation evidenced by abundant Myl2 (MLC2V) positivity and characteristic action potential kinetics; and (3) functional maturation with contractile forces and physiological responses such as a positive force-frequency behavior observed only in postnatal myocardium.^{35,46} Although functional β_1 -adrenergic signaling is minute in immature PSC-derived CMs,⁴⁷ defined EHM displayed a robust β_1 -mediated inotropic response. The cardiotoxic effect of elevated norepinephrine levels

further argues for relevant adrenergic signaling to model disease mechanisms of heart failure. Consistent with recent work, the biomechanical stimulation of EHM may accelerate β -adrenergic maturation in comparison with monolayer CMs.⁴⁷ Spontaneous contractions of EHM require specialized pacemaker cells. Random impalements with sharp electrodes for AP recordings did not identify bona fide pacemaker cells in defined, serum-free EHM. Optical imaging after loading with voltage-sensitive dyes or the use of genetically encoded voltage sensors⁴⁸ may help to better localize regions with pacemaker activity and guide detailed electrophysiological studies to define the underlying mechanisms of EHM automaticity.

Transcriptional profiling in 6-week EHM was in agreement with the structural and functional data, confirming an advanced degree of maturation in comparison with parallel monolayer cultures. However, reaching a fully adult phenotype remains a challenging task. In fact, unbiased global transcriptome profiling suggested that EHMs are, at large, similar to fetal human heart at 13 weeks of gestation, despite some morphological (M bands) and functional (Bowditch phenomenon) properties that develop postnatally. This suggests, on the one hand, that our defined, serum-free EHM protocol supports bona fide heart development in the dish to a notable extent, and, on the other hand, introduces an unbiased approach for the benchmarking of tissue-engineered myocardium.

Taken together, we conclude that the serum-free EHM protocol can serve as the foundation for the definition of specific biological, pharmacological, or biophysical interventions controlling heart development. Whether *in vitro* interventions will finally enable the speeding up of heart development in a dish beyond the pace of natural cardiomyogenesis remains to be elucidated. The principle propensity for advanced maturation was further supported by long-term *in vitro* culture and *in vivo* implantation studies. We consider this an important prerequisite for applications of EHM in disease modeling, drug screens, and tissue-engineered heart repair.

ACKNOWLEDGMENTS

The authors thank M. Hoch, I. Quentin, D. Reher, A. Schraut, and K. Sharkova for excellent technical assistance. The authors thank D. Ziebolz for providing gingiva samples, C. Rogge for preparing EHM during early phases of this study, and S. Lutz for sharing cardiac fibroblast cultures and antibodies. The authors also acknowledge B. Downie, T. Lingner, and G. Salinas from the Transcriptome and Genome Analysis Laboratory, University Medical Center Göttingen, for their support.

SOURCES OF FUNDING

This study was supported by DZHK (German Center for Cardiovascular Research), the German Federal Ministry for Sci-

ence and Education (BMBF FKZ 13GW0007A [CIRM-ET3]), the German Research Foundation (DFG ZI 708/7-1, 8-1, 10-1; SFB 937 TP18, SFB 1002 TPs B03, C04, S1; IRTG 1618), a Lower Saxony-Israel grant (11-76251-99-30/09), the European Union FP7 CARE-MI, the Foundation Leducq, and the National Institutes of Health (U01 HL099997). This study was also supported by the California Institute of Regenerative Medicine (CIRM DR2A-05394, CIRM TR3-05556, and CIRM RT3-07798). The collection and studies of fetal material is partly funded by NIRM (Netherlands Institute for Regenerative Medicine).

DISCLOSURES

A patent concerning serum-free engineered human myocardium generation for applications in drug screens and heart repair has been filed by the University of Göttingen with Drs Tiburcy, Hudson, and Zimmermann listed as inventors. Dr Zimmermann is the founder and scientific advisor of myriamed GmbH and Repairon GmbH.

AFFILIATIONS

From Institute of Pharmacology and Toxicology, University Medical Center Göttingen, Germany (M.T., J.E.H., P.B., S.S., T.M., M.-L.C.L., E.L., F.R., S.Z., E. Wettwer, W.-H.Z.); German Center for Cardiovascular Research (DZHK), partner site Göttingen, Germany (M.T., J.E.H., P.B., S.S., T.M., M.-L.C.L., E.L., F.R., S.Z., E. Wingender, W.A.L., W.-H.Z.); Institute of Bioinformatics, University Medical Center Göttingen, Germany (S.Z., E. Wingender); Stanford Cardiovascular Institute (J.R., M.W., J.D.G., J.C.W.) and Department of Radiology (J.D.G., J.C.W.), Molecular Imaging Program, Stanford University School of Medicine, CA; The Sohni Laboratory for Cardiac Electrophysiology and Regenerative Medicine, Technion-Israel Institute of Technology, Haifa (I.K., L.G.); Institute of Pharmacology and Toxicology, Technical University Dresden, Germany (E. Wettwer, U.R.); University Medical Center Utrecht and Hubrecht Institute, The Netherlands (P.D., L.W.v.L.); Leiden University Medical Center, The Netherlands (M.J.G.); Clinic for Cardiology and Pneumology, University Medical Center Göttingen, Germany (S.K., K.T., G.H., W.A.L.); Center for Applied Technology, Beckman Research Institute, City of Hope, Duarte, CA (L.A.C.); Department of Cardiovascular Physiology, Institute of Physiology, Ruhr University Bochum, Bochum, Germany (A.U., W.A.L.); New Laura and Isaac Perlmutter Cancer Center at New York University Langone (T.A., B.N.); and McEwen Centre for Regenerative Medicine, Toronto, Canada (G.K.). The current address for Dr Hudson is Laboratory for Cardiac Regeneration, School of Biomedical Sciences, The University of Queensland, Australia.

FOOTNOTES

Received June 24, 2016; accepted January 23, 2017.

The online-only Data Supplement is available with this article at <http://circ.ahajournals.org/lookup/suppl/doi:10.1161/CIRCULATIONAHA.116.024145/-/DC1>.

Circulation is available at <http://circ.ahajournals.org>.

REFERENCES

1. Thomson JA, Itskovitz-Eldor J, Shapiro SS, Waknitz MA, Swiergiel JJ, Marshall VS, Jones JM. Embryonic stem cell lines derived from human blastocysts. *Science*. 1998;282:1145–1147.
2. Takahashi K, Tanabe K, Ohnuki M, Narita M, Ichisaka T, Tomoda K, Yamanaka S. Induction of pluripotent stem cells from adult human fibroblasts by defined factors. *Cell*. 2007;131:861–872. doi: 10.1016/j.cell.2007.11.019.
3. Yang L, Soonpaa MH, Adler ED, Roepke TK, Kattman SJ, Kennedy M, Henckaerts E, Bonham K, Abbott GW, Linden RM, Field LJ, Keller GM. Human cardiovascular progenitor cells develop from a KDR+ embryonic-stem-cell-derived population. *Nature*. 2008;453:524–528.
4. Burridge PW, Keller G, Gold JD, Wu JC. Production of de novo cardiomyocytes: human pluripotent stem cell differentiation and direct reprogramming. *Cell Stem Cell*. 2012;10:16–28. doi: 10.1016/j.stem.2011.12.013.
5. Lian X, Bao X, Zilberter M, Westman M, Fisahn A, Hsiao C, Hazeltine LB, Dunn KK, Kamp TJ, Palecek SP. Chemically defined, albumin-free human cardiomyocyte generation. *Nat Methods*. 2015;12:595–596. doi: 10.1038/nmeth.3448.
6. Laflamme MA, Chen KY, Naumova AV, Muskheli V, Fugate JA, Dupras SK, Reinecke H, Xu C, Hassanipour M, Police S, O'Sullivan C, Collins L, Chen Y, Minami E, Gill EA, Ueno S, Yuan C, Gold J, Murry CE. Cardiomyocytes derived from human embryonic stem cells in pro-survival factors enhance function of infarcted rat hearts. *Nat Biotechnol*. 2007;25:1015–1024. doi: 10.1038/nbt1327.
7. Burridge PW, Matsa E, Shukla P, Lin ZC, Churko JM, Ebert AD, Lan F, Diecke S, Huber B, Mordwinkin NM, Plews JR, Abilez OJ, Cui B, Gold JD, Wu JC. Chemically defined generation of human cardiomyocytes. *Nat Methods*. 2014;11:855–860. doi: 10.1038/nmeth.2999.
8. Zimmermann WH, Fink C, Kralisch D, Remmers U, Weil J, Eschenhagen T. Three-dimensional engineered heart tissue from neonatal rat cardiac myocytes. *Biotechnol Bioeng*. 2000;68:106–114.
9. Radisic M, Park H, Shing H, Consi T, Schoen FJ, Langer R, Freed LE, Vunjak-Novakovic G. Functional assembly of engineered myocardium by electrical stimulation of cardiac myocytes cultured on scaffolds. *Proc Natl Acad Sci USA*. 2004;101:18129–18134. doi: 10.1073/pnas.0407817101.
10. Fink C, Ergün S, Kralisch D, Remmers U, Weil J, Eschenhagen T. Chronic stretch of engineered heart tissue induces hypertrophy and functional improvement. *FASEB J*. 2000;14:669–679.
11. Schaaf S, Shibamiya A, Mewe M, Eder A, Stöhr A, Hirt MN, Rau T, Zimmermann WH, Conradi L, Eschenhagen T, Hansen A. Human engineered heart tissue as a versatile tool in basic research and preclinical toxicology. *PLoS One*. 2011;6:e26397. doi: 10.1371/journal.pone.0026397.
12. Nunes SS, Miklas JW, Liu J, Aschar-Sobbi R, Xiao Y, Zhang B, Jiang J, Massé S, Gagliardi M, Hsieh A, Thavandiran N, Laflamme MA, Nanthakumar K, Gross GJ, Backx PH, Keller G, Radisic M. Biowire: a platform for maturation of human pluripotent stem cell-derived cardiomyocytes. *Nat Methods*. 2013;10:781–787. doi: 10.1038/nmeth.2524.
13. Tulloch NL, Muskheli V, Razumova MV, Korte FS, Regnier M, Hauch KD, Pabon L, Reinecke H, Murry CE. Growth of engineered human myocardium with mechanical loading and vascular coculture. *Circ Res*. 2011;109:47–59. doi: 10.1161/CIRCRESAHA.110.237206.
14. Kensah G, Roa Lara A, Dahlmann J, Zweigerdt R, Schwanke K, Hegermann J, Skvorc D, Gawol A, Azizian A, Wagner S, Maier LS, Krause A, Dräger G, Ochs M, Haverich A, Gruh I, Martin U. Murine and human pluripotent stem cell-derived cardiac bodies form contractile myocardial tissue *in vitro*. *Eur Heart J*. 2013;34:1134–1146. doi: 10.1093/eurheartj/ehs349.

15. Zhang D, Shadrin IY, Lam J, Xian HQ, Snodgrass HR, Bursac N. Tissue-engineered cardiac patch for advanced functional maturation of human ESC-derived cardiomyocytes. *Biomaterials*. 2013;34:5813–5820. doi: 10.1016/j.biomaterials.2013.04.026.
16. Soong PL, Tiburcy M, Zimmermann WH. Cardiac differentiation of human embryonic stem cells and their assembly into engineered heart muscle. *Curr Protoc Cell Biol*. 2012;55:23.8.1–23.8.21.
17. Riegler J, Tiburcy M, Ebert A, Tzatzalos E, Raaz U, Abilez OJ, Shen Q, Kooreman NG, Neofytou E, Chen VC, Wang M, Meyer T, Tsao PS, Connolly AJ, Couture LA, Gold JD, Zimmermann WH, Wu JC. Human engineered heart muscles engraft and survive long term in a rodent myocardial infarction model. *Circ Res*. 2015;117:720–730. doi: 10.1161/CIRCRESAHA.115.306985.
18. Weinberger F, Breckwoldt K, Pecha S, Kelly A, Geertz B, Starbatty J, Yorgan T, Cheng KH, Lessmann K, Stolen T, Scherrer-Crosbie M, Smith G, Reichenspurner H, Hansen A, Eschenhagen T. Cardiac repair in guinea pigs with human engineered heart tissue from induced pluripotent stem cells. *Sci Transl Med*. 2016;8:363ra148. doi: 10.1126/scitranslmed.aaf8781.
19. Kehat I, Kenyagin-Karsenti D, Snir M, Segev H, Amit M, Gepstein A, Livne E, Binah O, Itskovitz-Eldor J, Gepstein L. Human embryonic stem cells can differentiate into myocytes with structural and functional properties of cardiomyocytes. *J Clin Invest*. 2001;108:407–414. doi: 10.1172/JCI12131.
20. Costa M, Dottori M, Ng E, Hawes SM, Sourris K, Jamshidi P, Pera MF, Elefanti AG, Stanley EG. The hESC line Envy expresses high levels of GFP in all differentiated progeny. *Nat Methods*. 2005;2:259–260. doi: 10.1038/nmeth748.
21. Irion S, Luche H, Gadue P, Fehling HJ, Kennedy M, Keller G. Identification and targeting of the ROSA26 locus in human embryonic stem cells. *Nat Biotechnol*. 2007;25:1477–1482. doi: 10.1038/nbt1362.
22. Hudson J, Titmarsh D, Hidalgo A, Wolvetang E, Cooper-White J. Primitive cardiac cells from human embryonic stem cells. *Stem Cells Dev*. 2012;21:1513–1523. doi: 10.1089/scd.2011.0254.
23. Tohyama S, Hattori F, Sano M, Hishiki T, Nagahata Y, Matsuura T, Hashimoto H, Suzuki T, Yamashita H, Satoh Y, Egashira T, Seki T, Muraoka N, Yamakawa H, Ohgino Y, Tanaka T, Yoichi M, Yuasa S, Murata M, Suematsu M, Fukuda K. Distinct metabolic flow enables large-scale purification of mouse and human pluripotent stem cell-derived cardiomyocytes. *Cell Stem Cell*. 2013;12:127–137. doi: 10.1016/j.stem.2012.09.013.
24. Graichen R, Xu X, Braam SR, Balakrishnan T, Norfiza S, Sieh S, Soo SY, Tham SC, Mummery C, Colman A, Zweigerdt R, Davidson BP. Enhanced cardiomyogenesis of human embryonic stem cells by a small molecular inhibitor of p38 MAPK. *Differentiation*. 2008;76:357–370. doi: 10.1111/j.1432-0436.2007.00236.x.
25. Kim D, Perteau G, Trapnell C, Pimentel H, Kelley R, Salzberg SL. TopHat2: accurate alignment of transcriptomes in the presence of insertions, deletions and gene fusions. *Genome Biol*. 2013;14:R36. doi: 10.1186/gb-2013-14-4-r36.
26. Huang da W, Sherman BT, Lempicki RA. Systematic and integrative analysis of large gene lists using DAVID bioinformatics resources. *Nat Protoc*. 2009;4:44–57. doi: 10.1038/nprot.2008.211.
27. Benjamini Y, Hochberg Y. Controlling the false discovery rate - a practical and powerful approach to multiple testing. *J Roy Stat Soc B Met*. 1995;57:289–300.
28. Robinson MD, McCarthy DJ, Smyth GK. edgeR: a Bioconductor package for differential expression analysis of digital gene expression data. *Bioinformatics*. 2010;26:139–140. doi: 10.1093/bioinformatics/btp616.
29. Tiburcy M, Didié M, Boy O, Christalla P, Döker S, Naito H, Karikkineth BC, El-Armouche A, Grimm M, Nose M, Eschenhagen T, Zieseniss A, Katschinski DM, Hamdani N, Linke WA, Yin X, Mayr M, Zimmermann WH. Terminal differentiation, advanced organotypic maturation, and modeling of hypertrophic growth in engineered heart tissue. *Circ Res*. 2011;109:1105–1114. doi: 10.1161/CIRCRESAHA.111.251843.
30. Dubois NC, Craft AM, Sharma P, Elliott DA, Stanley EG, Elefanti AG, Gramolini A, Keller G. SIRPA is a specific cell-surface marker for isolating cardiomyocytes derived from human pluripotent stem cells. *Nat Biotechnol*. 2011;29:1011–1018. doi: 10.1038/nbt.2005.
31. Naito H, Melnychenko I, Didié M, Schneiderbanger K, Schubert P, Rosenkranz S, Eschenhagen T, Zimmermann WH. Optimizing engineered heart tissue for therapeutic applications as surrogate heart muscle. *Circulation*. 2006;114(1 suppl):I72–I78. doi: 10.1161/CIRCULATIONAHA.105.001560.
32. Severs NJ. The cardiac muscle cell. *Bioessays*. 2000;22:188–199.
33. Tracy RE, Sander GE. Histologically measured cardiomyocyte hypertrophy correlates with body height as strongly as with body mass index. *Cardiol Res Pract*. 2011;2011:658958. doi: 10.4061/2011/658958.
34. Lundy SD, Zhu WZ, Regnier M, Laflamme MA. Structural and functional maturation of cardiomyocytes derived from human pluripotent stem cells. *Stem Cells Dev*. 2013;22:1991–2002. doi: 10.1089/scd.2012.0490.
35. Wiegerinck RF, Cojoc A, Zeidenweber CM, Ding G, Shen M, Joyner RW, Fernandez JD, Kanter KR, Kirshbom PM, Kogon BE, Wagner MB. Force frequency relationship of the human ventricle increases during early postnatal development. *Pediatr Res*. 2009;65:414–419. doi: 10.1203/PDR.0b013e318199093c.
36. Mulieri LA, Hasenfuss G, Leavitt B, Allen PD, Alpert NR. Altered myocardial force-frequency relation in human heart failure. *Circulation*. 1992;85:1743–1750.
37. Flesch M, Kilter H, Cremers B, Lenz O, Südkamp M, Kuhn-Regnier F, Böhm M. Acute effects of nitric oxide and cyclic GMP on human myocardial contractility. *J Pharmacol Exp Ther*. 1997;281:1340–1349.
38. Cohn JN, Levine TB, Olivari MT, Garberg V, Lura D, Francis GS, Simon AB, Rector T. Plasma norepinephrine as a guide to prognosis in patients with chronic congestive heart failure. *N Engl J Med*. 1984;311:819–823. doi: 10.1056/NEJM198409273111303.
39. Dambrot C, Braam SR, Tertoolen LG, Birket M, Atsma DE, Mummery CL. Serum supplemented culture medium masks hypertrophic phenotypes in human pluripotent stem cell derived cardiomyocytes. *J Cell Mol Med*. 2014;18:1509–1518. doi: 10.1111/jcmm.12356.
40. Masson S, Latini R, Anand IS, Vago T, Angelici L, Barlera S, Missov ED, Clerico A, Tognoni G, Cohn JN, Val-He FTI. Direct comparison of B-type natriuretic peptide (BNP) and amino-terminal proBNP in a large population of patients with chronic and symptomatic heart failure: the Valsartan Heart Failure (Val-HeFT) data. *Clin Chem*. 2006;52:1528–1538.
41. Carlson C, Koonce C, Aoyama N, Einhorn S, Fiene S, Thompson A, Swanson B, Anson B, Kattman S. Phenotypic screening with human iPS cell-derived cardiomyocytes: HTS-compatible assays for interrogating cardiac hypertrophy. *J Biomol Screen*. 2013;18:1203–1211. doi: 10.1177/1087057113500812.
42. Zimmermann WH, Melnychenko I, Wasmeier G, Didié M, Naito H, Nixdorff U, Hess A, Budinsky L, Brune K, Michaelis B, Dhein S, Schwoerer A, Ehmke H, Eschenhagen T. Engineered heart tissue grafts improve systolic and diastolic function in infarcted rat hearts. *Nat Med*. 2006;12:452–458. doi: 10.1038/nm1394.
43. Li J, Pucéat M, Perez-Terzic C, Mery A, Nakamura K, Michalak M, Krause KH, Jaconi ME. Calreticulin reveals a critical Ca(2+) checkpoint in cardiac myofibrillogenesis. *J Cell Biol*. 2002;158:103–113. doi: 10.1083/jcb.200204092.
44. Ye L, Zimmermann WH, Garry DJ, Zhang J. Patching the heart: cardiac repair from within and outside. *Circ Res*. 2013;113:922–932. doi: 10.1161/CIRCRESAHA.113.300216.

45. Kamakura T, Makiyama T, Sasaki K, Yoshida Y, Wuriyanghai Y, Chen J, Hattori T, Ohno S, Kita T, Horie M, Yamanaka S, Kimura T. Ultrastructural maturation of human-induced pluripotent stem cell-derived cardiomyocytes in a long-term culture. *Circ J*. 2013;77:1307–1314.
46. Molenaar P, Bartel S, Cochrane A, Vetter D, Jalali H, Pohlner P, Burrell K, Karczewski P, Krause EG, Kaumann A. Both beta(2)- and beta(1)-adrenergic receptors mediate hastened relaxation and phosphorylation of phospholamban and troponin I in ventricular myocardium of Fallot infants, consistent with selective coupling of beta(2)-adrenergic receptors to G(s)-protein. *Circulation*. 2000;102:1814–1821.
47. Jung G, Fajardo G, Ribeiro AJ, Kooiker KB, Coronado M, Zhao M, Hu DQ, Reddy S, Kodo K, Sriram K, Insel PA, Wu JC, Pruitt BL, Bernstein D. Time-dependent evolution of functional vs. remodeling signaling in induced pluripotent stem cell-derived cardiomyocytes and induced maturation with biomechanical stimulation. *FASEB J*. 2016;30:1464–1479. doi: 10.1096/fj.15-280982.
48. Chang Liao ML, de Boer TP, Mutoh H, Raad N, Richter C, Wagner E, Downie BR, Unsöld B, Aroj I, Streckfuss-Bömeke K, Döker S, Luther S, Guan K, Wagner S, Lehnart SE, Maier LS, Stühmer W, Wettwer E, van Veen T, Morlock MM, Knöpfel T, Zimmermann WH. Sensing cardiac electrical activity with a cardiac myocyte-targeted optogenetic voltage indicator. *Circ Res*. 2015;117:401–412. doi: 10.1161/CIRCRESAHA.117.306143.

Defined Engineered Human Myocardium With Advanced Maturation for Applications in Heart Failure Modeling and Repair

Malte Tiburcy, James E. Hudson, Paul Balfanz, Susanne Schlick, Tim Meyer, Mei-Ling Chang Liao, Elif Levent, Farah Raad, Sebastian Zeidler, Edgar Wingender, Johannes Riegler, Mouer Wang, Joseph D. Gold, Izhak Kehat, Erich Wettwer, Ursula Ravens, Pieterjan Dierickx, Linda W. van Laake, Marie Jose Goumans, Sara Khadjeh, Karl Toischer, Gerd Hasenfuss, Larry A. Couture, Andreas Unger, Wolfgang A. Linke, Toshiyuki Araki, Benjamin Neel, Gordon Keller, Lior Gepstein, Joseph C. Wu and Wolfram-Hubertus Zimmermann

Circulation. 2017;135:1832-1847; originally published online February 6, 2017;
doi: 10.1161/CIRCULATIONAHA.116.024145

Circulation is published by the American Heart Association, 7272 Greenville Avenue, Dallas, TX 75231
Copyright © 2017 American Heart Association, Inc. All rights reserved.
Print ISSN: 0009-7322. Online ISSN: 1524-4539

The online version of this article, along with updated information and services, is located on the World Wide Web at:

<http://circ.ahajournals.org/content/135/19/1832>

Data Supplement (unedited) at:

<http://circ.ahajournals.org/content/suppl/2017/02/06/CIRCULATIONAHA.116.024145.DC1>

Permissions: Requests for permissions to reproduce figures, tables, or portions of articles originally published in *Circulation* can be obtained via RightsLink, a service of the Copyright Clearance Center, not the Editorial Office. Once the online version of the published article for which permission is being requested is located, click Request Permissions in the middle column of the Web page under Services. Further information about this process is available in the [Permissions and Rights Question and Answer](#) document.

Reprints: Information about reprints can be found online at:
<http://www.lww.com/reprints>

Subscriptions: Information about subscribing to *Circulation* is online at:
<http://circ.ahajournals.org/subscriptions/>

SUPPLEMENTAL MATERIAL

Defined Engineered Human Myocardium with Advanced Maturation for Applications in Heart Failure Modelling and Repair

Authors: Malte Tiburcy, MD^{1,2}; James E. Hudson, PhD^{1,2*}; Paul Balfanz^{1,2}; Susanne Schlick, MS^{1,2}; Tim Meyer, PhD^{1,2}; Mei-Ling Chang Liao, PhD^{1,2}; Elif Levent, PhD^{1,2}; Farah Raad, PhD^{1,2}; Sebastian Zeidler, PhD^{1,2,3}; Edgar Wingender, PhD^{2,3}; Johannes Riegler, PhD⁴; Mouer Wang, MD⁴; Joseph D. Gold, PhD^{4,5}; Izhak Kehat, MD PhD⁶; Erich Wettwer, PhD^{1,7}; Ursula Ravens, MD PhD⁷; Pieterjan Dierickx, PhD⁸; Linda W. van Laake, MD PhD⁸; Marie Jose Goumans, PhD⁹; Sara Khadjeh, PhD¹⁰; Karl Toischer, MD¹⁰; Gerd Hasenfuss, MD¹⁰; Larry A. Couture, PhD¹¹; Andreas Unger, PhD¹²; Wolfgang A. Linke, PhD^{2,10,12}; Toshiyuki Araki, PhD¹³; Benjamin Neel, MD PhD¹³; Gordon Keller, PhD¹⁴; Lior Gepstein, MD PhD⁶; Joseph C. Wu, MD PhD^{4,5}; Wolfram-Hubertus Zimmermann, MD^{1,2}

Affiliations: ¹Institute of Pharmacology and Toxicology, University Medical Center Goettingen, Goettingen, Germany. ²German Center for Cardiovascular Research (DZHK), partner site Goettingen, Goettingen, Germany. ³Institute of Bioinformatics, University Medical Center Goettingen, Goettingen, Germany. ⁴Stanford Cardiovascular Institute and ⁵Department of Radiology, Molecular Imaging Program, Stanford University School of Medicine, Stanford, CA, USA. ⁶The Sohnis Laboratory for Cardiac Electrophysiology and Regenerative Medicine, Technion-Israel Institute of Technology, Haifa, Israel. ⁷Institute of Pharmacology and Toxicology, Technical University Dresden, Dresden, Germany. ⁸University Medical Center Utrecht and Hubrecht Institute, Utrecht, The Netherlands. ⁹Leiden University Medical Center, Leiden, The Netherlands. ¹⁰Clinic for Cardiology and Pneumology, University Medical Center Goettingen, Goettingen, Germany. ¹¹Center for Applied Technology, Beckman Research Institute, City of Hope, Duarte, CA, USA. ¹²Department of Cardiovascular Physiology, Institute of Physiology, Ruhr University Bochum, Bochum, Germany. ¹³New Laura and Isaac Perlmutter Cancer Center at New York University Langone, New York. ¹⁴McEwen Centre for Regenerative Medicine, Toronto, Canada.

*Present address: Laboratory for Cardiac Regeneration, School of Biomedical Sciences, The University of Queensland, Australia

Corresponding author:

Wolfram-Hubertus Zimmermann, M.D.
Institute of Pharmacology and Toxicology
University Medical Center Goettingen
Georg-August-University
Robert-Koch-Str. 40
37075 Goettingen
Germany
Tel: +49-551-39-5781; Fax: +49-551-39-5699
Email: w.zimmermann@med.uni-goettingen.de

Supplemental Methods

Supplemental Tables 1-5

Supplemental Figures 1-11

Supplemental References

Supplemental Video Legends

Supplemental methods

EHM - Starting Protocol. First, a suspension of differentiated single cells was prepared: (1) EBs were digested with collagenase B (Roche, 1 mg/ml; H9.2), collagenase I (Sigma-Aldrich, 2 mg/ml) and/or trypsin/EDTA (Life Technologies, 0.25%/1 mmol/l; HES3, HES3-ENVY, HES2, hiPS-BJ) as described elsewhere¹⁻⁶; (2) monolayers (hES2-RFP, hiPS-G1) were digested with Accutase (Millipore), 0.0125% Trypsin (Life Technologies), and 20 µg/ml DNase (Calbiochem) for 10-15 mins at room temperature; and (3) human fibroblasts were dispersed using TrypLE (Life Technologies). Fibroblast culture was in DMEM with 4.5 g/l glucose, 15% fetal bovine serum, 100 U/ml penicillin, and 100 µg/ml streptomycin (all Life Technologies). Where indicated fibroblast were transduced with a lentivirus (pGIPZ, Addgene) for stable expression of GFP under the control of a ubiquitously active CMV promotor.

Freshly dispersed cells were counted using the electrical current exclusion method (CASY, Roche) before proceeding with EHM construction, using a modification of our original engineered heart tissue protocol⁷. Briefly, EHMs (reconstitution volume: 500 µl) were prepared by pipetting a mixture containing freshly dispersed ESC-derivatives (1×10^4 - 15×10^6 cells in Iscove-Medium with 20% fetal bovine serum, 1% non-essential amino acids, 2 mmol/l glutamine, 100 µmol/l β-mercaptoethanol, 100 U/ml penicillin, and 100 µg/ml streptomycin) with or without addition of fibroblasts as indicated, pH-neutralized collagen type I from rat tails (0.4 mg/EHM), MatrigelTM (10% v/v; Becton Dickenson), and concentrated serum-containing culture medium (2x DMEM, 20% horse serum, 4% chick embryo extract, 200 U/ml penicillin, and 200 µg/ml streptomycin) in circular molds

(inner/outer diameter: 2/4 mm; height: 5 mm - Starting Protocol, **Table 1**). EHM condensed quickly within the casting molds and were transferred onto static or dynamic stretch devices (110% of slack length)⁸⁻¹⁰ on culture day 3. Medium was exchanged every other day.

Definition of the EHM reconstitution and culture protocol towards cGMP. Initially, cells were reconstituted in a mixture of pH-neutralized medical grade bovine collagen (LLC Collagen Solutions, 0.4 mg/EHM), concentrated serum-containing culture medium (2x DMEM, 40% fetal calf serum, 200 U/ml penicillin, and 200 µg/ml streptomycin) and cultured in Iscove-Medium with 20% fetal calf serum, 1% non-essential amino acids, 2 mmol/l glutamine, 300 µmol/l ascorbic acid, 100 µmol/l β-mercaptoethanol, 100 U/ml penicillin, and 100 µg/ml streptomycin (Matrix Protocol, **Table 1**).

To generate defined, serum-free EHM, cells were reconstituted in a mixture of pH-neutralized medical grade bovine collagen (LLC Collagen Solutions, 0.4 mg/EHM), concentrated serum-free medium (2x RPMI, 8% B27 without insulin, 200 U/ml penicillin, and 200 µg/ml streptomycin) and cultured in Iscove-Medium with 4% B27 without insulin, 1% non-essential amino acids, 2 mmol/l glutamine, 300 µmol/l ascorbic acid, 100 ng/ml IGF1 (AF-100-11), 10 ng/ml FGF-2 (AF-100-18B), 5 ng/ml VEGF₁₆₅ (AF-100-20), 5 ng/ml TGF-β1 (AF-100-21C; mandatory during culture days 0-3), 100 U/ml penicillin, and 100 µg/ml streptomycin (Serum-free Protocol, **Table 1**). All growth factors were purchased from Peprotech as "animal-free recombinant human growth factors". Where indicated full B27 (Life Technologies, A1486701) was compared to B27 without antioxidants (Life Technologies, #10889038) and B27 without insulin (Life Technologies, #0050129SA).

Action potential recordings. We recorded spontaneous action potentials (APs) from individual cardiomyocytes in EHMs via conventional intracellular glass microelectrodes filled with 2.5 mol/l KCl in thermostatted (37°C) and pH-controlled (pH 7.4 under 5% O₂ and 95%

CO₂) extracellular solution (mmol/l: 126.7 NaCl, 5.4 KCl, 1.8 CaCl₂, 1.05 MgCl₂, 22 NaHCO₃, 0.42 NaH₂PO₄, 11 glucose).

Flow cytometry. Single cell suspensions were analysed either alive or fixed in 70% ice cold ethanol or 4% formaldehyde (Histofix, Roth). For live cell analysis, cells were incubated for 10 min in Sytox Red Dead Cell Stain (Life Technologies, 5 nmol/L) to exclude dead cells and Hoechst-3342 (Life Technologies, 10 µg/ml) to analyse nuclear DNA content and exclude cell doublets. The following gating strategy was applied: (1) gating of cells based on forward scatter area (FSC-A) and sideward scatter area (SSC-A), (2) gating of live cells (Sytox Red negative), (3) gating of single cells (based on DNA signal width), (4) gating of RFP-positive cells (cardiomyocytes), and (5) assessment of cardiomyocyte size based on median SSC-A or median RFP fluorescence intensity. Cardiomyocyte size measurements by flow cytometry were validated against morphometric measurements of cell area in microscopic images of identical samples using ImageJ software (**Supplementary Figure 9**).

Fixed cells were stained with Hoechst-3342 (Life Technologies, 10 µg/ml) to analyse nuclear DNA content and to exclude cell doublets.

The following flow cytometry parameters were established for the factorial screen (**Supplementary Figure 3**): (1) cell viability (100% minus percentage of cells in the sub-G1 DNA fraction), (2) cardiomyocyte and non-myocyte percentage (actinin-positive and -negative cells, respectively), (3) cardiomyocyte median actinin fluorescence intensity (MFI, as a quantitative surrogate for cardiomyocyte sarcomere content), (4) cardiomyocyte, and (5) non-myocyte size (based on median SSC-A). Refer to **Supplementary Table 2** for details on antibodies utilized in this study. Cells were run on a LSRII SORP Cytometer (BD Biosciences) and analysed using DIVA or Cyflogic software. At least 10,000 events were analysed per sample.

Immunofluorescence staining. EHM-derived cells or 2D monolayer cardiomyocytes were fixed in 4% formaldehyde (Histofix, Roth). After 3 washes with PBS, cells were incubated with primary antibodies in PBS, 5% goat serum (Thermo Scientific), 1% bovine serum albumin, 0.5% Triton-X (both Sigma-Aldrich) for 2 hours at room temperature or overnight at 4°C. The antibodies used in this study are summarized in **Supplementary Table 2**. After several washes, appropriate secondary antibodies and Hoechst-33342 (Life Technologies, 10 µg/ml) to detect nuclear DNA were added for 1 hour at room temperature. Where indicated Alexa Fluor coupled phalloidin (Thermo Scientific) to stain f-actin was added (1:60 dilution). Immunostainings were imaged using a Zeiss LSM710 confocal microscope¹¹. For sarcomere length measurements individual cardiomyocytes were semi-automatically analyzed using a custom-made Matlab (version 2014b) script. Briefly, individual actinin-stained sarcomeres were interactively traced using `impoly` command. Intensity values of the resulting pixel trace were smoothed (5 pixel moving average) and Z-bands were identified by the `findpeaks` command with a manually adjustable `MinPeakProminence` Parameter (default 50 for 8 bit images). Pixel X and Y indices were scaled to their respective physical length and converted to positions along the trace line by cumulatively summing the norms of vectors connecting neighboring pixel.

Supplemental Tables

Supplementary Table 1

PSC line	Cardiomyocyte differentiation	Input cells/500 μ l EHM	Contractions (defined areas / whole construct)	Experimental data
H9.2	Spontaneous, EB; Kehat et al. ²	10,000	local: 2-3 days after casting / whole: not observed	n.a.
H9.2		250,000	local: 2-3 days after casting / whole: not observed	n.a.
HES3-ENVY	Spontaneous, EB; ESI ¹	10,000	local: 2 days after casting / whole: not observed	n.a.
HES3-ENVY		100,000	local: 2 days after casting / whole: not observed	n.a.
HES3-ENVY		250,000	local: 1-2 days after casting / whole: not observed	n.a.
HES3-ENVY		1.5x10 ⁶	local: 1 day after casting / whole: 3 days after casting	Figure 2f
HES3-ENVY		15x10 ⁶	local: 1 day after casting / whole: 3 days after casting	n.a.
HES3	Spontaneous, EB; ESI ¹	1.5x10 ⁶	local: 1 day after casting / whole: 3 days after casting	n.a.
HES2	Directed, EB; Yang et al. ⁵	1.5x10 ⁶	local: 1 day after casting / whole: 3 days after casting	Figure 1b Suppl. Fig. 1f, 3d
HES2-RFP	Directed, monolayer; refer to methods	1.5x10 ⁶	local: 1 day after casting / whole: 3 days after casting	Figure 1a-e, 2c,f, 3a-f, 4a-g Suppl. Fig. 1a-f, 2a-d, 3, 4a, 5, 6, 7, 8, 9b, 10
hiPS-G1	Directed, monolayer; refer to methods	1.5x10 ⁶	local: 1 day after casting / whole: 3 days after casting	Figure 1f, 2a-e, 3a,b Suppl. Fig. 4b,c, 5, 7b, 9a,b
H7	Directed, EB; Riegler et al. ⁶	1.5x10 ⁶	local: 1 day after casting / whole: 3 days after casting	Figure 1f, 5b-g Suppl. Figure 1f, 10
hiPS-BJ	Directed, EB, Yang et al. ⁵	1.5x10 ⁶	local: 1 day after casting / whole: 3 days after casting	Figure 1b
iCell [®] CM	CDI-undisclosed	1.5x10 ⁶	local: 1 day after casting / whole: 3 days after casting	Figure 1f, 3a,b Suppl. Video 2

Supplementary Table 1: Overview of EHM generation from various pluripotent stem cell lines. n.a.: not applicable, EB: embryoid body differentiation protocol

Supplementary Table 2

Primary Antibodies	Dilution	Vendor	Order Nr./ Clone
Sarcomeric α -actinin	1:1000-4000	Sigma-Aldrich	A7811
CD31 (Pecam1)	1:100	Abcam	ab28364
Human Anti-Integrin β 1 (CD29)	1:200	Millipore	MAB1965
Human β Myosin heavy chain	1:100	Dev. Studies Hybridoma Bank	A4.951
β Myosin heavy chain	1:500	Dev. Studies Hybridoma Bank	MF20
Human cardiac Troponin T	1:200	Abcam	ab45932
MLC2V	1:500	Synaptic Systems	310003
MLC2A	1:500	Synaptic Systems	56F5
Myomesin-1	1:500	Proteintech	20360-1-AP
N-cadherin (CDH2)	1:50	Sigma-Aldrich	HPA058574
Ki67	1:100	Thermo Scientific	SP6
Secondary Antibodies			
Secondary Antibodies	Dilution	Vendor	Order Nr.
Goat anti mouse Alexa Fluor 488	1:1000	Thermo Scientific	A-11001
Goat anti mouse Alexa Fluor 633	1:1000	Thermo Scientific	A-21052
Goat anti rabbit Alexa Fluor 633	1:1000	Thermo Scientific	A-21070
Goat anti rabbit Alexa Fluor 546	1:1000	Thermo Scientific	A-11010

Supplementary Table 2: Overview of primary and secondary antibodies

Supplementary Table 3: Cardiomyocyte transcriptome

Gene Symbol	Embryonic cardiomyocytes		Fetal Heart		Adult Heart	
	RPKM	Rank	RPKM	Rank	RPKM	Rank
MYL7	16361,38	1	9101,30	1	566,72	30
TNNT2	5660,97	2	5983,81	2	5411,26	2
NPPA	3082,65	3	474,08	21	20,00	265
MYL4	2393,09	4	1248,75	8	60,04	142
POPDC2	2314,59	5	2016,64	5	1155,05	18
PLN	2009,90	6	842,31	13	886,30	22
RGS5	1969,40	7	625,01	15	1607,16	11
ANKRD1	1923,96	8	257,27	44	671,88	26
MYL3	1816,20	9	1633,33	6	1688,51	10
FABP3	1585,57	10	994,91	10	1260,77	15
ENO3	1427,43	11	504,95	20	1130,04	19
ACTC1	1324,64	12	1195,42	9	1353,81	14
MYL2	1264,78	13	754,32	14	4607,74	3
DMD	1235,66	14	2043,98	4	2030,08	8
COL4A5	1100,94	15	275,27	41	46,48	171
MYH7	835,00	16	2533,40	3	6175,99	1
CSRP3	688,62	17	309,49	34	511,22	31
NPPB	683,10	18	17,56	305	26,28	234
HSPB7	655,45	19	573,42	18	1188,17	16
CGNL1	639,91	20	524,56	19	173,74	62
CCDC141	575,53	21	910,89	12	390,40	38
SMPX	554,44	22	237,39	46	187,07	59
NPNT	498,38	23	459,41	24	7,67	397
PDK1	491,20	24	467,19	23	78,33	114
MYOCD	483,98	25	594,64	16	226,24	56
IGFBP2	447,11	26	119,56	79	70,69	119
THBS4	413,05	27	138,25	74	308,39	45
NEBL	374,05	28	275,68	40	344,30	42
CKM	369,60	29	443,76	25	1048,87	20
TNNI3	364,60	30	441,83	27	1694,21	9
TTN	362,14	31	917,23	11	1507,67	12
MYH6	342,66	32	48,72	161	246,49	50
YPEL2	336,44	33	188,34	60	162,78	66
LAPTM4B	314,51	34	138,02	75	61,08	139
MYBPC3	288,67	35	467,56	22	823,87	23
COL15A1	285,00	36	1275,76	7	896,22	21
MLIP	283,44	37	257,64	43	451,71	34
TNNI1	282,25	38	172,27	65	7,76	396
C7	279,36	39	89,24	101	47,91	164
SPINT2	278,17	40	35,57	199	11,56	337
TECRL	270,33	41	208,48	53	398,22	37
APOA1	266,33	42	4,58	520	30,89	212
SH3BGR	253,18	43	163,18	67	69,22	124

APOE	247,27	44	14,83	331	10,64	347
ACTN2	244,16	45	311,96	33	585,17	29
CPE	235,06	46	63,61	137	67,32	125
DES	225,84	47	368,58	29	3582,77	5
NREP	220,12	48	267,10	42	6,23	440
MYOZ2	219,75	49	123,07	77	288,10	46
MDK	211,09	50	216,22	52	1,44	701
LDB3	209,64	51	592,56	17	708,59	25
CRIP2	198,67	52	216,36	51	240,89	53
VCAM1	192,47	53	31,91	218	5,88	447
APOBEC2	183,71	54	120,20	78	114,52	83
IGF2	183,17	55	81,03	110	17,30	285
SMYD1	179,38	56	190,82	57	108,57	86
MB	178,19	57	338,22	32	3935,68	4
ATP1B1	176,58	58	111,40	85	109,36	85
CRYAB	167,14	59	299,07	35	1356,53	13
EEF1A2	163,59	60	193,86	56	374,60	40
MYOM1	162,53	61	351,96	31	379,57	39
PPP1R9A	154,28	62	352,17	30	200,43	58
CHD7	153,08	63	287,88	37	145,24	70
MLF1	148,57	64	216,44	50	87,82	100
FZD3	143,28	65	84,50	106	21,78	254
GPR22	142,67	66	292,76	36	96,27	95
HSPB3	138,05	67	198,24	55	114,77	82
CNN1	134,83	68	60,26	138	107,67	87
KRT8	133,29	69	23,28	264	12,26	330
SLC25A4	130,57	70	88,87	102	243,91	52
ACTA1	127,98	71	6,17	471	3251,70	6
CKMT2	127,66	72	157,95	69	479,49	33
TMEM71	126,37	73	287,57	38	91,01	98
PROX1	122,15	74	243,57	45	157,24	67
HAND2	121,52	75	171,09	66	64,04	132
SLC8A1	119,35	76	218,76	49	93,51	96
LMOD2	115,44	77	58,19	142	253,56	48
SNTA1	112,27	78	93,32	96	61,19	138
HOOK1	111,61	79	36,37	196	20,36	261
ITGB1BP2	108,97	80	58,13	144	31,58	209
NCAM1	107,50	81	157,35	70	168,72	64
PLCL2	104,18	82	200,50	54	98,02	91
BMP5	101,44	83	64,21	133	2,10	630
EPHA4	100,69	84	17,99	303	19,06	272
BVES	99,74	85	85,28	104	28,43	222
HRC	99,35	86	67,72	126	320,85	43
UNC45B	96,94	87	104,97	88	59,75	143
PRKCH	96,64	88	72,92	122	46,95	168
GUCY1A3	96,63	89	80,72	111	38,94	186
ALDOC	96,58	90	118,45	80	96,41	93

RAPGEF4	93,68	91	82,37	109	38,73	187
CASQ2	92,57	92	221,88	48	423,11	35
PKP2	91,55	93	80,47	112	118,92	77
CPVL	89,22	94	31,47	220	43,53	178
GCNT2	87,87	95	139,39	73	67,02	126
XPO4	87,30	96	63,68	135	16,30	289
TRIM63	86,95	97	103,35	89	72,27	118
SORBS2	86,57	98	395,76	28	261,56	47
EDNRA	84,49	99	67,51	127	21,16	256
PPP1R14C	82,68	100	59,38	140	30,81	213
STOX2	82,23	101	189,87	59	129,03	72
SERPINA5	82,14	102	0,55	725	2,38	611
PTP4A3	81,41	103	98,44	90	169,25	63
AK4	80,96	104	84,78	105	117,92	79
ABLIM1	79,99	105	109,04	87	253,18	49
ANK2	79,14	106	158,12	68	123,04	76
RBM24	79,06	107	183,20	62	64,63	131
PPP1R13B	79,05	108	174,49	63	117,75	80
HEPH	78,29	109	34,17	207	6,37	436
LRRRC17	77,05	110	14,80	332	1,07	765
CORIN	76,98	111	111,14	86	26,47	233
ADPRHL1	74,96	112	93,86	94	118,51	78
PPP1R12B	73,46	113	173,23	64	146,24	69
FITM1	72,84	114	38,22	188	24,72	240
PPARGC1A	72,36	115	89,28	100	77,39	115
ILDR2	72,00	116	64,77	132	28,39	223
TCAP	71,70	117	34,34	205	720,26	24
SIPA1L2	71,11	118	80,41	113	45,25	175
FIGN	70,60	119	154,16	71	47,61	165
SERPINI1	69,93	120	11,94	369	11,24	341
FREM1	69,70	121	115,32	83	7,64	400
C1orf105	68,10	122	3,79	542	3,16	559
DTNA	66,99	123	53,10	150	102,19	90
ASB2	66,88	124	44,72	174	55,38	149
RYR2	66,65	125	189,96	58	487,71	32
LRRRC10	66,31	126	58,14	143	20,29	263
PPM1K	66,09	127	26,52	243	81,30	108
CYP2J2	65,34	128	32,48	214	44,30	176
AGL	65,05	129	49,83	158	28,07	227
COL21A1	64,68	130	117,92	81	22,82	247
KLHL31	64,50	131	48,89	160	309,59	44
CHN2	64,17	132	65,20	130	55,22	150
AQP1	62,87	133	33,85	210	57,38	147
COL14A1	62,61	134	45,12	173	15,11	303
NKX2-5	62,33	135	50,30	157	46,71	170
RIMKLA	61,99	136	50,40	156	45,93	172
FAM134B	61,89	137	64,02	134	130,78	71

HIF3A	61,72	138	285,54	39	86,64	101
MMP15	61,66	139	43,48	177	22,80	248
TBX20	59,65	140	183,83	61	36,83	194
FNDC5	58,02	141	51,66	153	163,29	65
TSPAN18	57,37	142	96,54	91	103,93	89
RRAD	56,71	143	94,14	93	62,84	136
RNF207	55,59	144	225,81	47	50,05	159
MYO18B	55,21	145	93,10	97	85,51	102
XIRP1	55,17	146	77,97	116	244,86	51
TRDN	55,14	147	26,03	249	58,39	145
NDRG2	54,36	148	45,37	171	78,79	113
DLK1	53,79	149	93,32	95	14,92	304
DMKN	52,30	150	38,01	190	5,44	459
GREB1	51,94	151	82,53	108	28,35	224
MYLK3	51,37	152	47,66	164	60,48	141
IFI44L	50,65	153	2,77	578	82,32	106
TMEM178A	50,59	154	48,21	163	4,73	481
RRAGD	48,74	155	27,00	240	30,18	218
ITGA9	47,43	156	88,79	103	97,14	92
MTUS1	47,18	157	65,37	129	79,37	110
CASQ1	46,92	158	5,40	492	24,06	245
FILIP1	46,57	159	58,98	141	63,19	134
LRRRC39	46,42	160	56,69	146	47,99	163
PDGFD	45,48	161	20,51	283	9,86	358
B4GALNT4	45,34	162	8,87	415	1,77	657
CCDC69	44,84	163	26,48	245	39,60	185
PYGM	44,39	164	25,38	252	56,47	148
JPH2	43,84	165	44,67	175	40,86	180
CORO6	43,74	166	92,27	98	29,40	219
PCDH7	42,92	167	73,32	121	37,36	193
GATA4	42,92	168	49,26	159	37,46	192
ISYNA1	42,49	169	30,67	224	8,85	370
NAP1L3	41,63	170	9,96	399	2,95	569
MTTP	41,20	171	0,64	721	7,10	413
LLGL2	40,13	172	25,77	251	5,78	449
RAB3IP	38,59	173	43,87	176	16,13	292
PRSS42	38,44	174	127,77	76	52,35	155
SLC47A1	37,87	175	13,96	345	15,15	302
ST6GAL1	37,17	176	24,33	257	24,30	243
AGT	36,99	177	18,42	300	33,79	199
TMEM176B	36,90	178	23,03	267	22,23	251
VTN	36,81	179	0,95	693	16,25	290
RNASE1	36,71	180	20,48	284	37,57	191
SPINK5	36,31	181	2,71	582	4,89	477
RBM38	36,17	182	32,14	216	15,96	294
RCAN2	35,76	183	23,40	263	124,38	74
S1PR1	35,55	184	29,14	230	20,32	262

EPB41L3	35,41	185	36,54	195	3,21	554
KCNQ1	35,22	186	45,87	170	48,09	162
FAM84B	35,16	187	34,41	204	2,77	589
TPD52L1	34,79	188	9,77	403	47,07	167
RAB9B	34,75	189	16,01	316	13,46	321
CFI	34,63	190	2,56	588	8,16	386
B4GALNT3	34,26	191	70,13	124	13,57	319
DENND5B	34,24	192	27,71	238	16,23	291
RAMP2	34,11	193	141,11	72	82,86	105
MST1	33,98	194	11,96	368	3,35	547
ERBB3	33,90	195	29,16	229	13,79	314
RCS1	33,85	196	57,10	145	17,58	282
GCA	33,81	197	20,57	282	6,92	417
PGM5	33,76	198	55,84	148	92,21	97
RAMP1	33,74	199	43,09	179	75,32	116
ARHGAP42	33,32	200	18,18	302	4,41	495
COLEC11	33,31	201	42,52	182	5,02	475
LPL	33,31	202	442,26	26	2467,43	7
BST2	33,17	203	0,67	719	12,09	331
DUSP27	32,85	204	26,76	242	85,29	104
SLAIN1	32,27	205	21,80	275	12,64	329
APOB	31,62	206	0,74	713	3,54	538
IGSF3	31,10	207	14,19	341	4,88	479
BMP7	31,09	208	28,98	231	2,32	618
PRRG3	30,47	209	115,96	82	14,36	309
CTNNA3	30,31	210	46,35	169	31,90	205
FAM189A2	30,25	211	63,62	136	11,90	333
EDA	30,16	212	29,91	228	15,41	299
CMYA5	30,16	213	47,52	165	653,71	27
PLEKHA7	29,75	214	96,34	92	20,18	264
COL4A6	29,60	215	5,66	487	3,94	524
CDKN1C	29,57	216	14,46	337	11,27	340
TRIM24	29,48	217	20,77	281	3,96	522
SMTNL2	29,41	218	2,60	586	8,27	384
TRIM54	29,36	219	28,13	234	73,33	117
ITGA7	29,25	220	38,04	189	123,29	75
ALPK3	29,00	221	52,28	152	50,64	158
PARM1	28,98	222	41,23	184	31,67	207
FAM78A	28,80	223	21,17	278	8,89	369
PTPRD	28,73	224	28,83	232	3,58	533
TMOD1	28,67	225	33,28	213	34,33	197
CLGN	28,46	226	25,90	250	32,71	202
GAB1	28,07	227	69,20	125	19,52	266
NAALAD2	27,76	228	47,50	166	5,57	454
SLC4A3	27,63	229	83,16	107	96,31	94
ADCY5	27,49	230	42,78	180	40,37	182
BCL2L11	27,42	231	46,41	168	19,32	269

SYNPO2L	27,35	232	24,54	255	70,34	122
MYH7B	27,19	233	80,09	115	37,68	190
ABCB4	27,12	234	65,19	131	31,62	208
PROM1	26,88	235	23,06	266	22,75	249
TSTD1	26,42	236	26,24	247	3,48	541
CADPS	26,14	237	12,89	354	8,76	373
VSNL1	26,13	238	10,27	391	14,14	311
BCAM	25,85	239	51,64	154	25,35	238
GARNL3	25,34	240	76,22	119	64,97	129
TMEM133	25,34	241	12,63	356	2,88	577
VASH1	25,28	242	12,25	363	4,07	515
KCNH2	25,04	243	34,22	206	25,83	237
RBM20	24,99	244	72,17	123	50,91	156
ADHFE1	24,98	245	80,23	114	61,48	137
DSG2	24,30	246	15,97	317	14,11	312
RAB3C	24,16	247	2,08	615	1,32	720
FRAS1	23,79	248	48,36	162	4,39	496
CSRNP3	23,58	249	25,05	253	12,04	332
ADAMTS9	23,47	250	30,22	227	22,29	250
DOK7	23,27	251	33,37	212	34,53	196
ACOT11	23,21	252	77,92	117	40,30	183
RASL11B	22,36	253	10,47	387	2,11	629
UNC13D	22,29	254	10,91	381	9,26	365
DUSP26	21,86	255	9,12	410	18,25	278
STAT4	21,77	256	27,98	235	1,48	696
MED12L	21,76	257	23,80	260	7,83	391
FAM160A1	21,62	258	19,05	297	63,57	133
GATM	21,61	259	8,85	418	8,61	375
CACNB2	21,37	260	56,67	147	26,52	231
CIB2	21,35	261	10,88	382	2,93	571
NIPSNAP3B	21,18	262	17,21	310	24,12	244
TTC39A	21,07	263	2,61	585	9,04	368
ICA1	21,03	264	23,45	262	26,18	236
SRL	20,85	265	77,04	118	128,90	73
SGCA	20,65	266	46,83	167	70,15	123
ATRN1	20,45	267	4,54	522	9,88	357
FAM81A	20,39	268	42,34	183	4,04	516
COX6A2	20,19	269	60,10	139	347,99	41
HOPX	20,14	270	7,97	432	5,36	464
PDE4D	19,90	271	16,83	314	18,41	276
EGLN3	19,77	272	19,90	292	52,90	151
PRKAA2	19,61	273	30,31	226	60,97	140
MAN1C1	19,50	274	8,17	426	6,49	428
SCN5A	19,49	275	36,04	197	57,61	146
ZNRF2	19,47	276	10,39	390	5,65	452
SLC1A3	19,41	277	33,84	211	26,26	235
CLIC5	19,19	278	18,90	299	107,56	88

FGF12	19,02	279	112,31	84	50,73	157
CADM4	18,85	280	7,01	449	3,01	567
LAD1	18,81	281	2,19	608	4,17	510
RASSF4	18,74	282	15,60	321	15,23	301
CMTM5	18,60	283	5,25	501	6,47	429
TMEM56	18,60	284	12,38	360	14,88	306
OBSCN	18,24	285	43,34	178	79,35	111
EPHA7	18,16	286	19,97	291	3,37	546
PPP1R1C	18,07	287	12,39	359	52,53	154
OSBP2	18,00	288	12,03	366	5,84	448
PLCXD3	17,92	289	53,01	151	26,51	232
CAND2	17,87	290	12,07	365	20,66	260
GJA3	17,71	291	24,67	254	9,92	356
INPP5J	17,51	292	9,56	405	32,03	204
AKAP6	17,44	293	34,14	208	45,79	173
MURC	17,42	294	18,42	301	19,35	268
PRICKLE1	17,32	295	14,93	330	3,99	521
SPHKAP	17,27	296	51,55	155	38,07	189
RASSF5	17,13	297	14,66	335	7,37	406
PPP1R1A	16,83	298	21,88	274	10,57	348
FAM184A	16,82	299	9,70	404	1,79	653
SLC38A3	16,74	300	7,19	446	6,45	430
HTRA3	16,72	301	15,32	323	24,38	242
PLCB2	16,62	302	32,20	215	15,89	296
FXVD6	16,54	303	35,44	200	5,54	456
PPFIA4	16,42	304	31,61	219	8,51	377
ITIH3	16,35	305	1,44	657	2,33	617
ANO5	16,31	306	20,28	287	30,25	217
ACSM3	16,11	307	15,49	322	18,09	279
EFNA1	15,92	308	11,25	375	10,29	353
F5	15,87	309	10,15	397	14,42	308
SLC40A1	15,84	310	23,72	261	13,65	315
SHC2	15,79	311	11,10	378	6,43	434
PPM1L	15,76	312	35,63	198	70,66	120
MTSS1	15,73	313	33,96	209	10,90	345
ZNF711	15,71	314	21,99	273	1,44	700
GPRIN3	15,66	315	38,23	187	7,31	408
SLC2A4	15,65	316	15,11	328	47,17	166
VSTM2L	15,57	317	7,41	443	1,49	693
SSTR2	15,46	318	5,74	484	5,39	462
KLHL3	15,44	319	17,69	304	7,66	398
CXADR	15,38	320	12,26	362	10,06	354
GPX3	15,16	321	7,90	435	175,17	61
RASL10B	15,13	322	4,26	528	4,16	511
CAMK2B	15,09	323	14,74	333	44,30	177
PPP1R3A	15,05	324	5,25	500	58,72	144
SLC7A2	14,76	325	4,66	516	13,65	316

HEY2	14,66	326	31,94	217	11,67	335
HHATL	14,61	327	26,49	244	237,29	54
DYSF	14,23	328	10,03	398	24,40	241
TMEM176A	14,22	329	9,81	402	10,45	350
METTL7A	13,93	330	5,91	479	5,12	472
ESRRG	13,81	331	28,18	233	14,35	310
ERBB4	13,78	332	37,56	192	3,49	539
WNK2	13,68	333	90,80	99	79,09	112
PLBD1	13,66	334	14,28	339	7,78	393
COLQ	13,65	335	12,29	361	2,70	595
FRMD4B	13,65	336	37,82	191	4,12	512
FBXO40	13,63	337	31,13	222	79,87	109
TNNT1	13,55	338	14,70	334	40,78	181
SELP	13,51	339	1,38	663	2,28	619
COL9A3	13,40	340	17,12	313	4,41	493
MTUS2	13,38	341	54,74	149	18,49	275
PTGES3L	13,28	342	11,14	377	5,08	473
HEY1	13,05	343	4,19	532	4,88	480
GRIA4	12,89	344	2,82	574	1,37	712
FTCD	12,87	345	5,03	506	2,07	632
TXLNB	12,79	346	22,18	271	31,75	206
TESC	12,72	347	13,41	351	33,68	200
TMEM38A	12,69	348	6,35	464	11,44	338
DERL3	12,56	349	14,08	343	2,59	597
EPHX2	12,35	350	8,85	417	8,68	374
FSD2	12,18	351	21,09	279	13,29	323
NGFR	11,85	352	2,90	568	7,45	405
GUCY1B3	11,83	353	19,87	293	14,78	307
SORCS1	11,82	354	2,96	565	1,33	717
RXRG	11,81	355	1,53	649	3,42	544
SPSB4	11,73	356	11,33	374	1,85	646
SLC16A12	11,54	357	8,68	419	2,37	614
KCNJ5	11,52	358	8,11	427	6,38	435
SPON1	11,45	359	11,08	379	4,47	491
PPARGC1B	11,34	360	26,12	248	40,20	184
CHRNA3	11,30	361	2,35	600	2,82	584
RASGRP3	11,24	362	26,76	241	19,41	267
KIAA1324L	11,23	363	2,36	599	1,61	676
JPH1	11,12	364	10,85	383	7,00	415
ACVR2B	11,11	365	8,39	423	3,13	560
EPB41L4A	11,09	366	37,55	193	9,93	355
AMT	11,07	367	12,03	367	6,77	421
HRASLS	11,02	368	5,33	493	2,26	621
IRX4	10,90	369	16,74	315	4,11	513
KLHL30	10,88	370	7,83	437	5,95	444
ADSSL1	10,84	371	23,92	259	38,20	188
RBPMS2	10,69	372	20,16	288	31,53	211

GAS7	10,29	373	13,90	347	13,52	320
ENPEP	10,24	374	66,44	128	32,56	203
REEP1	10,15	375	14,19	342	7,77	394
RCOR2	10,14	376	6,62	459	1,39	705
CA3	10,01	377	2,09	614	9,36	364
APLNR	9,96	378	36,72	194	17,41	283
FHIT	9,93	379	11,61	372	9,18	366
INHA	9,92	380	2,00	619	4,04	517
WBSCR17	9,89	381	6,82	453	22,02	252
ATP1B2	9,80	382	35,31	201	7,51	403
TET1	9,78	383	17,16	312	1,54	686
IGSF1	9,76	384	0,08	769	1,77	656
PDE9A	9,56	385	8,96	413	4,27	503
SLCO2B1	9,50	386	15,24	325	81,61	107
SH3BGRL2	9,34	387	3,73	545	2,78	587
RNF144A	9,13	388	11,64	371	7,31	407
TPD52	9,11	389	5,04	504	2,90	574
FBXL22	9,09	390	22,40	270	5,89	446
ASB11	9,07	391	17,21	309	27,29	228
SEPP1	9,04	392	5,71	485	10,30	352
CREB5	8,97	393	40,32	185	20,97	258
HCN4	8,93	394	8,57	422	4,44	492
CP	8,93	395	0,37	733	1,28	727
MYOM2	8,90	396	22,50	269	422,21	36
NEURL2	8,88	397	7,93	433	3,40	545
FGF18	8,86	398	24,34	256	13,23	325
TSPAN12	8,86	399	20,02	290	18,01	280
ADCY1	8,78	400	22,08	272	19,31	270
C6	8,66	401	5,26	499	115,06	81
ESAM	8,58	402	45,26	172	65,67	128
RNF165	8,56	403	20,16	289	7,13	412
USP2	8,53	404	13,93	346	27,07	229
KIAA0895	8,50	405	6,89	450	1,32	719
TNFSF10	8,37	406	2,11	612	15,94	295
C11orf21	8,36	407	0,35	735	6,75	423
CNTN4	8,32	408	31,30	221	3,62	532
TMC6	8,29	409	15,20	326	6,36	437
MARK1	8,26	410	12,47	358	5,49	457
PCDHB5	8,18	411	0,66	720	1,25	734
PAIP2B	8,09	412	30,56	225	29,28	220
GADD45G	8,07	413	2,87	570	21,81	253
ADD2	8,05	414	21,24	277	1,49	692
CCL21	8,03	415	7,26	444	2,27	620
PTH1R	7,93	416	5,01	507	3,32	549
CCDC3	7,75	417	8,93	414	3,00	568
PRKCZ	7,75	418	7,02	448	2,82	583
NRAP	7,74	419	19,84	294	607,96	28

ATP1A3	7,74	420	34,92	203	85,41	103
TGFB3	7,73	421	9,20	408	10,99	344
ARHGAP26	7,70	422	17,52	308	15,54	298
SLC29A2	7,42	423	10,84	384	4,88	478
CAMK2A	7,27	424	7,93	434	3,68	530
RBFOX1	7,21	425	26,38	246	30,62	214
SPATA25	7,11	426	10,67	386	3,87	525
PTGER3	7,05	427	6,30	467	2,02	636
MAPK4	6,97	428	0,87	701	13,40	322
GCOM1	6,95	429	21,44	276	16,79	288
C10orf35	6,94	430	1,40	659	1,13	755
ITM2A	6,94	431	17,54	306	18,70	273
SHE	6,84	432	42,78	181	65,72	127
AMY2B	6,82	433	12,62	357	6,98	416
ADORA1	6,81	434	2,91	567	2,44	604
NT5M	6,77	435	9,07	412	2,81	585
GKAP1	6,73	436	12,81	355	7,46	404
LRRTM3	6,73	437	19,00	298	5,72	451
ATP1A2	6,73	438	6,43	462	149,03	68
HAND1	6,67	439	8,07	430	6,51	426
ACACB	6,64	440	30,87	223	32,85	201
FAM13C	6,60	441	6,87	452	2,91	573
CPNE5	6,57	442	5,27	496	26,85	230
SLC44A5	6,52	443	1,60	642	1,21	741
SLC5A1	6,44	444	27,72	237	30,46	216
IGSF9B	6,34	445	75,23	120	52,64	153
ASXL3	6,30	446	17,53	307	3,29	550
L3MBTL4	6,28	447	8,26	424	1,76	658
CELSR1	6,28	448	15,27	324	4,09	514
RELN	6,26	449	2,82	573	1,72	662
RASGRP2	6,15	450	4,52	523	5,28	465
EGF	6,15	451	4,03	537	6,45	431
ELOVL2	6,04	452	2,00	620	2,38	610
TYRP1	6,00	453	0,43	731	70,35	121
ADAM11	5,98	454	24,14	258	2,17	626
SPTB	5,96	455	14,47	336	28,35	225
COL23A1	5,70	456	4,10	534	8,11	388
MPPED2	5,66	457	15,81	319	2,47	602
TNNI3K	5,62	458	15,90	318	7,65	399
AIF1L	5,62	459	14,24	340	6,51	427
B3GNT7	5,62	460	3,32	556	1,35	715
RALYL	5,59	461	0,78	709	4,03	518
DSC2	5,54	462	5,78	481	5,43	460
MPP7	5,54	463	6,00	474	4,17	509
NEB	5,45	464	0,88	700	7,61	401
AUTS2	5,37	465	13,41	352	2,90	575
ACE2	5,35	466	12,21	364	8,44	381

RAB6B	5,33	467	3,44	555	9,66	361
BCO2	5,32	468	15,61	320	30,51	215
ABCG1	5,26	469	7,12	447	7,09	414
EFHC2	5,23	470	6,88	451	8,47	378
WNT11	5,18	471	4,09	535	1,89	644
ZNF853	5,18	472	5,28	495	4,25	505
SORBS1	5,13	473	38,62	186	209,93	57
SFMBT2	5,01	474	3,72	546	4,26	504
XIRP2	4,94	475	5,96	476	1165,62	17
CXXC4	4,92	476	4,23	531	1,81	651
PDE3B	4,91	477	9,08	411	4,30	501
PIP5K1B	4,87	478	20,38	285	23,77	246
TMEM179	4,86	479	6,05	472	2,71	592
NAP1L2	4,85	480	0,13	762	3,03	566
LGI2	4,83	481	2,66	583	1,46	699
TRIL	4,83	482	7,62	439	1,14	752
ARHGAP4	4,74	483	9,51	406	3,81	527
NTRK1	4,68	484	0,83	706	4,23	507
FAM222A	4,67	485	1,22	673	2,43	606
MGAT3	4,60	486	0,85	705	1,75	660
C14orf180	4,56	487	13,20	353	20,73	259
ART3	4,55	488	10,45	389	111,21	84
ST6GALNAC3	4,53	489	2,37	598	1,06	768
PTPRE	4,53	490	2,25	604	9,14	367
SYTL1	4,49	491	2,51	591	1,84	647
DYNC111	4,49	492	0,17	754	11,04	343
NUP210	4,46	493	8,18	425	1,04	770
KCNA4	4,44	494	9,16	409	3,56	536
SOBP	4,41	495	10,23	396	6,77	420
LDHD	4,41	496	10,26	392	28,74	221
CASZ1	4,34	497	11,51	373	6,44	432
DUSP13	4,21	498	0,33	741	8,77	371
BCL11A	4,19	499	11,77	370	3,54	537
LGI4	4,15	500	2,20	607	2,86	578
CDK18	4,15	501	23,06	265	64,75	130
TMEM88	4,13	502	10,69	385	6,86	418
PRKCB	4,05	503	2,90	569	1,36	713
COBL	3,99	504	22,74	268	21,50	255
MOG	3,93	505	1,83	627	2,21	625
CPEB3	3,87	506	6,82	454	5,26	466
TSHZ2	3,71	507	1,64	637	1,21	739
RIC3	3,69	508	0,88	699	5,37	463
NRK	3,69	509	15,14	327	1,71	663
ZMAT1	3,69	510	10,26	394	9,71	360
VAV3	3,65	511	2,40	597	1,29	725
SLC30A3	3,65	512	5,77	482	2,15	627
RASGEF1B	3,61	513	5,51	490	2,66	596

NMNAT3	3,60	514	4,14	533	3,17	558
PTPN6	3,59	515	4,63	518	4,99	476
KIF26A	3,58	516	3,94	539	3,35	548
PARK2	3,58	517	3,01	563	8,16	387
AFAP1L2	3,56	518	4,70	515	2,37	613
MERTK	3,53	519	5,67	486	4,18	508
LMOD3	3,42	520	13,61	350	46,82	169
MPZL2	3,42	521	0,67	717	3,42	543
CACNA1H	3,40	522	1,15	680	1,94	640
SKIDA1	3,40	523	3,53	551	1,18	744
ATG9B	3,35	524	6,22	470	2,01	637
TMEM74B	3,34	525	1,84	626	2,40	608
ELMO1	3,29	526	13,68	348	9,44	363
VANGL2	3,26	527	3,86	541	1,39	708
MCF2L	3,25	528	7,59	440	10,89	346
PLEKHH1	3,25	529	3,49	553	1,71	664
C10orf71	3,24	530	13,66	349	35,80	195
S100A8	3,24	531	1,45	654	5,77	450
PNMT	3,22	532	3,57	549	2,52	598
KBTBD11	3,16	533	4,78	514	3,17	557
RALGPS1	3,16	534	8,67	420	4,69	484
SAMSN1	3,14	535	1,52	651	1,31	721
MGAT4A	3,12	536	2,98	564	5,21	469
PCDHB15	3,08	537	1,57	645	3,23	552
MYADML2	3,08	538	1,44	656	1,54	685
PRDM16	3,05	539	15,03	329	6,06	443
NR0B2	3,05	540	0,14	760	2,07	631
EPHA3	3,02	541	5,93	478	4,37	498
SCARF1	2,99	542	7,51	441	5,04	474
CTNND2	2,99	543	5,27	498	6,31	438
RAB17	2,92	544	1,55	648	1,37	711
SYT17	2,91	545	10,46	388	2,72	590
XK	2,91	546	2,58	587	3,85	526
ABRA	2,89	547	1,69	635	48,97	161
SPN	2,81	548	10,26	393	1,32	718
SLC16A10	2,80	549	6,70	457	4,27	502
SLC35F1	2,74	550	2,01	618	3,05	564
PRSS45	2,74	551	4,97	508	3,44	542
ADAMTS8	2,73	552	8,86	416	1,70	669
CES1	2,73	553	4,05	536	7,29	410
KCNJ4	2,73	554	5,30	494	8,42	382
HMGCS2	2,72	555	0,07	771	3,57	535
CA2	2,70	556	1,98	622	4,63	486
PCDHB14	2,67	557	1,40	660	1,83	648
KIAA1958	2,66	558	3,07	562	1,47	697
HRH2	2,66	559	19,66	295	12,78	328
SPINK7	2,63	560	27,18	239	5,46	458

PACRG	2,61	561	6,32	466	4,51	489
FAM110C	2,59	562	0,67	718	1,15	750
ESRRB	2,58	563	4,62	519	6,60	424
CA14	2,57	564	9,84	401	3,22	553
APOBEC4	2,54	565	6,00	473	2,37	615
ARHGAP44	2,54	566	5,96	475	3,20	556
HFM1	2,53	567	10,24	395	4,02	519
MYH11	2,42	568	4,24	530	17,33	284
RAP1GAP	2,41	569	1,73	632	1,24	735
PCDHB12	2,41	570	2,03	616	1,55	684
EBF4	2,40	571	3,12	560	1,39	706
WT1	2,40	572	3,31	557	1,88	645
JAG2	2,39	573	1,72	633	4,02	520
HPR	2,38	574	3,45	554	15,29	300
RGS16	2,38	575	1,12	681	2,47	603
P2RY1	2,35	576	1,77	630	1,48	694
ST8SIA6	2,35	577	11,16	376	10,51	349
SEMA6B	2,31	578	1,60	641	4,23	506
NTN1	2,28	579	2,25	602	6,14	441
MAOB	2,23	580	20,33	286	45,57	174
ELF3	2,22	581	0,16	757	1,07	767
SULT1C4	2,22	582	8,61	421	1,59	679
CPNE4	2,19	583	1,61	640	8,45	379
SEMA5B	2,19	584	27,84	236	8,45	380
NINJ2	2,17	585	9,94	400	2,80	586
ABLIM2	2,15	586	1,07	684	6,56	425
VWA7	2,13	587	1,98	623	4,53	488
HP	2,13	588	0,62	722	1,42	703
GABRB1	2,12	589	6,35	465	11,67	334
KCNJ11	2,09	590	1,60	643	2,72	591
DNAJC5G	2,08	591	6,64	458	2,26	622
NFATC2	2,06	592	2,47	593	1,52	691
GNG7	2,04	593	6,75	455	8,20	385
SEC14L5	2,02	594	5,27	497	3,09	563
CLYBL	2,00	595	1,88	625	1,46	698
ZNF385B	1,98	596	0,76	711	1,19	742
P2RY14	1,95	597	0,85	703	1,71	665
PIK3AP1	1,94	598	0,85	704	1,78	655
CXCR4	1,93	599	7,20	445	1,15	751
TMC8	1,93	600	4,26	529	5,21	468
SUSD4	1,93	601	1,24	670	1,81	652
CRIP3	1,92	602	6,27	468	31,57	210
YBX2	1,91	603	4,51	524	2,40	609
KCNJ12	1,89	604	1,32	667	3,12	561
FAM155B	1,84	605	0,11	766	3,80	528
RTN4RL1	1,83	606	1,37	664	1,38	710
RD3L	1,80	607	2,81	575	8,76	372

FAM110D	1,79	608	1,00	689	4,32	499
FXYD1	1,78	609	1,21	676	1,08	761
DHRS7C	1,71	610	6,39	463	9,74	359
MSI1	1,69	611	2,45	595	1,03	774
SLCO5A1	1,67	612	0,25	747	9,44	362
ADRA2B	1,66	613	0,93	695	1,70	666
SCN2B	1,66	614	2,17	609	2,95	570
GRM1	1,60	615	2,21	606	12,83	327
EDNRB	1,58	616	7,83	438	8,33	383
SLC26A9	1,57	617	2,03	617	4,41	494
VIP	1,51	618	0,95	692	1,01	776
ZBTB16	1,49	619	5,94	477	34,14	198
UGT2B4	1,46	620	0,09	768	14,91	305
PHACTR3	1,46	621	4,47	525	1,07	766
YPEL1	1,46	622	6,24	469	1,26	731
FAM107A	1,46	623	0,69	716	21,09	257
DLG2	1,45	624	7,88	436	3,57	534
CSF3R	1,45	625	0,33	738	1,39	709
THSD7A	1,43	626	4,27	527	1,01	775
IGSF5	1,43	627	1,62	638	1,65	673
PDK4	1,42	628	17,19	311	185,18	60
PACSIN1	1,41	629	0,29	744	2,07	633
METTL11B	1,41	630	2,49	592	1,28	729
VWC2	1,40	631	2,54	590	3,73	529
HLA-DRB1	1,39	632	1,62	639	28,18	226
CHDH	1,38	633	1,24	671	1,40	704
PRSS46	1,36	634	0,33	739	1,14	754
FGF9	1,36	635	3,95	538	2,82	582
MYO5C	1,36	636	3,49	552	1,10	759
TMEM74	1,34	637	2,84	571	1,28	728
C2orf71	1,32	638	2,25	603	5,42	461
EPN3	1,32	639	4,86	512	2,24	623
UPB1	1,29	640	1,39	661	1,30	723
TREM1	1,27	641	0,17	753	1,26	732
METTL24	1,26	642	0,76	710	1,26	733
TPRG1	1,25	643	0,70	715	1,15	749
GATA3	1,25	644	1,21	675	2,42	607
CHRD2	1,23	645	0,47	728	13,91	313
RERG	1,22	646	1,52	650	2,33	616
TLL2	1,20	647	2,81	576	2,37	612
FAM47E	1,19	648	2,55	589	1,70	668
GPD1	1,18	649	0,46	729	2,84	580
VWF	1,17	650	21,03	280	89,66	99
TMEM139	1,17	651	4,65	517	1,04	772
PLIN5	1,17	652	6,72	456	11,38	339
SYT2	1,17	653	4,93	511	1,43	702
RGS1	1,16	654	0,45	730	3,21	555

VIPR2	1,16	655	5,52	489	4,70	482
KLHL38	1,15	656	5,77	483	18,57	274
HTR4	1,12	657	3,87	540	2,52	600
BCL6B	1,11	658	7,98	431	4,68	485
ST8SIA5	1,09	659	0,52	727	1,27	730
RNF43	1,09	660	2,82	572	1,74	661
FAM151A	1,07	661	3,74	544	2,71	594
SPOCK2	1,07	662	2,72	580	2,71	593
SLC38A8	1,03	663	0,04	775	1,13	756
ZDHHC15	1,02	664	1,55	647	1,17	745
MEP1B	1,02	665	6,45	461	2,93	572
CYYR1	1,00	666	4,79	513	11,24	342
QRFPR	0,99	667	2,72	581	1,07	763
PLXDC1	0,98	668	1,73	631	6,78	419
MYH14	0,98	669	1,22	672	19,09	271
DUSP8	0,98	670	1,01	687	4,30	500
PZP	0,94	671	3,75	543	1,39	707
CEACAM1	0,93	672	3,22	558	1,94	641
MAEL	0,91	673	2,17	610	1,69	670
SRGAP3	0,90	674	0,71	714	2,90	576
GABRP	0,89	675	3,67	547	1,17	747
SLC6A13	0,88	676	2,44	596	1,92	642
C1orf168	0,88	677	0,86	702	4,69	483
PDE1B	0,87	678	0,97	690	1,28	726
DAND5	0,86	679	0,75	712	2,84	579
RGS6	0,85	680	8,08	428	17,07	286
ST6GALNAC1	0,82	681	0,29	745	1,36	714
SLC15A2	0,80	682	1,15	679	1,65	674
MYOM3	0,74	683	0,94	694	226,28	55
IFNK	0,74	684	0,91	697	1,21	738
IRX6	0,74	685	0,17	755	5,56	455
SERPINA3	0,72	686	0,07	772	5,15	471
ENAM	0,72	687	1,08	683	2,22	624
SLC22A7	0,71	688	0,97	691	3,04	565
SEMA3G	0,69	689	2,00	621	5,16	470
PCP4	0,67	690	0,90	698	1,55	683
POF1B	0,66	691	1,58	644	2,43	605
GRIK5	0,65	692	0,33	737	1,15	748
RASD2	0,64	693	5,56	488	1,48	695
RNASE6	0,64	694	5,86	480	1,53	689
ABCC8	0,64	695	0,61	723	8,59	376
LRMP	0,64	696	2,10	613	1,97	639
HEYL	0,63	697	4,31	526	10,33	351
NRXN1	0,61	698	0,93	696	1,54	687
CA8	0,60	699	1,22	674	2,51	601
MS4A6A	0,59	700	2,47	594	7,59	402
GLT1D1	0,58	701	0,15	759	1,04	771

HFE2	0,57	702	0,12	763	13,65	317
TSPAN7	0,57	703	1,30	668	2,52	599
CPT1B	0,57	704	2,76	579	1,05	769
PLA1A	0,56	705	0,25	748	1,23	736
CILP	0,55	706	2,65	584	5,22	467
GUCY2C	0,55	707	1,96	624	1,82	650
GIMAP5	0,55	708	14,30	338	63,09	135
LSP1	0,55	709	1,47	653	7,84	390
ASB10	0,54	710	1,39	662	6,29	439
KBTBD13	0,49	711	1,12	682	1,82	649
PLVAP	0,47	712	9,21	407	2,83	581
RORB	0,47	713	0,21	752	1,12	757
KCNT1	0,46	714	1,00	688	1,21	740
PEBP4	0,45	715	0,22	751	49,17	160
ARHGEF15	0,44	716	35,00	202	52,80	152
CYSLTR2	0,44	717	4,54	521	7,82	392
FXYD2	0,44	718	3,15	559	1,08	762
COL19A1	0,43	719	5,07	503	2,04	634
ITK	0,42	720	0,23	749	1,59	678
ALOX5	0,41	721	1,04	685	1,70	667
PAQR9	0,40	722	0,32	742	7,77	395
TNNT3	0,40	723	19,16	296	16,05	293
STAB1	0,40	724	5,49	491	15,82	297
CLEC7A	0,40	725	0,61	724	1,17	746
ASB12	0,39	726	0,03	777	1,75	659
KCNIP1	0,38	727	5,04	505	3,11	562
ZBTB7C	0,38	728	0,35	736	1,03	773
SV2B	0,37	729	2,33	601	7,29	409
PRIMA1	0,37	730	1,17	678	1,22	737
SMOC2	0,35	731	4,97	509	13,24	324
ASB4	0,33	732	10,92	380	6,75	422
TKTL1	0,32	733	1,78	629	2,02	635
GLP1R	0,30	734	13,99	344	1,59	681
PREX2	0,30	735	3,53	550	7,14	411
NPR1	0,29	736	6,55	460	4,38	497
LYZ	0,29	737	1,68	636	3,62	531
GIMAP4	0,29	738	4,93	510	11,60	336
TMEM252	0,28	739	1,35	665	1,53	688
GABRA4	0,28	740	3,65	548	6,09	442
ADRB1	0,27	741	0,22	750	17,97	281
LPAR5	0,27	742	0,33	740	1,29	724
AQP7	0,27	743	0,39	732	18,39	277
PCLO	0,26	744	0,37	734	1,79	654
CD38	0,25	745	1,45	655	5,62	453
SH2D3C	0,20	746	7,48	442	7,98	389
GRM8	0,20	747	0,10	767	1,60	677
ABCD2	0,18	748	0,05	773	3,94	523

GIMAP6	0,18	749	5,24	502	13,20	326
MFNG	0,18	750	1,49	652	2,77	588
ZPBP	0,17	751	0,80	707	1,11	758
CYBB	0,17	752	3,11	561	4,47	490
SOX7	0,16	753	2,80	577	3,49	540
PIK3CG	0,16	754	1,57	646	1,07	764
PDCD1	0,15	755	0,05	774	1,01	777
ASB15	0,14	756	1,34	666	13,65	318
MS4A4A	0,13	757	1,72	634	6,43	433
P2RX3	0,13	758	2,96	566	5,93	445
KLHL6	0,12	759	1,20	677	1,18	743
TCF15	0,12	760	1,79	628	4,56	487
TDRD10	0,12	761	1,29	669	1,97	638
CBFA2T3	0,11	762	0,26	746	1,53	690
HS6ST3	0,11	763	0,12	764	1,56	682
SGSM1	0,09	764	0,29	743	3,26	551
KLHL34	0,08	765	0,14	761	1,67	672
MOGAT1	0,07	766	1,04	686	1,09	760
GIMAP8	0,07	767	2,25	605	16,80	287
ADRA1A	0,06	768	0,52	726	42,79	179
HLA-DOA	0,05	769	0,16	756	1,35	716
DSC1	0,05	770	0,07	770	1,14	753
HLA-DQB1	0,05	771	0,15	758	1,92	643
TAL1	0,04	772	2,11	611	1,63	675
FCGR2B	0,03	773	0,04	776	2,11	628
CLEC10A	0,03	774	0,11	765	1,68	671
AVPR1A	0,03	775	1,42	658	1,59	680
OR51E1	0,02	776	0,78	708	1,31	722
F13A1	0,01	777	8,08	429	25,33	239

Supplementary Table 3: Cardiomyocyte transcriptome. Cardiomyocyte-specific gene transcription in pluripotent stem cell-derived (embryonic) cardiomyocytes (pooled from HES2, hiPS-G1 and hiPS-CDI [iCell] cardiomyocytes; n=3/group), fetal heart (3 biopsies from single donor), and adult hearts (4 biopsies from the left ventricles of 4 non-failing hearts). Data displayed for direct comparison as RPKM and ranked by expression level.

Supplementary Table 4: Fibroblasts transcriptome

Gene Symbol	Fibroblasts RPKM	Rank	Fetal Heart RPKM	Rank	Adult Heart RPKM	Rank
THBS1	23522,73	1	490,55	1	806,46	1
LGALS1	3703,66	2	193,07	2	183,77	3
S100A6	2439,53	3	60,68	9	138,79	4
NT5E	1353,17	4	14,13	34	10,74	52
PLAU	1177,94	5	15,59	29	45,20	11
ANXA2	1104,48	6	117,85	6	35,17	13
CYP1B1	1003,39	7	14,37	33	388,64	2
SERPINE1	631,35	8	2,33	122	6,82	74
S100A4	620,19	9	34,70	13	41,94	12
ANXA1	593,94	10	33,27	15	18,17	26
WNT5B	588,34	11	9,61	46	1,89	149
MME	529,60	12	1,04	156	2,06	143
NQO1	515,39	13	4,92	81	6,57	75
CCND1	509,69	14	24,96	18	35,03	14
FRMD6	497,35	15	16,08	27	12,31	48
RND3	489,36	16	20,73	21	13,84	44
SERPINE2	486,16	17	34,92	12	16,49	32
POSTN	460,05	18	167,40	3	13,88	43
FBLN1	450,11	19	121,04	5	108,06	5
CTSK	428,50	20	4,58	84	3,35	107
COLEC12	416,90	21	38,59	11	47,76	10
SRGN	371,06	22	9,56	49	27,89	21
MFAP5	340,78	23	7,35	59	29,42	18
PTX3	323,98	24	1,85	129	1,93	147
CD44	269,12	25	2,94	105	8,13	66
MT2A	242,95	26	5,52	73	17,99	27
ALDH1A3	221,42	27	2,18	125	8,07	67
TNFRSF11B	214,04	28	0,34	187	10,34	55
HMGA1	191,50	29	15,85	28	6,43	77
IL7R	182,48	30	1,20	147	1,91	148
LIMA1	177,15	31	15,22	31	15,03	38
COL12A1	166,64	32	101,64	7	52,32	8
HIST1H2BB	165,35	33	147,58	4	2,39	137
SPHK1	164,24	34	4,32	88	9,69	60
LAYN	162,25	35	5,78	71	5,26	81
CRIM1	154,12	36	25,09	17	29,77	17
HPCAL1	150,69	37	13,68	35	25,60	22
TAGLN2	150,05	38	18,33	24	23,62	23
STC2	139,14	39	6,77	67	1,10	193
MMP2	138,29	40	33,83	14	23,44	24
COL8A1	136,22	41	2,72	112	17,32	29
ADM	133,07	42	2,57	115	2,87	125
HMOX1	126,20	43	4,56	85	3,75	98

COTL1	125,90	44	4,60	83	2,91	122
PID1	120,25	45	20,24	23	15,91	36
LOX	118,68	46	5,86	70	1,17	191
RGMB	114,73	47	15,53	30	9,25	62
AXL	113,53	48	7,29	61	6,47	76
PTGS1	107,02	49	2,67	113	2,56	132
PAMR1	102,93	50	3,01	103	3,35	106
CLDN11	93,90	51	1,10	151	1,07	194
EMP1	92,50	52	10,76	43	10,79	51
LPAR1	92,06	53	7,29	60	3,38	105
CD9	84,76	54	7,10	64	14,13	40
GPR176	84,05	55	2,07	126	1,25	188
STC1	81,55	56	0,69	171	3,21	112
EDN1	79,58	57	4,16	91	1,59	164
CLMP	79,43	58	5,34	77	2,15	140
NBL1	75,91	59	5,05	78	12,74	46
ANPEP	72,79	60	1,74	136	1,30	184
DPP4	72,03	61	1,84	131	3,06	118
PCOLCE	61,63	62	11,69	37	10,52	53
EGFR	59,08	63	7,90	54	10,42	54
SLC1A1	58,99	64	0,87	163	6,91	73
F3	58,08	65	21,27	20	32,65	16
FBLN5	53,07	66	9,42	51	16,15	34
FGF2	51,44	67	5,03	79	2,42	136
CLEC11A	51,04	68	5,01	80	1,43	178
LTBP2	50,96	69	2,35	121	16,13	35
TBC1D2	48,84	70	1,06	155	1,57	166
MR1	48,42	71	2,56	116	8,69	64
DAB2	48,34	72	11,04	42	15,81	37
DCN	48,27	73	53,45	10	60,83	7
SH3GL2	46,60	74	11,17	40	33,49	15
CPED1	45,23	75	4,73	82	17,18	30
ATP8B1	44,48	76	5,66	72	7,50	69
MGLL	44,29	77	3,42	98	22,23	25
NTN4	43,44	78	5,46	75	28,83	19
CCBE1	41,52	79	0,67	173	1,05	196
MYO10	41,14	80	4,47	87	3,31	108
FAM20C	40,33	81	7,11	63	8,60	65
MLPH	39,86	82	0,50	178	28,77	20
CXCL1	38,07	83	0,99	158	1,44	175
DRAM1	37,37	84	0,95	161	2,47	134
C8orf4	37,37	85	7,46	57	11,27	50
LOXL3	36,90	86	2,89	107	1,47	173
ARHGAP22	35,90	87	0,63	174	1,82	153
PCDH18	35,89	88	20,59	22	3,28	110
LPXN	34,75	89	2,96	104	3,11	116
SYTL2	34,51	90	14,91	32	5,69	80

HIST1H1A	33,25	91	79,55	8	2,65	128
VEGFC	33,13	92	7,62	55	4,14	92
MYC	32,76	93	4,52	86	9,26	61
ATOH8	31,95	94	13,30	36	13,96	42
SLC14A1	31,68	95	0,91	162	5,01	83
VASN	30,05	96	2,91	106	3,12	115
ENPP2	26,69	97	1,61	141	2,57	131
CPXM2	26,56	98	2,06	127	3,17	113
CD109	25,74	99	9,51	50	4,87	85
ADAM33	24,21	100	6,85	65	3,89	97
CAMK2N1	24,20	101	1,39	143	3,58	101
L1CAM	22,02	102	0,26	190	1,60	163
ARSJ	21,90	103	1,93	128	1,02	199
EHF	21,56	104	1,76	135	1,69	156
IL6	21,48	105	0,13	194	1,52	168
ADAMTS2	21,42	106	9,57	48	1,38	179
SLFN5	21,10	107	3,35	100	5,10	82
ARHGEF28	20,44	108	3,06	102	1,61	161
ENG	20,24	109	18,20	26	48,11	9
DOCK10	19,44	110	3,69	94	1,18	190
SH2D4A	19,26	111	1,78	133	1,61	162
FAM180A	18,67	112	0,35	185	9,75	59
SLC16A4	18,26	113	6,56	68	2,63	129
MRGPRF	17,43	114	1,22	146	1,04	197
CTSF	17,04	115	7,39	58	16,18	33
CRLF1	16,97	116	0,73	167	5,86	79
ALDH3B1	16,69	117	3,58	96	1,47	172
NOV	16,62	118	3,15	101	1,87	150
MAMDC2	16,60	119	0,99	159	2,38	138
BDNF	16,22	120	2,47	117	4,43	88
RGCC	15,83	121	9,62	45	17,13	31
NEK10	15,59	122	10,43	44	8,02	68
SQRDL	15,58	123	0,41	183	2,92	121
VGLL3	15,13	124	2,39	119	1,30	183
DDX3Y	14,62	125	0,00	197	9,86	58
SVEP1	13,14	126	3,37	99	3,66	99
CD248	12,25	127	3,62	95	2,43	135
COLEC10	11,78	128	0,29	189	4,90	84
CDKN2C	11,72	129	7,29	62	2,91	123
ERAP2	11,56	130	1,08	153	2,83	127
ITPR3	11,01	131	3,82	93	3,45	103
SLFN11	9,61	132	1,64	140	9,18	63
NFASC	9,24	133	1,16	149	10,30	56
SFRP4	8,90	134	0,68	172	1,43	177
OSR2	8,77	135	0,16	193	2,09	142
MT1X	8,73	136	1,74	137	14,61	39
PRR16	8,28	137	3,93	92	4,12	93

ALPL	7,63	138	0,97	160	2,99	120
LRRN4CL	7,50	139	1,22	145	1,94	146
ABCG2	7,39	140	2,73	111	1,33	182
SYNE3	7,08	141	1,74	138	4,07	96
BST1	7,01	142	2,40	118	1,02	200
RASSF2	6,99	143	6,78	66	1,63	160
ANKRD29	6,80	144	3,44	97	3,09	117
DLL4	6,63	145	9,26	53	14,09	41
ELN	6,49	146	31,57	16	10,02	57
GPR68	6,43	147	1,82	132	1,66	158
OLFML1	5,48	148	11,66	38	4,09	95
NAALADL1	5,38	149	2,73	110	2,28	139
PRDM1	5,29	150	2,36	120	1,87	151
TRPA1	5,16	151	1,00	157	1,04	198
SAMD9L	5,05	152	1,08	152	3,27	111
FAM162B	4,85	153	2,18	124	3,17	114
CCDC144A	4,76	154	11,35	39	4,29	91
ACTG2	4,23	155	0,69	170	1,47	174
SHISA3	3,94	156	1,33	144	1,63	159
CLEC14A	3,87	157	7,55	56	13,80	45
NEGR1	3,60	158	1,84	130	1,44	176
EBF3	3,58	159	11,10	41	3,55	102
SPESP1	3,53	160	2,84	108	1,49	169
LRRK1	3,52	161	1,07	154	1,20	189
NGF	3,05	162	2,25	123	1,70	155
SLC37A2	2,94	163	1,12	150	1,11	192
HSPA2	2,92	164	2,66	114	2,84	126
CTSS	2,83	165	0,72	168	2,51	133
ZFY	2,80	166	0,00	198	1,36	180
NR4A2	2,79	167	0,43	182	1,48	171
ADAMTS5	2,78	168	2,79	109	1,86	152
BHMT2	2,77	169	0,40	184	2,10	141
TCF21	2,70	170	6,16	69	1,49	170
PTGER4	2,57	171	0,57	176	4,32	90
APOD	2,41	172	1,76	134	104,00	6
OAS2	2,17	173	0,79	165	4,32	89
LAMA3	2,12	174	4,21	90	2,03	144
TDRD1	1,92	175	0,34	186	1,29	185
DIO2	1,81	176	0,31	188	6,38	78
CCDC36	1,63	177	5,51	74	1,68	157
MKRN3	1,12	178	1,65	139	2,00	145
NKAPL	1,11	179	1,18	148	3,30	109
USP9Y	0,98	180	0,00	200	1,55	167
MUSK	0,77	181	0,49	179	1,06	195
SLCO4A1	0,69	182	0,19	191	3,43	104
UTY	0,64	183	0,00	199	1,34	181
ZNF662	0,59	184	9,60	47	2,58	130

CCL11	0,58	185	0,17	192	4,87	86
ADH1B	0,57	186	0,44	181	7,39	71
FMO2	0,56	187	0,84	164	17,36	28
GIMAP2	0,54	188	4,28	89	7,42	70
CDH19	0,50	189	1,56	142	12,33	47
CD34	0,49	190	18,26	25	12,27	49
HLA-DMB	0,47	191	0,71	169	3,01	119
CLEC3B	0,44	192	9,29	52	4,74	87
VIT	0,38	193	0,02	196	2,88	124
CCR1	0,25	194	0,56	177	1,59	165
LTF	0,21	195	0,45	180	1,77	154
CSF2RB	0,18	196	0,76	166	1,28	186
PRELP	0,16	197	0,60	175	7,08	72
PEG3	0,15	198	23,85	19	4,10	94
MEOX2	0,15	199	5,44	76	3,63	100
COMP	0,14	200	0,02	195	1,26	187

Supplementary Table 4: Fibroblasts transcriptome. Fibroblast-specific gene transcription in fibroblasts (pooled from heart, skin, and gingiva derived fibroblast cultures; n=3/group), fetal heart (3 biopsies from single donor), and adult hearts (4 biopsies from the left ventricles of 4 non-failing hearts). Data displayed for direct comparison as RPKM and ranked by expression level.

Supplementary Table 5: Gene clusters according to the trajectory of cardiomyocyte-specific gene transcription in embryonic, fetal, and adult cardiomyocytes.

Adult CM genes	Embryonic CM genes	CM genes without directed pattern
ABCC8	ACVR2B	ABCB4
ABLIM1	ADAMTS9	ABCD2
ABLIM2	AFAP1L2	ABCG1
ACACB	AMT	ABLIM2
ACTC1	APOBEC2	ABRA
ACTN2	APOE	ACACB
ADPRHL1	ARHGAP42	ACE2
ADRA1A	ATP1B1	ACOT11
ADRA2B	B4GALNT4	ACSM3
ADRB1	C10orf35	ACTA1
ADSSL1	C1orf105	ADAM11
AK4	C7	ADAMTS8
AKAP6	CADM4	ADCY1
ANO5	CCDC3	ADCY5
AQP7	CDKN1C	ADD2
ARHGEF15	CIB2	ADHFE1
ART3	CLYBL	ADORA1
ASB10	CNTN4	AGL
ASB11	COL14A1	AGT
ASB15	COL4A5	AIF1L
ATP1A2	COL4A6	ALDOC
ATP1A3	COL9A3	ALPK3
AVPR1A	CPT1B	AMY2B
BCO2	CSRNP3	ANK2
C10orf71	CXADR	ANKRD1
C14orf180	CXXC4	APLNR
C2orf71	DENND5B	APOA1
CA8	DLK1	APOB
CAMK2B	DMKN	APOBEC4
CAND2	DSC2	AQP1
CASQ2	DSG2	ARHGAP26
CCDC69	EBF4	ARHGAP4
CD38	EDNRA	ARHGAP44
CDK18	EFNA1	ASB12
CES1	ENPEP	ASB2
CKM	EPB41L3	ASB4
CKMT2	EPHA3	ASXL3
CLEC7A	EPHX2	ATG9B
CLGN	ERBB3	ATP1B2
CLIC5	FAM184A	ATRNL1
CMYA5	FAM84B	AUTS2
COL23A1	FTCD	B3GNT7

COX6A2	FXYD1	B4GALNT3
CPNE4	FXYD2	BCAM
CRIP2	FZD3	BCL11A
CRIP3	GABRP	BCL2L11
CRYAB	GAS7	BCL6B
CTNND2	GATM	BMP5
CYBB	GCA	BMP7
CYP2J2	GRIA4	BST2
CYSLTR2	GUCY1A3	BVES
CYYR1	HAND1	C11orf21
DAND5	HEPH	C1orf105
DES	HOOK1	C1orf168
DHRS7C	HOPX	C6
DOK7	HRASLS	CA14
DTNA	IGF2	CA2
DUSP27	IGFBP2	CA3
DYSF	IGSF3	CACNA1H
EDNRB	ISYNA1	CACNB2
EEF1A2	JPH1	CADPS
EFHC2	KBTBD11	CAMK2A
ENAM	KCNIP1	CASQ1
ESAM	KCNJ5	CASZ1
ESRRB	KIAA0895	CBFA2T3
F13A1	KIAA1324L	CCDC141
F5	KRT8	CCL21
FABP3	LAPTM4B	CEACAM1
FAM107A	LLGL2	CELSR1
FAM134B	LRRC17	CFI
FBXO40	MAN1C1	CGNL1
FILIP1	MDK	CHD7
GABRA4	MERTK	CHDH
GABRB1	METTL7A	CHN2
GIMAP4	MMP15	CHRD2
GIMAP5	MPP7	CHRNA3
GIMAP6	MST1	CILP
GIMAP8	NAP1L3	CLEC10A
GNG7	NRK	CMTM5
GRM1	P2RY1	CNN1
HEYL	PCDHB12	COBL
HHATL	PDE9A	COL15A1
HPR	PDGFD	COL19A1
HRC	PLBD1	COL21A1
HSPB7	PLEKHH1	COL9A3
IFNK	PRICKLE1	COLEC11
IGSF5	PRKCZ	COLQ
INPP5J	PROM1	CORIN
IRX6	PTH1R	CORO6

ITGA7	RAB17	CP
ITGA9	RAB3C	CPE
ITM2A	RAP1GAP	CPEB3
KBTBD13	RASGEF1B	CPNE5
KCNJ11	RASL10B	CPVL
KCNJ12	RASL11B	CREB5
KCNJ4	RASSF4	CSF3R
KCNQ1	RELN	CSRP3
KCNT1	RNF43	CTNNA3
KLHL31	SAMSN1	CXCR4
KLHL34	SERPINI1	DERL3
KLHL38	SH3BGRL2	DLG2
LDB3	SHC2	DMD
LDHD	SLAIN1	DNAJC5G
LMOD3	SLC40A1	DSC1
LPAR5	SLC44A5	DUSP13
LPL	SORCS1	DUSP26
LSP1	SPINT2	DUSP8
MAOB	SPOCK2	DYNC111
MB	SPON1	EDA
MCF2L	ST6GAL1	EGF
MFNG	ST6GALNAC3	EGLN3
MLIP	SYTL1	ELF3
MOGAT1	TMC6	ELMO1
MS4A4A	TMEM133	ELOVL2
MS4A6A	TMEM139	ENO3
MTUS1	TMEM176B	EPB41L4A
MURC	TMEM88	EPHA4
MYADML2	TNNI1	EPHA7
MYBPC3	TPD52	EPN3
MYH11	TRIM24	ERBB4
MYH7	TSHZ2	ESRRG
MYL2	TSTD1	FAM110C
MYL3	UNC13D	FAM110D
MYLK3	VANGL2	FAM13C
MYOM1	VCAM1	FAM151A
MYOM2	WNT11	FAM155B
MYOM3	ZNF853	FAM160A1
MYOZ2	ZNRF2	FAM189A2
NCAM1		FAM222A
NDRG2		FAM47E
NEBL		FAM78A
NGFR		FAM81A
NIPSNAP3B		FBXL22
NRAP		FCGR2B
NTN1		FGF12
OBSCN		FGF18

OR51E1
P2RX3
PCLO
PCP4
PDE1B
PDK4
PGM5
PIP5K1B
PLIN5
PLN
PLXDC1
PPARGC1B
PPM1L
PPP1R1C
PPP1R3A
PREX2
PRIMA1
PRKAA2
PRSS46
PYGM
RAB6B
RASGRP2
RBFOX1
RBPMS2
RCAN2
RD3L
RGS5
RGS6
RNASE1
RORB
RRAGD
RYS2
SCN2B
SCN5A
SELP
SEMA3G
SFMBT2
SGCA
SGSM1
SH2D3C
SHE
SLC25A4
SLC26A9
SLC2A4
SLC35F1
SLC4A3
SLC5A1

FGF9
FHIT
FIGN
FITM1
FNDC5
FRAS1
FREM1
FRMD4B
FSD2
FXD6
GAB1
GADD45G
GARNL3
GATA3
GATA4
GCNT2
GCOM1
GJA3
GKAP1
GLP1R
GLT1D1
GPD1
GPR22
GPRIN3
GPX3
GREB1
GRIK5
GRM8
GUCY1B3
GUCY2C
HAND2
HCN4
HEY1
HEY2
HFE2
HFM1
HIF3A
HLA-DOA
HLA-DQB1
HLA-DRB1
HMGCS2
HOOK1
HP
HRH2
HS6ST3
HSPB3
HTR4

SLCO2B1
SORBS1
SOX7
SPTB
SRL
ST8SIA5
STAB1
SYNPO2L
TCF15
TDRD10
TECRL
TGFB3
THBS4
TKTL1
TMC8
TMEM252
TMEM38A
TMOD1
TNNI3
TNNT1
TRDN
TRIM54
TSPAN18
TTN
TXLNB
USP2
VSNL1
VWC2
VWF
WBSCR17
XIRP1
XIRP2
XK
ZBTB16
ZPBP

HTRA3
ICA1
IFI44L
IGSF1
IGSF9B
ILDR2
INHA
IRX4
ISYNA1
ITGB1BP2
ITIH3
ITK
JAG2
JPH2
KCNA4
KCNH2
KIAA0895
KIAA1324L
KIAA1958
KIF26A
KLHL3
KLHL30
KLHL6
KRT8
L3MBTL4
LAD1
LGI2
LGI4
LMOD2
LRMP
LRRC10
LRRC39
LRRTM3
LYZ
MAEL
MAPK4
MARK1
MED12L
MEP1B
METTL11B
METTL24
MGAT3
MGAT4A
MLF1
MOG
MPPED2
MPZL2

MSI1
MTSS1
MTTP
MTUS2
MYH14
MYH6
MYH7B
MYL4
MYL7
MYO18B
MYO5C
MYOCD
NAALAD2
NAP1L2
NEB
NEURL2
NFATC2
NINJ2
NKX2-5
NMNAT3
NPNT
NPPA
NPPB
NPR1
NR0B2
NREP
NRXN1
NT5M
NTRK1
NUP210
OSBP2
P2RY14
PACRG
PACSIN1
PAIP2B
PAQR9
PARK2
PARM1
PCDH7
PCDHB14
PCDHB15
PCDHB5
PDCD1
PDE3B
PDE4D
PDK1
PEBP4

PHACTR3
PIK3AP1
PIK3CG
PKP2
PLA1A
PLCB2
PLCL2
PLCXD3
PLEKHA7
PLVAP
PNMT
POF1B
POPDC2
PPARGC1A
PPFIA4
PPM1K
PPP1R12B
PPP1R13B
PPP1R14C
PPP1R1A
PPP1R9A
PRDM16
PRKCB
PRKCH
PROX1
PRRG3
PRSS42
PRSS45
PTGER3
PTGES3L
PTP4A3
PTPN6
PTPRD
PTPRE
PZP
QRFPR
RAB3IP
RAB9B
RALGPS1
RALYL
RAMP1
RAMP2
RAPGEF4
RASD2
RASGRP3
RASSF5
RBM20

RBM24
RBM38
RCOR2
RCSD1
REEP1
RERG
RGS1
RGS16
RIC3
RIMKLA
RNASE6
RNF144A
RNF165
RNF207
RRAD
RTN4RL1
RXRG
S100A8
S1PR1
SCARF1
SEC14L5
SEMA5B
SEMA6B
SEPP1
SERPINA3
SERPINA5
SH3BGR
SIPA1L2
SKIDA1
SLC15A2
SLC16A10
SLC16A12
SLC1A3
SLC22A7
SLC29A2
SLC30A3
SLC38A3
SLC38A8
SLC47A1
SLC6A13
SLC7A2
SLC8A1
SLCO5A1
SMOC2
SMPX
SMTNL2
SMYD1

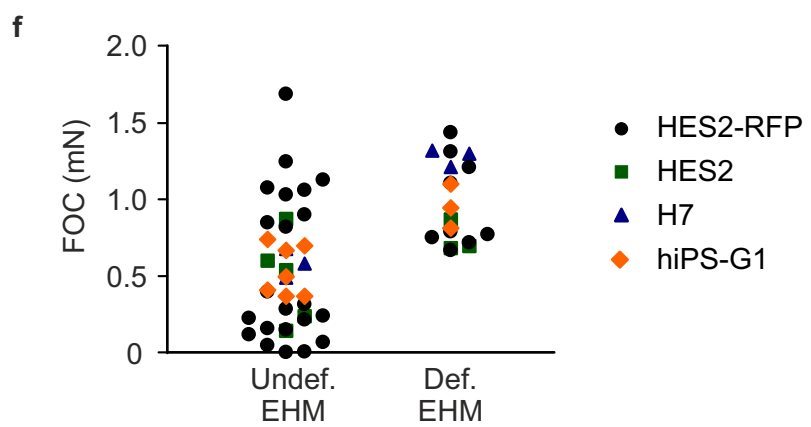
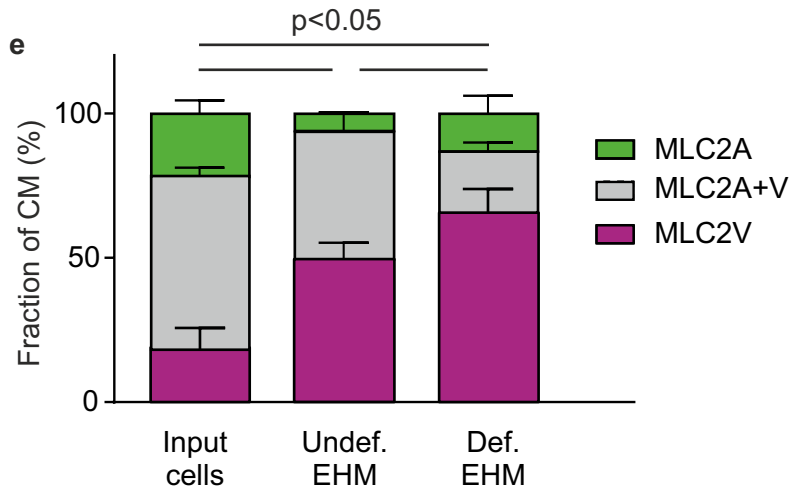
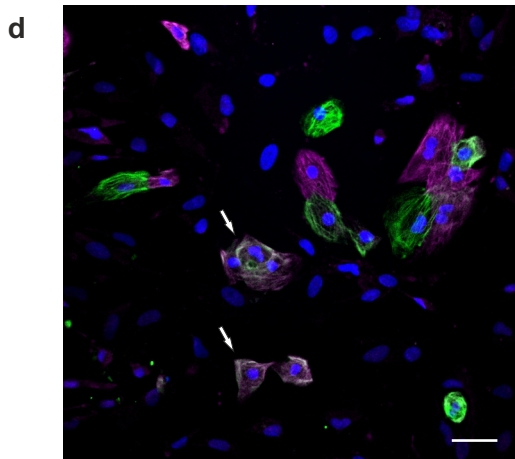
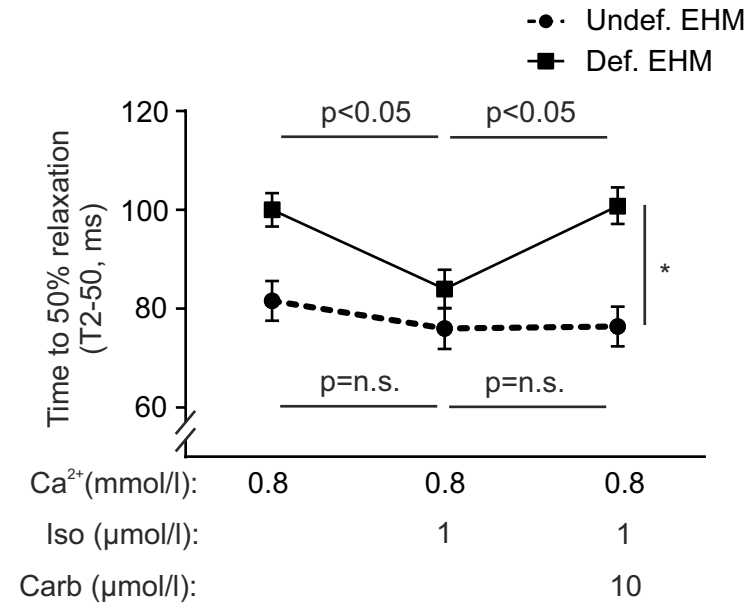
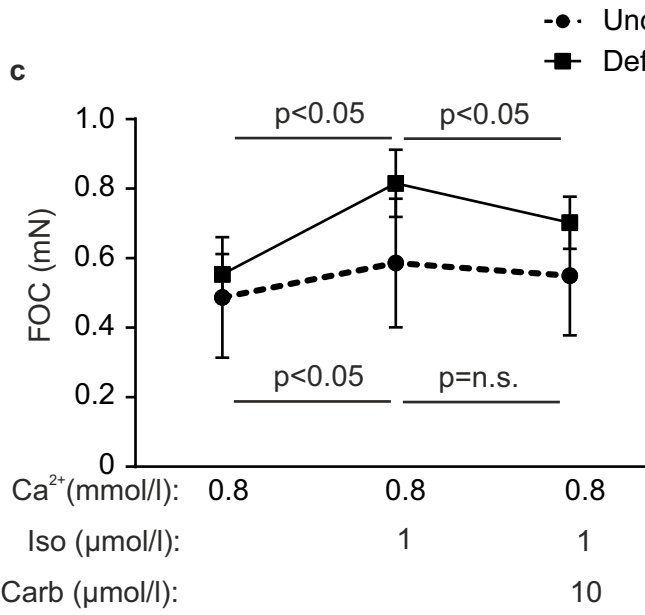
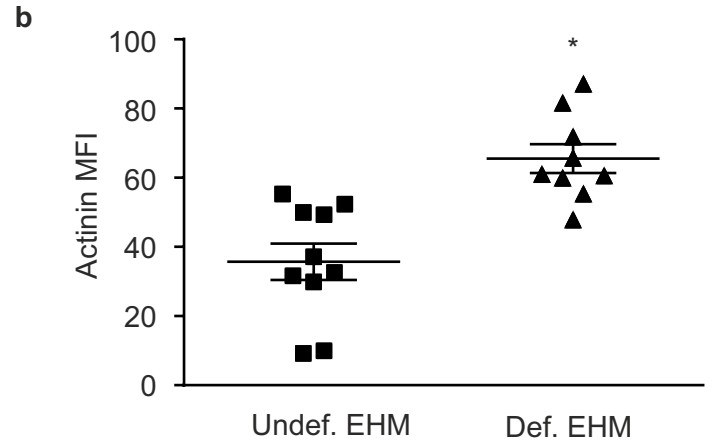
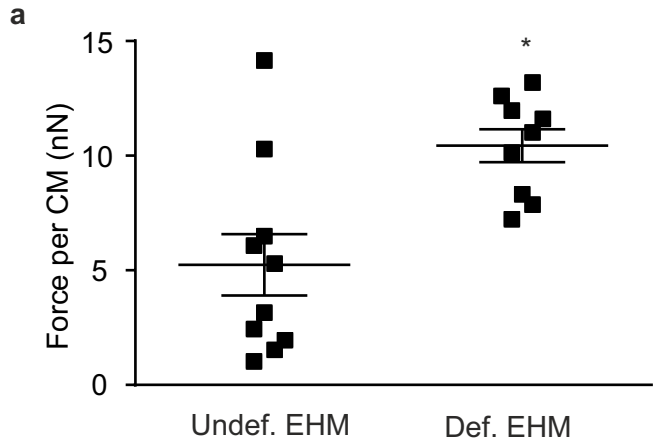
SNTA1
SOBP
SORBS2
SPATA25
SPHKAP
SPINK5
SPINK7
SPN
SPSB4
SRGAP3
SSTR2
ST6GALNAC1
ST8SIA6
STAT4
STOX2
SULT1C4
SUSD4
SV2B
SYT17
SYT2
TAL1
TBX20
TCAP
TESC
TET1
THSD7A
TLL2
TMEM176A
TMEM178A
TMEM179
TMEM56
TMEM71
TMEM74
TMEM74B
TNFSF10
TNNI3K
TNNT2
TNNT3
TPD52L1
TPRG1
TREM1
TRIL
TRIM63
TSPAN12
TSPAN7
TTC39A
TYRP1

UGT2B4
UNC45B
UPB1
VASH1
VAV3
VIP
VIPR2
VSTM2L
VTN
VWA7
WNK2
WT1
XPO4
YBX2
YPEL1
YPEL2
ZBTB7C
ZDHHC15
ZMAT1
ZNF385B
ZNF711

Supplementary Table 5: Gene clusters according to the trajectory of cardiomyocyte-specific gene transcription in embryonic, fetal, and adult cardiomyocytes. Adult CM genes (progressively up in HES2-CM monolayer culture<fetal heart<adult heart), embryonic CM genes (progressively down in HES2-CM monolayer culture>fetal heart>adult heart), and CM genes without a uniform increase or decrease from embryo (HES2-CM monolayer culture) to fetal and finally adult stages.

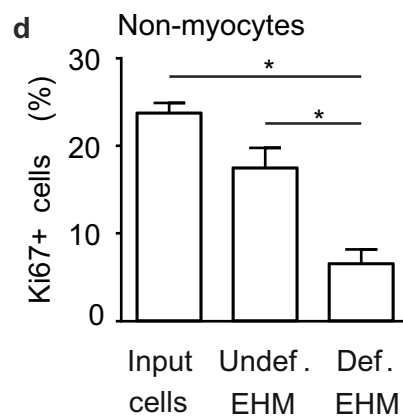
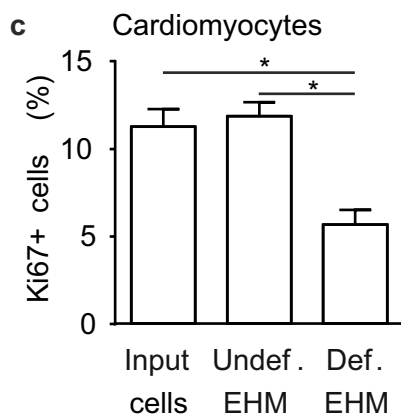
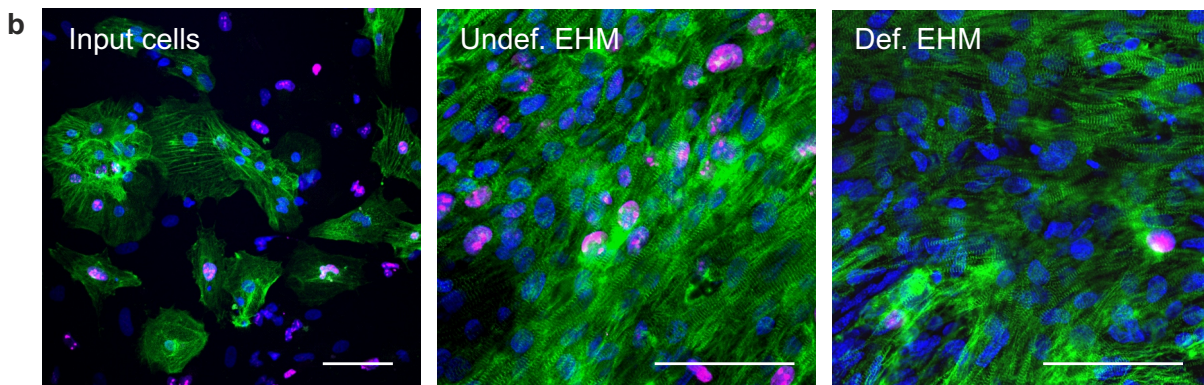
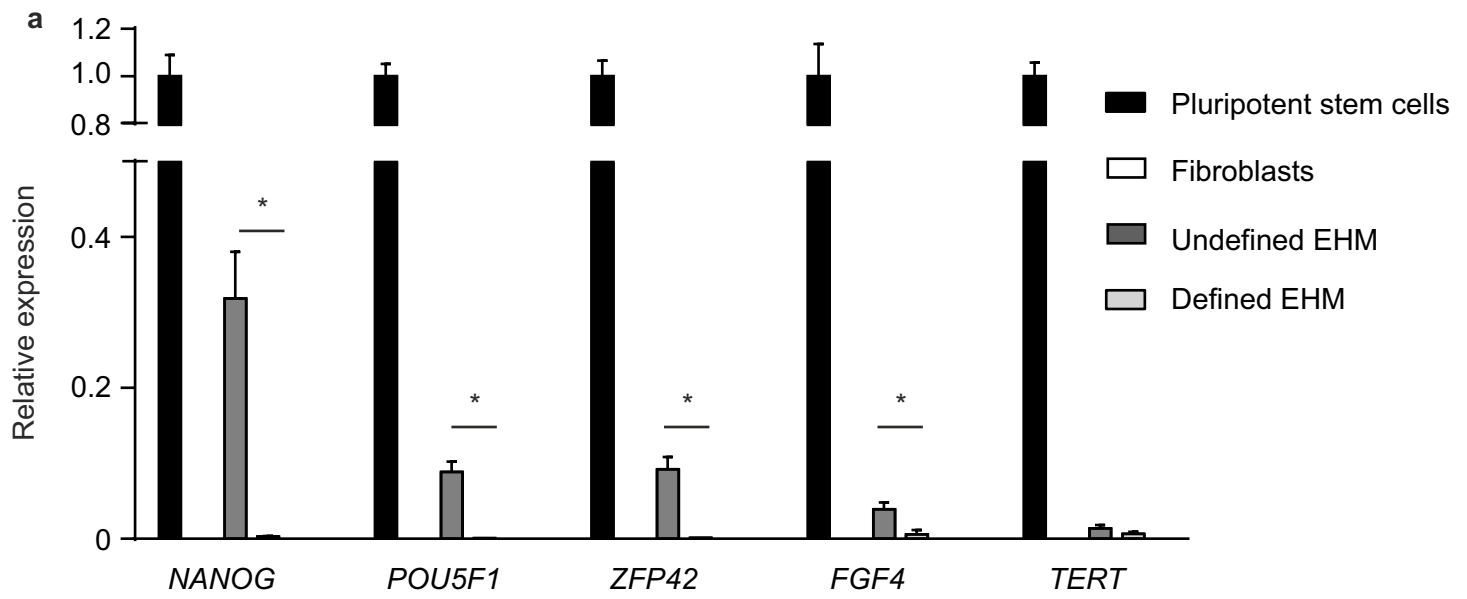
Supplemental Figures

Supplementary Figure 1



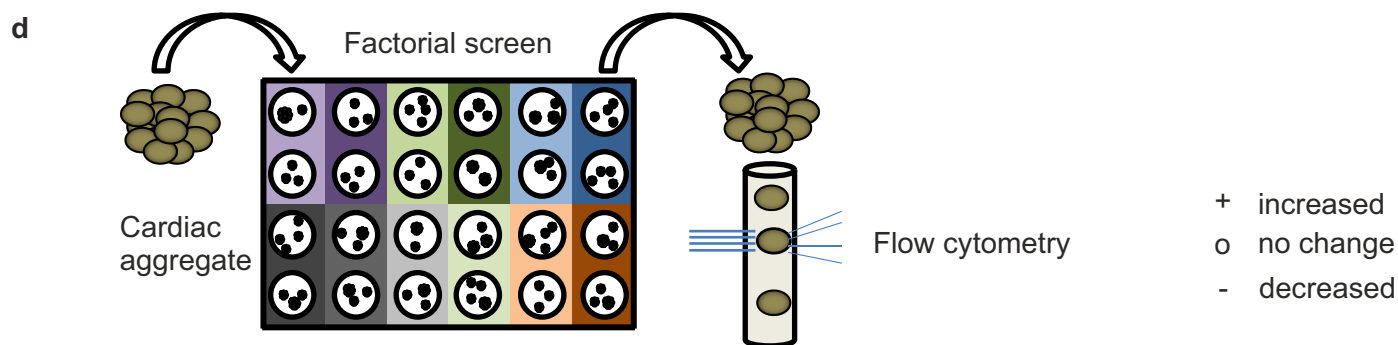
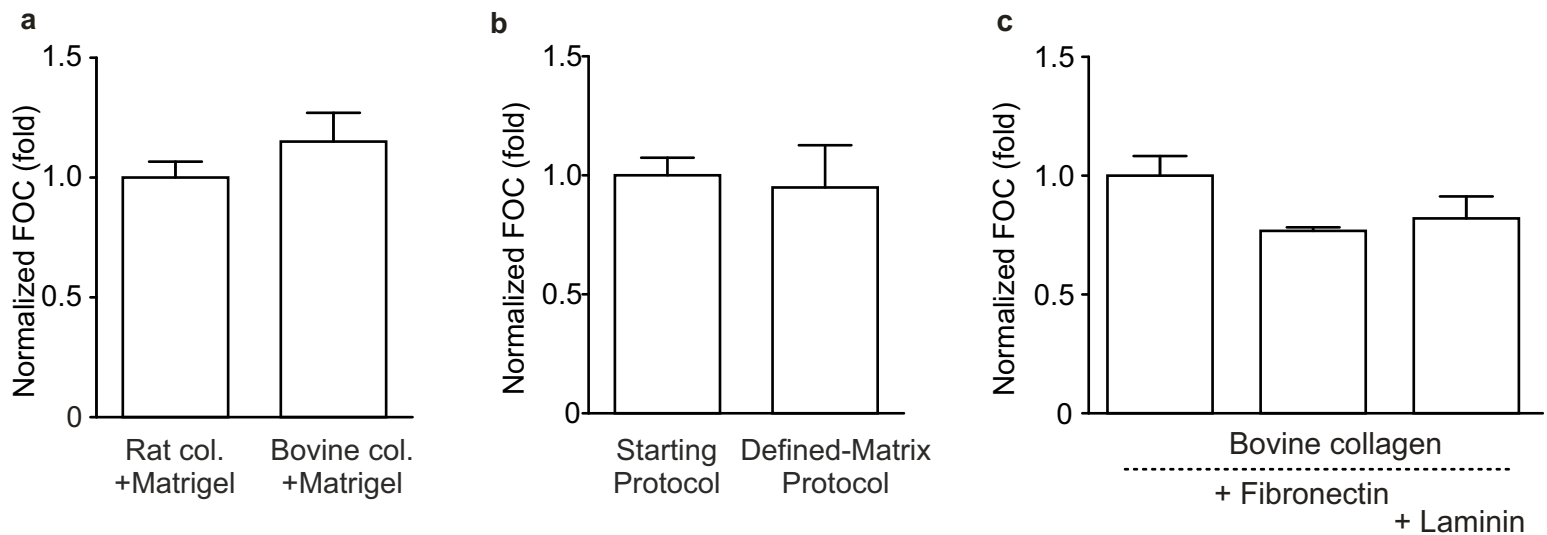
Supplementary Figure 1. Maturation of EHM constructed from defined cardiomyocyte and non-myocyte populations. (a) Force per cardiomyocyte (CM) in undefined vs. defined EHM. (b) Actinin median fluorescence intensity (MFI) assessed by flow cytometry in cardiomyocytes isolated from undefined vs. defined EHM. (c) Inotropic response (left panel) and time-to-50%-relaxation (right panel) in undefined vs. defined EHM in response to 1 $\mu\text{mol/L}$ isoprenaline followed by 10 $\mu\text{mol/L}$ carbachol at 0.8 mmol/L calcium. (d) Immunostaining of MLC2A (green), MLC2V (magenta) and nuclei (blue) in cardiomyocyte monolayer culture. Note grey appearance of double positive cells (arrows); bar: 20 μm . (e) Quantification of MLC2A single positive (green), MLC2V single positive (magenta), and MLC2A/V double-positive (grey) cardiomyocytes before EHM generation (“input cells”) and after isolation from undefined vs. defined EHM (“output cells”). (f) Maximal FOC in undefined and defined EHM from indicated PSC lines; each label represents one EHM. (a-c) undefined (n=10) vs. defined (n=9) EHM: *p<0.05 by two-tailed, unpaired Student’s t-test (a,b) and *p<0.05 by 2-way repeated-measures ANOVA followed by Tukey’s multiple comparison test (c); (e) n=3-4 cell pools/group, p<0.05 by 1-way ANOVA followed by Tukey’s multiple comparison test for MLC2A/V double-positive cardiomyocytes.

Supplementary Figure 2

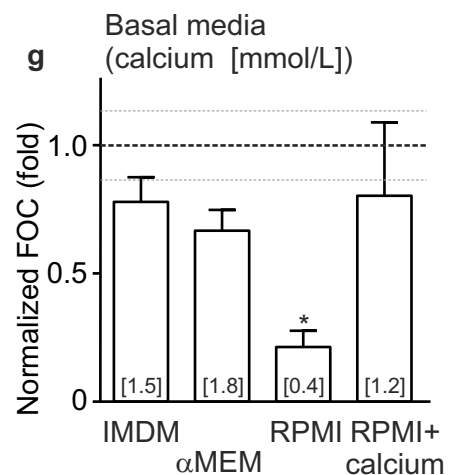
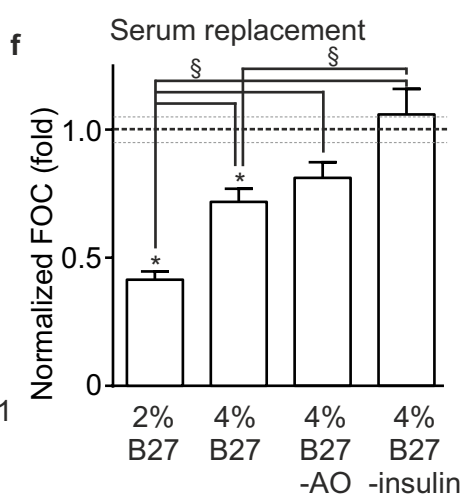
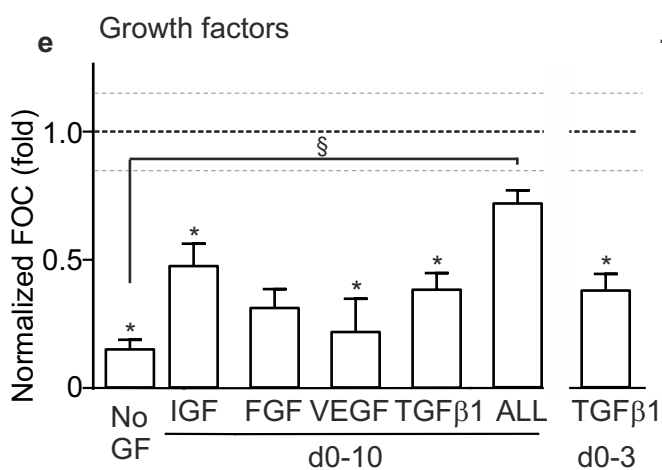


Supplementary Figure 2. Expression of pluripotency associated genes and cell cycle activity in defined vs. undefined EHM. (a) Expression of indicated pluripotency genes relative to pluripotent stem cells (HES2) in human foreskin fibroblasts (HFF), 2-week-old undefined EHM (HES2), and 2-week-old defined EHM made from purified cardiomyocytes (HES2) and HFF; n=3-6 per group, *p<0.05 undefined EHM vs. defined EHM by two-tailed, unpaired Student's t-test. (b) Representative immunostaining of cell cycle marker Ki67 in monolayer cardiomyocytes before EHM generation ("input cells"), in 2-week-old undefined EHM, and in 2-week-old defined EHM (all HES2). Actinin (green), Ki67 (magenta), Nuclei (blue); bars: 50 μ m. (c) Quantification of Ki67⁺ cardiomyocytes (actinin⁺ cells) and (d) Ki67⁺ non-myocytes (actinin⁻ cells) in monolayer cultures before EHM generation ("input cells"), 2-week-old undefined EHM, and 2-week-old defined EHM by flow cytometry. n=3-6 per condition, *p<0.05 by 1-way ANOVA followed by Tukey's multiple comparison test.

Supplementary Figure 3



	Factor	Viability	CM actinin content	CM size	NM size	CM/NM ratio
Medium supplements	B27 plus insulin 2%	-	o	-	-	o
	B27 plus insulin 4%	+	-	-	o	-
	B27 minus insulin 2%	-	-	-	-	o
	B27 minus insulin 4%	-	o	-	o	o
Growth factors	TGF- β 1 (5 ng/ml)	o	+	o	o	o
	TGF- β 2 (5 ng/ml)	-	-	+	+	o
	TGF-inhibitor (100 nmol/L)	+	o	-	-	o
	IGF-1 (20 ng/ml)	+	+	+	+	o
	VEGF ₁₆₅ (5 ng/ml)	o	+	o	o	o
	FGF-2 (10 ng/ml)	o	o	+	o	-
	PDGF-BB (10 ng/ml)	-	o	+	+	-
	Cardiotrophin-1 (10 ng/ml)	-	+	+	+	o
	Neuregulin-1 (10 ng/ml)	-	o	+	+	-
	EGF (10 ng/ml)	+	o	o	-	o

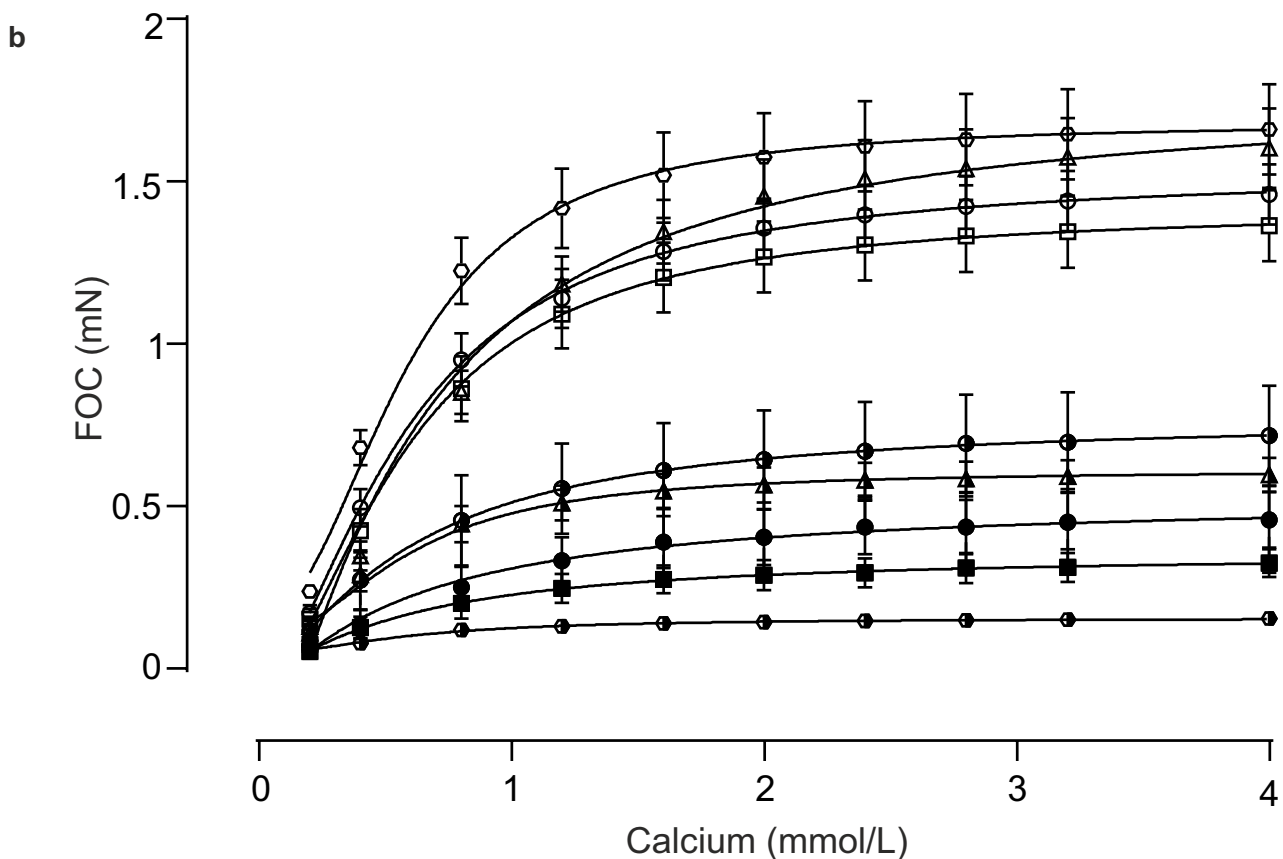


Supplementary Figure 3. Definition of defined, serum-free EHM. (a) Normalized force of contraction (FOC) at 2 mmol/L calcium of EHM made with rat collagen and MatrigelTM (n=12) or bovine collagen and MatrigelTM (n=14). (b) Normalized FOC at 2 mmol/L calcium of EHM made according to the Starting Protocol (n=12) and Matrix Protocol (n=9); see **Table 1** for details. (c) Normalized FOC at 2 mmol/L calcium of EHM made with bovine collagen only (0.4 mg/EHM), bovine collagen plus fibronectin (5 µg/EHM), or bovine collagen plus laminin (5 µg/EHM) as indicated; n=4/group. (d) Factorial screen in cardiac aggregate cultures: aggregates were cultured for 10 days in the presence or absence of respective factors and then analyzed by flow cytometry. Table of tested medium supplements and growth factors with a semi-quantitative analysis of viability, cardiomyocyte (CM) actinin content, CM and non-myocyte (NM) size, and CM/NM ratio. Comparison is either to serum-containing medium (Matrix Protocol) for medium supplements or control medium (αMEM with 2% B27 with insulin) without growth factor supplementation for the indicated growth factors (n=1-3 biological replicates). (e) Normalized FOC in EHM cultured for the indicated days in the presence of the indicated growth factors (GF: 100 ng/ml IGF-1 [n=10], 10 ng/ml FGF-2 [n=3], 5 ng/ml VEGF₁₆₅ [n=3], 5 ng/ml TGFβ1 [n=6], combination [ALL] of IGF-1, FGF-2, VEGF₁₆₅, TGFβ1 [n=16]) compared to serum-free medium (Iscove's with 4% B27 plus insulin) without respective growth factor supplementation (No GF, n=6). (f) Normalized FOC in EHM cultured in 2% full B27 (n=9), 4% full B27 (n=16), 4% B27 without antioxidants (-AO, n=5), or 4% B27 without insulin (-insulin, n=6) in the presence of ALL growth factors. (g) Normalized FOC in EHM cultured in indicated basal media, Iscove's (IMDM, n=9), αMEM (n=12), RPMI (n=9), and RPMI supplemented with calcium (total free calcium ~1.2 mM, n=3) in the presence of 4% B27 and ALL growth factors as indicated in (e); numbers in square brackets indicate free calcium concentration of respective medium. (e-g) Dashed lines indicate mean (black) and SEM (grey) of normalized FOC in Matrix Protocol EHM (refer to **Table 1**); *p<0.05 vs. Matrix Protocol EHM and §p<0.05 for indicated comparisons by 1-way ANOVA followed by Tukey's multiple comparison test.

Supplementary Figure 4

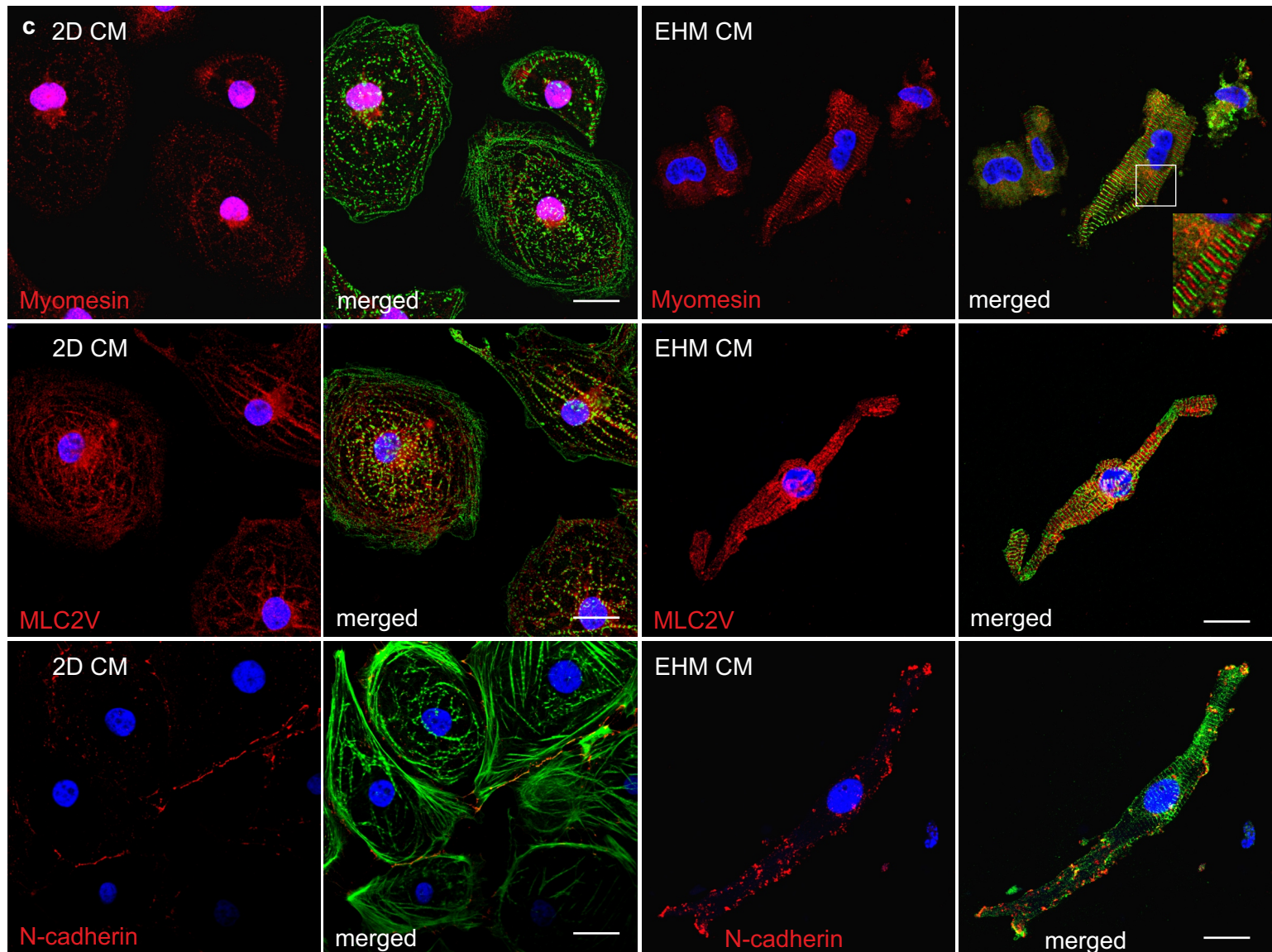
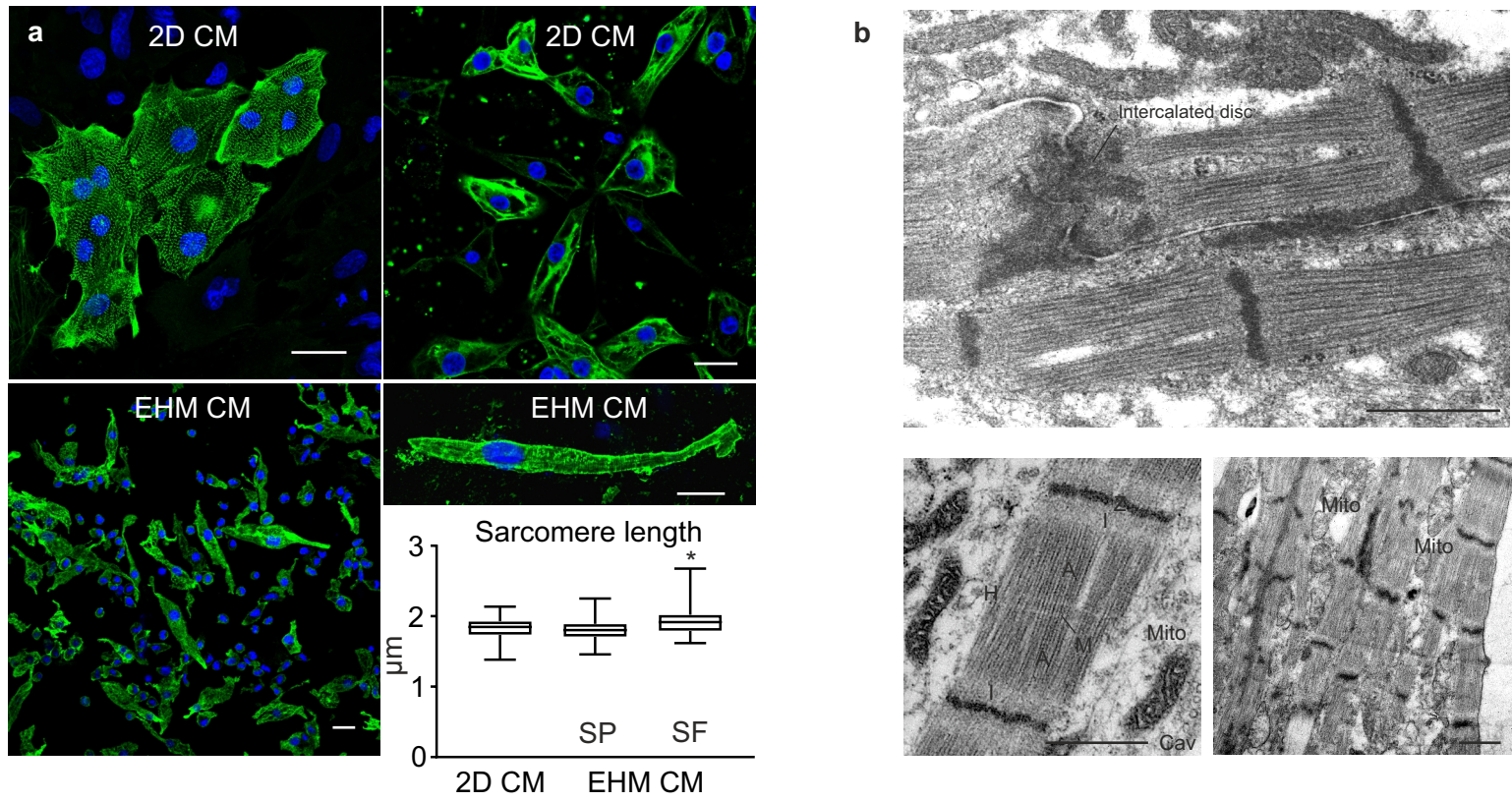
a

		Protocols		
Cell lines		Starting, undefined	Matrix, undefined	Serum-free, defined
HESC	HES2	■ n=8, W4	▣ n.d.	□ n=24, W4 *
	H7	▲ n.d.	▴ n=3, W4	△ n=7, W4 *
iPSC	hiPS-G1	● n=11, W4	◐ n=4, W4	○ n=18, W4 *
	iCell®	◐ n.d.	◑ n=4, W4	◒ n=10, W4 *



Supplementary Figure 4. EHM protocol development. (a) Summary of EHM constructed according to indicated protocols (details in **Table 1**) from different pluripotent stem cell lines (details in **Supplementary Table 1**). (b) Force of contraction (FOC) recorded in EHM (after 4 weeks in culture [W4]; constructed from indicated pluripotent stem cell lines; refer to **Supplementary Table 1**) under isometric conditions, electrical field-stimulation at 1.5 Hz, and increasing extracellular calcium concentrations. EHM were constructed according to the indicated protocols (**Table 1**): Starting Protocol with undefined cell composition, Matrix Protocol with undefined cell composition, Serum-free Protocol with defined cell composition (n-numbers indicated in (a); n.d.: not determined; *p<0.05 serum-free, defined vs. serum-containing (Starting or Matrix protocol), undefined EHM by 2-way ANOVA with Tukey's multiple comparison test.

Supplementary Figure 5

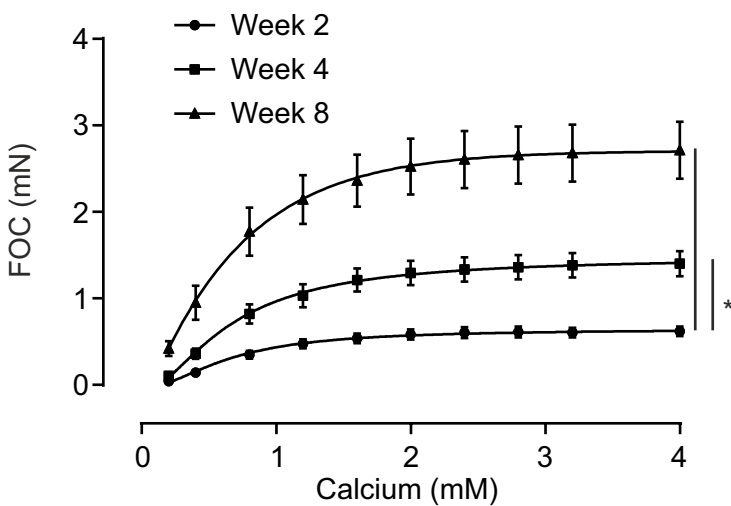
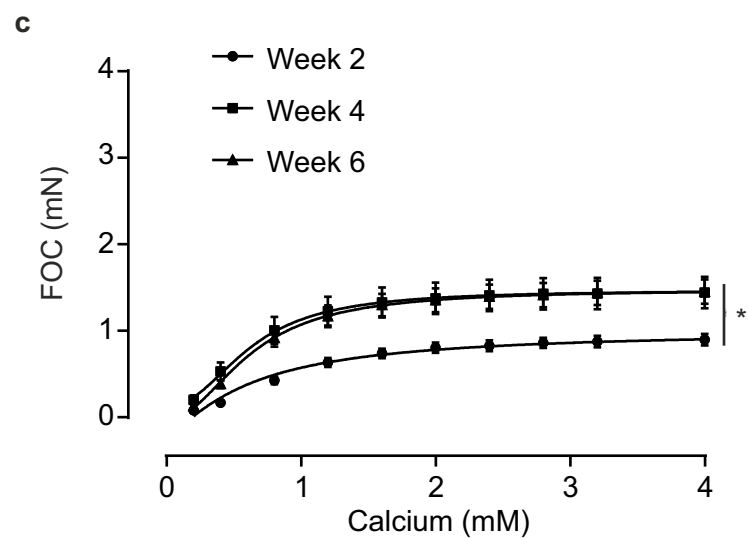
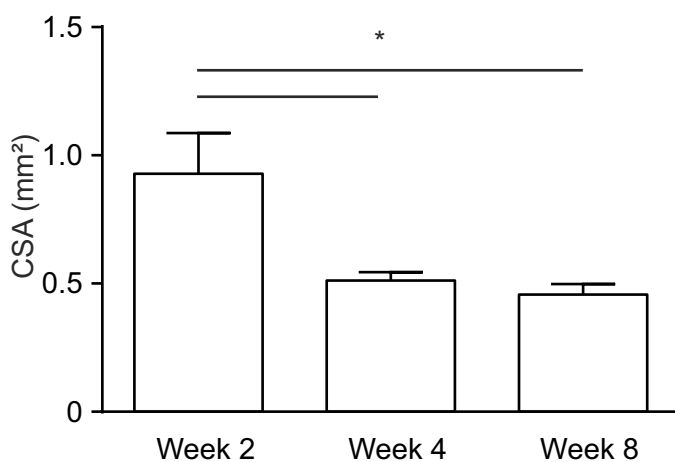
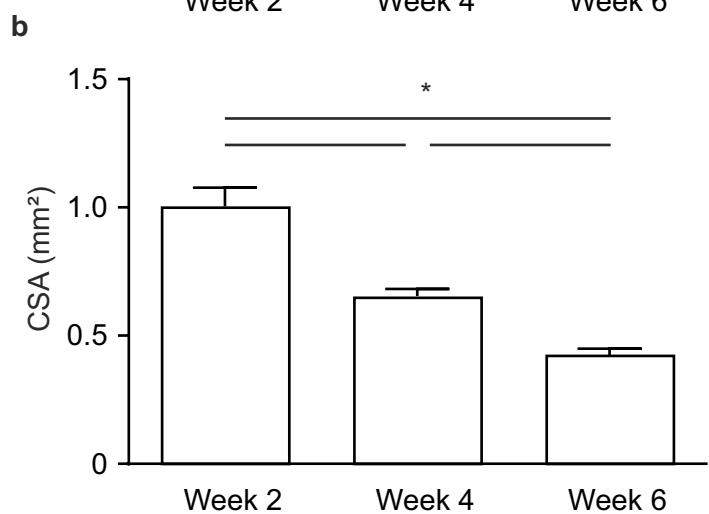
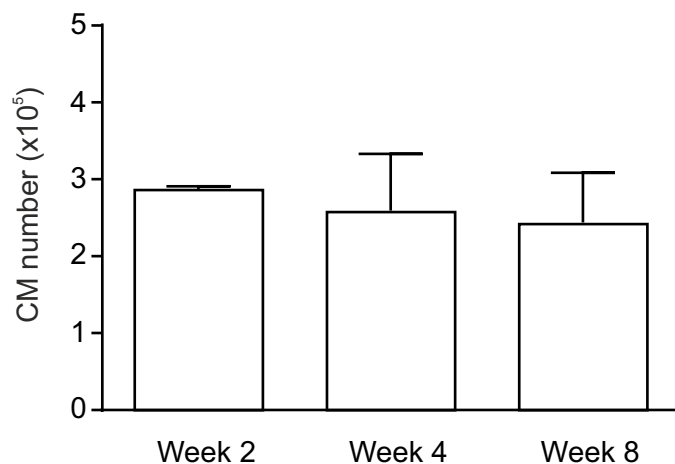
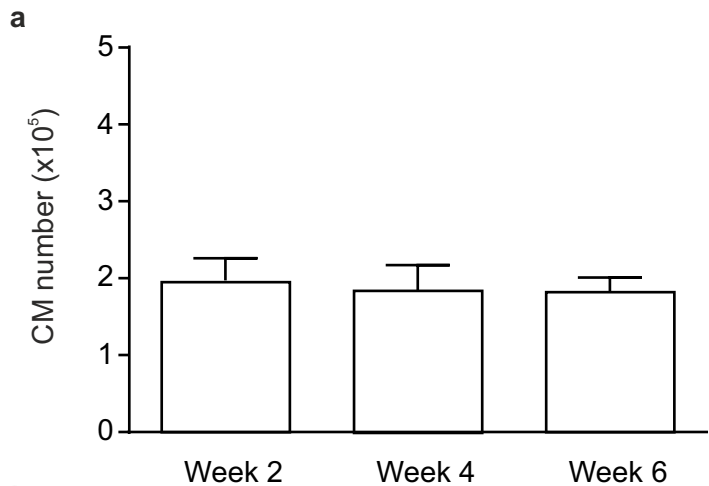


Supplementary Figure 5. Morphology of EHM-derived cardiomyocytes. (a) Immunostaining of sarcomeric actinin (left) and myosin heavy chain (right) in 2D monolayer cardiomyocytes (top row) or EHM-derived cardiomyocytes (lower row). Graph depicts the average sarcomere size with minimal to maximal values of 2D monolayer cardiomyocytes (2D CM), Starting Protocol (SP), or Serum-free Protocol (SF) EHM-derived cardiomyocytes (EHM CM); bars: 20 μm ; * $p < 0.05$ by 1-way ANOVA followed by Tukey's multiple comparison test. (b) Electron micrographs of 4 week serum-free EHM (hiPS-G1); characteristic sarcomere structures, organelles, and cell-cell contacts are labelled (Mito: mitochondria, Cav: caveolae); bars: 1 μm . (c) Immunostaining of myomesin (M-band protein), MLC2V, and n-cadherin (associated with intercalated disc) in 2D monolayer cardiomyocytes (left panels) and EHM-derived cardiomyocytes (right panels); bars: 20 μm

Supplementary Figure 6

HES2

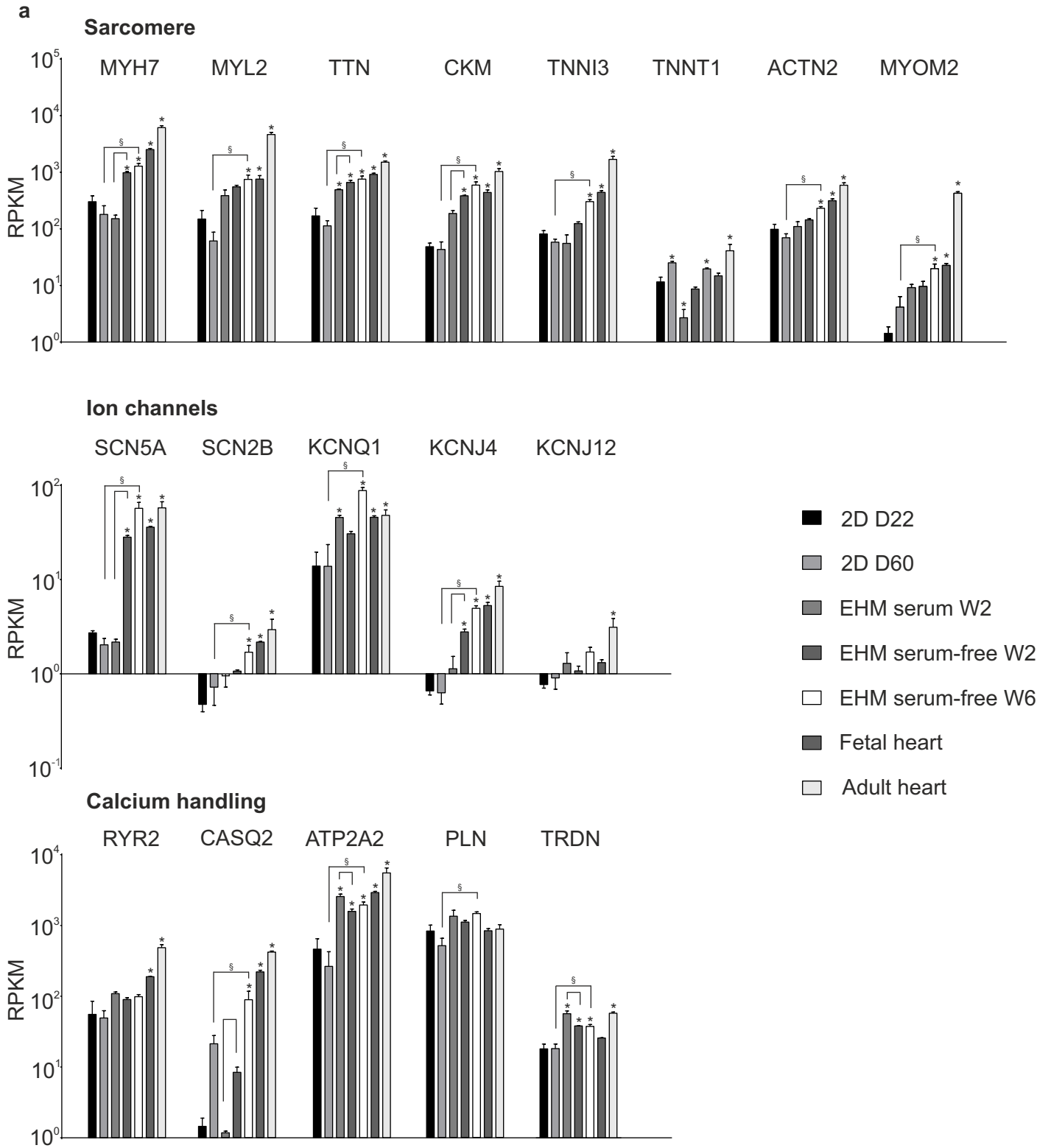
hiPS-G1



Supplementary Figure 6. Cellularity and dimensions of EHM during long-term culture.

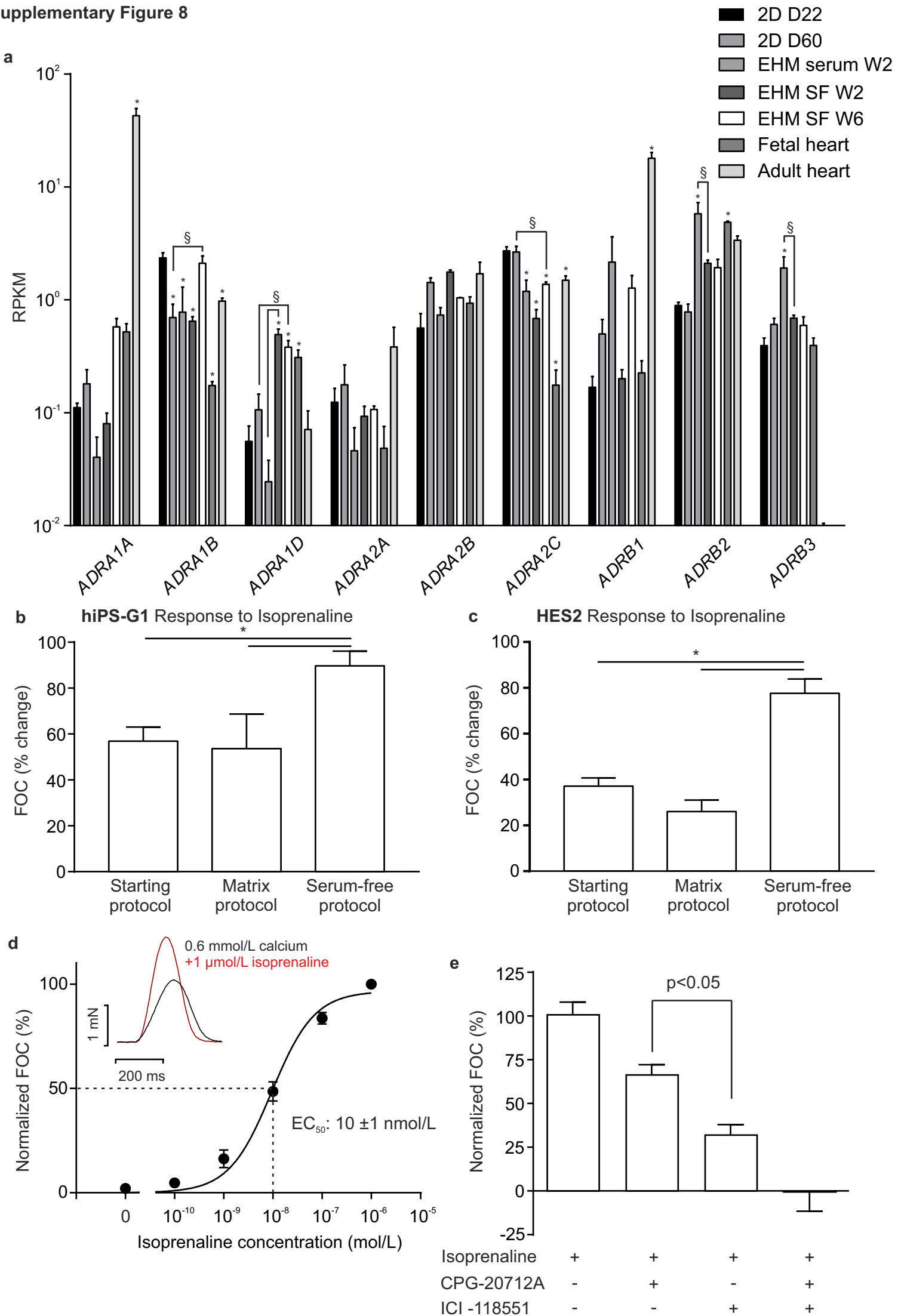
(a) Output cardiomyocyte (CM) number for HES2 (left panel) and hiPS-G1 (right panel) EHM after 2, 4, and 6/8 weeks in culture. n=12/10/3 for weeks 2/4/6 in HES2 EHM, n=4/7/6 for weeks 2/4/8 in hiPS-G1 EHM. (b) Cross sectional area (CSA) of HES2-RFP EHM (left panel) and hiPS-G1 EHM (right panel) at 2, 4, and 6/8 weeks in culture. n=12/10/8 for weeks 2/4/6 in HES2 EHM; n=7/10/8 for weeks 2/4/8 in hiPS-G1 EHM; *p<0.05 by 1-way ANOVA followed by Tukey's multiple comparison test. (c) Absolute uncorrected FOC of HES2 EHM (left panel) and hiPS-G1 EHM (right panel) at 2, 4, and 6/8 weeks in culture. *p<0.05 by 2-way ANOVA followed by Tukey's multiple comparison test; n=12/14/8 for weeks 2/4/6 in HES2 EHM and n=7/10/8 for weeks 2/4/8 in hiPS-G1 EHM.

Supplementary Figure 7



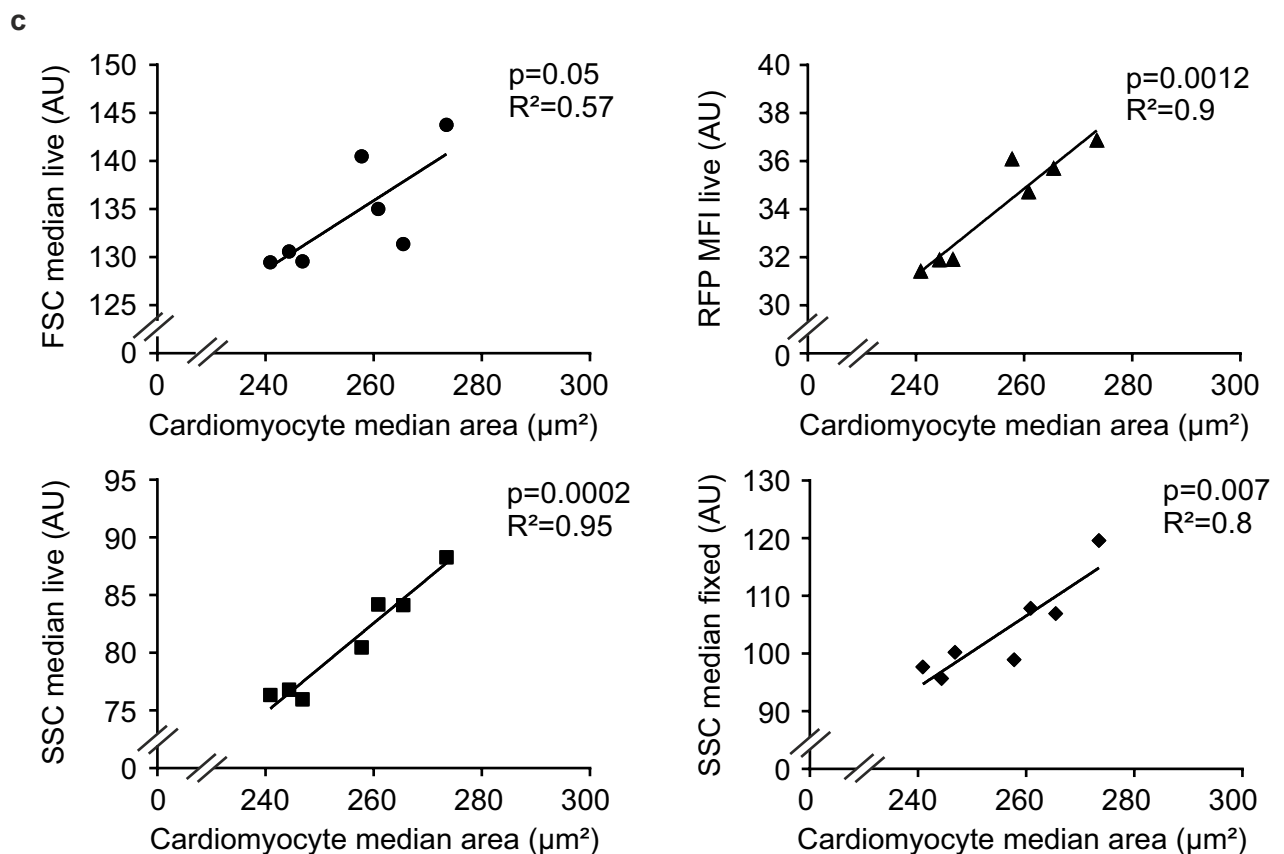
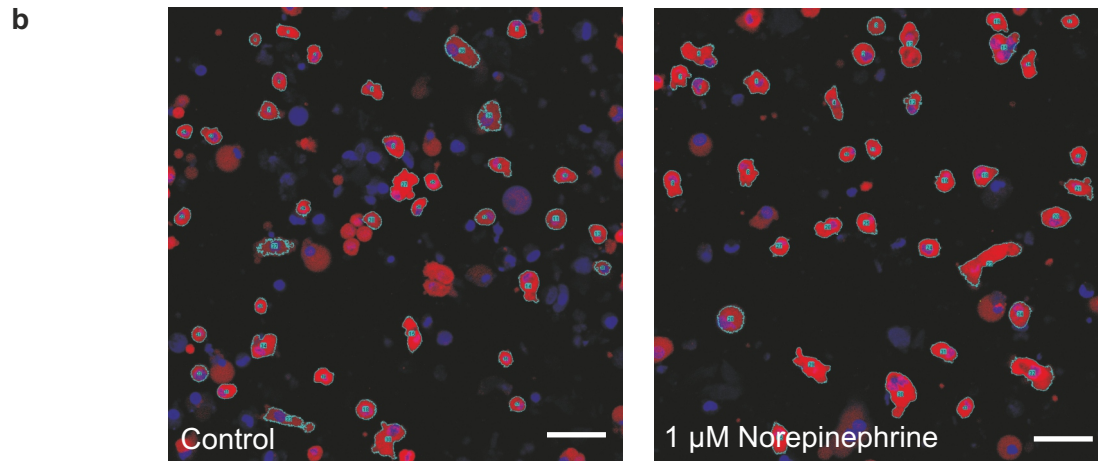
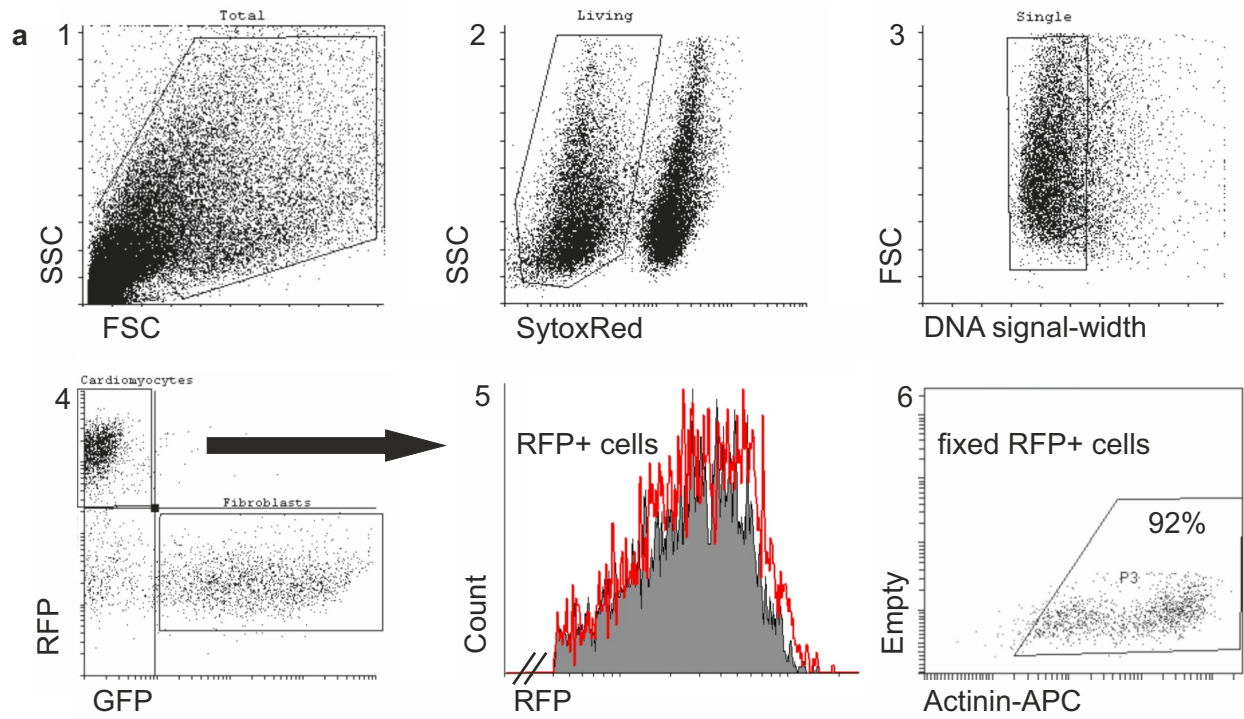
Supplementary Figure 7. Cardiomyocyte maturation transcripts. Expression of cardiomyocyte (CM) genes (according to analyses in **Figure 3a**) with a developmental trajectory (up: “adult” CM genes; down: “embryonic” CM genes) in: 22-day-old cardiomyocyte monolayer cultures (2D D22); 60-day-old cardiomyocyte monolayer cultures (2D D60); 2-week-old undefined, serum-containing EHM (EHM serum W2, Matrix Protocol); 2-week-old defined, Serum-free Protocol EHM (EHM serum-free W2); 6-week-old defined, Serum-free Protocol EHM (EHM serum-free W6); fetal and adult heart; n=3-4/group. *p<0.05 vs. 2D D22 and §p<0.05 for indicated comparisons by 1-way ANOVA followed by Tukey’s multiple comparison test. Note that the 6 weeks EHM culture is preceded by 3 weeks of cardiomyocyte differentiation and selection; hence EHM and 2D D60 have been cultured for a similar duration under similar culture medium conditions.

Supplementary Figure 8



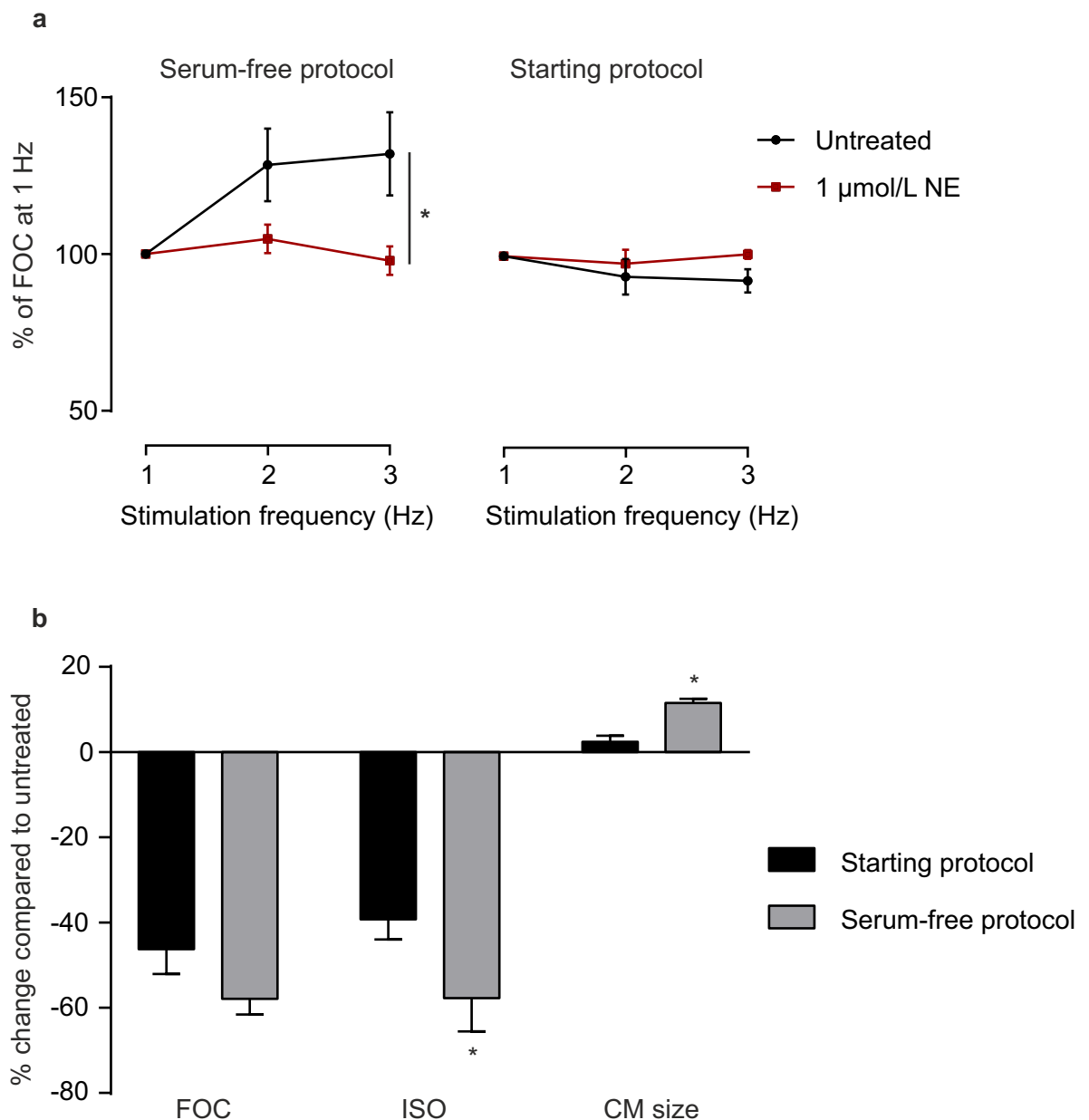
Supplementary Figure 8. Adrenoceptor expression and function in EHM. (a) RPKM of adrenoceptor subtypes: 22-day-old and 60-day-old monolayer CM culture (2D D22 and 2D D60); 2 week undefined, serum-containing EHM cultures (EHM serum W2); 2 and 6 week defined, Serum-free Protocol EHM cultures (EHM SF W2 and EHM SF W6); fetal and adult heart; n=3-4/group. *p<0.05 vs. 2D d22 and §p<0.05 and indicated comparisons by 1-way ANOVA followed by Tukey's multiple comparison test. Note that the 6 weeks EHM culture is preceded by 3 weeks of cardiomyocyte differentiation and selection; hence EHM and 2D D60 have been cultured for a similar duration under similar culture medium conditions. (b) hiPS-G1 EHM and (c) HES2 EHM change in force of contraction (FOC) in response to 1 µmol/L isoprenaline at EC₅₀ extracellular calcium; EHM were constructed according to: (1) undefined Starting Protocol (n=11/20); (2) Matrix Protocol (n=11/32) and (3) defined, Serum-free Protocol (n=15/18); *p<0.05 by 1-way ANOVA followed by Tukey's multiple comparison test. (d) Inotropic response of EHM to isoprenaline at 0.6 mmol/L extracellular calcium in percent of baseline force of contraction (FOC; n=11); inset: original contraction traces of unstimulated EHM (black) and after exposure to 1 µmol/L isoprenaline (red). (e) Inotropic effect of isoprenaline (100 nmol/L; n=11) alone or after 30 min pre-incubation with the specific β1-adrenoceptor antagonist (CPG-20712A, 300 nmol/L, n=7), the specific β2-adrenoceptor antagonist (ICI-118551, 50 nmol/L, n=7), or both (n=5); *p<0.05 CPG vs. ICI by two-tailed, unpaired Student's t-test.

Supplementary Figure 9



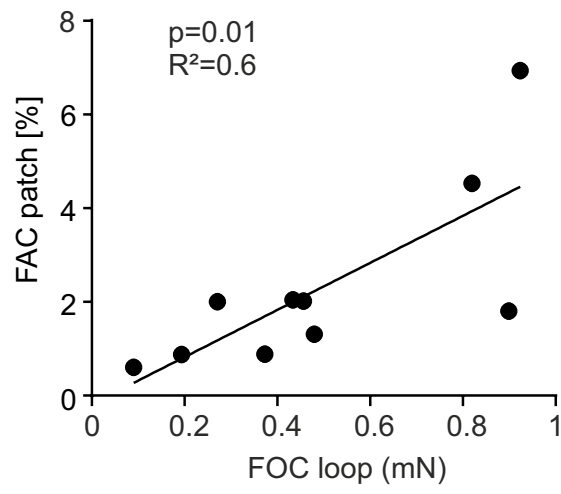
Supplementary Figure 9. Validation of flow cytometry-based cardiomyocyte size measurements. (a) Panel 1: flow cytometry gating strategy for the enumeration of EHM-derived cells: total cells; panel 2: live cells (negative for SytoxRed stain); panel 3: single cells (homogenous nuclear DNA signal to exclude doublets); panel 4: RFP⁺ cardiomyocytes vs. GFP⁺ fibroblasts; panel 5: cardiomyocyte size analyzed by RFP median fluorescence intensity (MFI; representative distribution of cardiomyocytes from control [grey area] and NE-treated [1 μmol/L, red line] EHM); panel 6: RFP⁺ cells stained for sarcomeric actinin after fixation to confirm cardiomyocyte identity. (b) Measurement of RFP⁺ cardiomyocyte cell area by fluorescence microscopy; representative images of cells derived enzymatically from control EHM and EHM treated with 1 μmol/L NE for 7 days; bars: 50 μm. (c) Correlation of cardiomyocyte area measured by fluorescence microscopy and flow cytometry parameters for size approximation (FSC: forward scatter; SSC: sideward scatter, live cells and cells fixed with 70% ethanol).

Supplementary Figure 10



Supplementary Figure 10. Serum masks chronic catecholamine stimulation induced heart failure phenotype. (a) Force frequency response in defined, serum-free EHM (Serum-free Protocol, $n=4$) and undefined, serum-containing EHM (Starting Protocol, $n=4$) after treatment with 1 $\mu\text{mol/L}$ norepinephrine (NE) for 7 days. $*p<0.05$ by 2-way repeated-measures ANOVA followed by Sidak's multiple comparison test. (b) Overview of change in force of contraction (FOC), acute isoprenaline response (ISO), and cardiomyocyte (CM) size after treatment with 1 $\mu\text{mol/L}$ NE for 7 days compared to untreated controls in undefined, serum-containing EHM (Starting Protocol, black bars, $n=8$) and defined, serum-free EHM (Serum-free Protocol; grey bars, $n=11$). $*p<0.05$ Starting vs. Serum-free Protocol by two-tailed, unpaired Student's t-test.

Supplementary Figure 11



Supplementary Figure 11. EHM patch function. Correlation of force of contraction (FOC) and fractional area change (FAC) recorded in small EHM loops and patches from the same production runs (n=10 production runs).

Supplemental references

1. Xu C, Police S, Rao N, Carpenter MK. Characterization and enrichment of cardiomyocytes derived from human embryonic stem cells. *Circ Res.* 2002; 91:501-508.
2. Kehat I, Kenyagin-Karsenti D, Snir M, Segev H, Amit M, Gepstein A, Livne E, Binah O, Itskovitz-Eldor J, Gepstein L. Human embryonic stem cells can differentiate into myocytes with structural and functional properties of cardiomyocytes. *J Clin Invest.* 2001; 108:407-414.
3. Mummery C, Ward-van Oostwaard D, Doevendans P, Spijker R, van den Brink S, Hassink R, van der Heyden M, Opthof T, Pera M, de la Riviere AB, Passier R, Tertoolen L. Differentiation of human embryonic stem cells to cardiomyocytes: role of coculture with visceral endoderm-like cells. *Circulation.* 2003; 107:2733-2740.
4. Passier R, Oostwaard DW, Snapper J, Kloots J, Hassink RJ, Kuijk E, Roelen B, de la Riviere AB, Mummery C. Increased cardiomyocyte differentiation from human embryonic stem cells in serum-free cultures. *Stem Cells.* 2005; 23:772-780.
5. Yang L, Soonpaa MH, Adler ED, Roepke TK, Kattman SJ, Kennedy M, Henckaerts E, Bonham K, Abbott GW, Linden RM, Field LJ, Keller GM. Human cardiovascular progenitor cells develop from a KDR+ embryonic-stem-cell-derived population. *Nature.* 2008; 453:524-528
6. Riegler J, Tiburcy M, Ebert A, Tzatzalos E, Raaz U, Abilez OJ, Shen Q, Kooreman NG, Neofytou E, Chen VC, Wang M, Meyer T, Tsao PS, Connolly AJ, Couture LA, Gold JD, Zimmermann WH, Wu JC. Human Engineered Heart Muscles Engraft and Survive Long Term in a Rodent Myocardial Infarction Model. *Circ Res.* 2015; 117:720-730.

7. Zimmermann WH, Schneiderbanger K, Schubert P, Didie M, Munzel F, Heubach JF, Kostin S, Neuhuber WL, Eschenhagen T. Tissue engineering of a differentiated cardiac muscle construct. *Circ Res.* 2002; 90:223-230.
8. Zimmermann WH, Melnychenko I, Wasmeier G, Didie M, Naito H, Nixdorff U, Hess A, Budinsky L, Brune K, Michaelis B, Dhein S, Schwoerer A, Ehmke H, Eschenhagen T. Engineered heart tissue grafts improve systolic and diastolic function in infarcted rat hearts. *Nat Med.* 2006; 12:452-458.
9. Soong PL, Tiburcy M, Zimmermann WH. Cardiac differentiation of human embryonic stem cells and their assembly into engineered heart muscle. *Curr Prot Cell Biol.* 2012;55: 23.8.1-23.8.21.
10. Tiburcy M, Meyer T, Soong PL, Zimmermann WH. Collagen-based engineered heart muscle. *Methods Mol Biol.* 2014; 1181:167-176.
11. Tiburcy M, Didie M, Boy O, Christalla P, Doker S, Naito H, Karikkineth BC, El-Armouche A, Grimm M, Nose M, Eschenhagen T, Zieseniss A, Katschinski DM, Hamdani N, Linke WA, Yin X, Mayr M, Zimmermann WH. Terminal differentiation, advanced organotypic maturation, and modeling of hypertrophic growth in engineered heart tissue. *Circ Res.* 2011; 109:1105-1114.

Supplemental Video Legends:

Supplementary Video 1: Defined, serum-free small EHM loop (2 weeks old) on flexible holders.

Supplementary Video 2: High purity cardiomyocyte (CM) EHM (left) and 70:30% CM:HFH EHM (right); input cardiomyocyte were from identical cardiomyocyte pools (iCell CM; CDI).

Supplementary Video 3: Free floating defined, serum-free small EHM loop (4 weeks old).

Supplementary Video 4: Color-coded EHM on flexible holders. Sequential recordings of GFP⁺-fibroblasts, RFP⁺-cardiomyocytes, and EHM in transmitted light.

Supplementary Video 5: Defined, serum-free EHM patch (1.5x1.7 cm, 3 weeks old) on a 3D printed array of flexible holders.